

**CHEMICAL TRANSFORMATIONS USING
TUNGSTEN AND MOLYBDENUM HYDROGEN
BRONZES**

By

PHANI KIRAN S. BOLLAPRAGADA

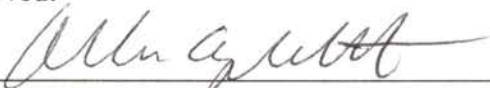
Bachelor of Science
Pune University
Pune, India
1995

Master of Science
Pune University
Pune, India
1997

Submitted to the Faculty of the
Graduate College of the
Oklahoma State University
in partial fulfillment of
the requirements for
the Degree of
DOCTOR OF PHILOSOPHY
August, 2003


**CHEMICAL TRANSFORMATIONS USING
TUNGSTEN AND MOLYBDENUM HYDROGEN
BRONZES**

Thesis Approved:




Thesis Adviser











Dean of the Graduate College

ACKNOWLEDGMENTS

I wish to express my sincere appreciation and gratefulness to my thesis advisor, Dr. Allen Apblett for his intelligent supervision, constructive guidance, inspiration and friendship. My sincere appreciation extends to my other committee members Dr. Neil Purdie, Dr. Elizabeth Holt, Dr Nicholas Materer, Dr. Nicholas Kotov, Dr. LeGrande Slaughter and Dr. Karen High, whose guidance, assistance and friendship have been very valuable to me during this investigation. I also wish to thank Dr. K. D. Berlin for his valuable guidance and discussions during this investigation.

Moreover, I wish to express my sincere gratitude to all my labmates and friends who provided me suggestions, encouragement and support during this study.

I would also like to give my special thanks to my parents and sister for their valuable suggestions to my research, their strong encouragement at times of difficulty, love and understanding throughout the whole investigation.

I would also like to thank the Chemistry Department and the Environmental Institute of Oklahoma State University for supporting my research during these five years of study.

TABLE OF CONTENTS

CHAPTER 1: INTRODUCTION	1
Aim of Experiments.....	1
Introduction to oxide bronzes.....	1
Hydrogen bronzes of transition metal oxides	3
Location of hydrogen in hydrogen bronzes	6
Applications of metal bronzes	9
Conclusions.....	14
References.....	14
CHAPTER 2: SYNTHESIS OF W AND Mo HYDROGEN BRONZES	17
Background.....	17
Experimental.....	20
Results and discussion.....	22
Characterization of the bronzes.....	29
References.....	31
CHAPTER 3: REACTIONS OF CHLOROMETHANES.....	33
Introduction.....	33
Experimental.....	35
Results and discussion.....	37
Conclusions.....	48
References.....	49
CHAPTER 4: REACTIONS OF BENZYLIC HALIDES	51
Introduction.....	51
Experimental.....	53
Results and discussion.....	54
Conclusions.....	68
References.....	68
CHAPTER 5: REACTIONS OF ALKENES WITH METAL BRONZES ...	71
Background.....	71
Experimental.....	71
Results and discussion.....	72
Conclusions.....	79
References.....	80

CHAPTER 6: REACTIONS OF ACETYLENES WITH BRONZES	82
Introduction.....	82
Experimental.....	83
Results and discussion.....	84
Conclusions.....	88
References.....	89
 CHAPTER 7: REACTIONS OF NITRILES WITH METAL BRONZES	90
Introduction.....	90
Experimental.....	91
Results and discussion.....	91
Conclusions.....	96
References.....	96
 CHAPTER 8: HEAVY METAL REMEDIATION USING Mo BRONZE ...	97
Introduction.....	97
Experimental.....	100
Results and discussion.....	102
Conclusions.....	116
References.....	116

LIST OF TABLES

Table	Page
1.1 Hydrogen bronzes of tungsten and molybdenum oxides	4
2.1 Classification of hydrogen bronzes of tungsten and molybdenum	19
2.2 XRD data for various MoO ₃ :molybdenum bronze (MB) mixtures.....	23
2.3 Percentage of bronze produced from alcohols.....	24
2.4 Analysis of alcohol used in molybdenum bronze synthesis.....	25
2.5 Results of reaction between molybdenum bronze and alcohols.....	26
3.1 Pseudo first order rate constants at 150 ^o C	40
3.2 Apparent activation energies of chlorocarbons.....	42
3.3 Adsorption data for chlorocarbons onto tungsten blue at 25 ^o C	43
4.1 Reactions between molybdenum bronze and benzylic halides.....	54
4.2 Reactions between tungsten bronze and benzylic halides.....	55
4.3 Reactions between benzyl chloride and aromatic substrates.....	60
4.4 Reactions of various benzylic monohalides with tungsten brnnze	61
4.5 Reaction between 0.25 g of α -chloroisodurene and 2.5 g of tungsten hydrogen bronze at 100 ^o C.....	64
4.6 Reaction between α -chloroisodurene and tungsten bronze in anisole.....	66
5.1 Alkenes used and the products obtained	73
6.1 Reactions of various C \equiv C with tungsten and molybdenum bronzes	85
6.2 Effect of reuse of tungsten bronze in the hydration reactions	88
7.1 Reaction of nitriles with tungsten and molybdenum bronze	93

7.2 Effect of Reuse of tungsten bronze in hydration of nitriles.....	95
8.1 Methods used to analyze filtrates of metal uptake reactions	101
8.2 Experimental conditions for metal uptake reactions.....	103
8.3 Results of metal uptake experiments.....	105
8.4 Results of competition experiments between calcium and uranium	106
8.5 Results of competition experiments between calcium and lead.....	107
8.6 Metal-oxygen stretching frequencies observed in the infrared spectra (cm^{-1}).....	108
8.7 Results of TGA experiments	110

LIST OF FIGURES

Figure	Page
1.1 Structures based on ReO_3 structure, a) WO_3 b) H_xWO_3	7
1.2a Structure of $\text{H}_{0.34}\text{MoO}_3$	9
1.2b Structure of $\text{H}_{1.7}\text{MoO}_3$	9
1.3 Representation of typical permeable reactive barriers (PRB)	13
2.1 (Graph1) Graph of percent MB Vs. ratio ($\text{area}_{\text{MB}}/\text{area}_{\text{MoO}_3}$)	23
2.2 Proposed mechanism for reaction of alcohols with molybdenum blue	27
2.3 Interaction of acetylacetone with acids and bases	28
2.4 Scanning electron micrographs	31
3.1 Proposed mechanism for reaction between CCl_4 and molybdenum bronze.....	38
3.2(A) Concentration of CCl_4 versus time for reaction with tungsten blue at 150°C	39
3.2(B) First order reaction kinetics for reaction of CCl_4 with tungsten blue at 150°C	39
3.3 Reaction between 2-methyl-2-phenyl-1-chloropropane and tungsten hydrogen bronze.....	46
3.4 AT and ET mechanisms for reductive dehalogenations	47
4.1 Reaction between tungsten bronze and α,α,α trichlorotoluene	55
4.2 Reaction between tungsten bronze and α,α -dichlorotoluene.....	56
4.3 Stepwise mechanism for reaction between tungsten bronze with α,α,α trichlorotoluene and α,α -dichlorotoluene	57
4.4 Reaction between benzyl chloride and tungsten bronze.....	58

4.5 Proposed mechanism for reaction between benzyl chloride and tungsten bronze.....	59
4.6 Reaction of α -chloroisodurene reaction with tungsten bronze	62
4.7 Graph of α -chloroisodurene reaction with tungsten bronze	64
4.8 General reactions of polyalkylbenzenes with acids.....	65
4.9 Reaction between CID and tungsten bronze in presence of aromatics	66
4.10 Proposed mechanism for the formation of Ar-CH ₂ -Ar.....	67
5.1 Reaction of cyclopentene with tungsten bronze	74
5.2 Possible products from the reaction between indene and tungsten blue....	76
5.3 Proposed mechanism for the reaction of 1-hexene and hydrogen bronzes.	78
5.4 Proposed mechanism for the dimerization of stilbene.....	79
6.1 General reaction for hydration of an alkyne.....	82
6.2 Reaction of C \equiv C with tungsten and molybdenum bronzes	84
6.3 Proposed mechanism for hydration of alkynes by metal bronzes.....	87
7.1 General reaction for conversion of a nitrile to an amide	92
7.2 Reaction of nitriles with tungsten and molybdenum bronzes	94
8.1 Graph of metal capacity versus metal solution.....	105
8.2 Graph of uranium: calcium ratio versus weight percent of uranium absorbed	107
8.3 X-Ray powder diffraction pattern for the reaction between lead nitrate and molybdenum bronze.....	111
8.4 SEM pictures.....	112
8.5 Complete cycle of the uranium remediation process.....	115

CHAPTER 1

INTRODUCTION

AIM OF EXPERIMENTS

This study utilized a series of laboratory experiments to explore the feasibility of applying redox techniques for the remediation of ground water contaminated with chlorocarbons and heavy metals. Considerable success in achieving the above objective was gained by using molybdenum and tungsten hydrogen bronzes as reducing agents to remediate wastewater. These hydrogen bronzes are simply products obtained from hydrogen insertion into tungsten and molybdenum trioxides. While much is known about the structure and properties of these bronzes, there are not many reports available in literature documenting the different types of chemical reactions feasible by the use of the bronzes. In this investigation, numerous interesting results were obtained upon using these bronzes as reagents in various chemical conversions. Therefore, this thesis will provide an account of the chemical transformations that can be effected by these bronzes and the potential applications of these in synthetic and environmental chemistry.

INTRODUCTION TO OXIDE BRONZES

Insertion compounds of transition metal oxides are called “ bronzes” due to their similarity to metallic bronzes in color and luster [1]. Therefore, it is appropriate to term these compounds as “oxide bronzes” so that they can be easily differentiated from metallic bronzes. Oxide bronzes are a group of well-defined, non-stoichiometric, insertion compounds having the general formula $M_xT_yO_z$, where, (i) M is a relatively

electropositive metal like Na, K, Group II metals, lanthanides, or hydrogen, (ii) T is a transition metal, (iii) T_yO_z is the metal's highest binary oxide state, and (iv) x is a variable falling in the range $0 < x < 2$. Such compounds are intensely colored, possess electrical conductivity (either metallic or semiconductor), and show sequences of various crystalline phases as "x" is varied. Particular phases can possess definite values of x or can exist over a wide compositional range. Although the bronzes constitute a unique class of non-stoichiometric compounds, they show similarities to other inorganic systems. They resemble the silicates and tungstosilicates in their structural properties; the alloys in the wide range of homogeneity of successive phases; and the solutions of alkali metals in liquid ammonia due to their typical free electron behavior that underlies their optical and electrical properties [2].

The structures of these oxide bronzes depend upon not only the character of the T_yO_z subarray, but also on the choice of element M, the concentration of the guest ion, and on the temperature of preparation. Each phase of the bronze has a compositional range, the limits of which vary with the equilibrium temperature. The number of crystallographic sites available to the M atoms approaches saturation as the value of x increases, but the value of x for which the phase $M_xT_yO_z$ stops being thermodynamically stable is generally less than the concentration of crystallographically available sites. Typically, for the value of x corresponding to crystallographic saturation, either another phase stabilizes with a slight variation in structure, or there is a disproportionation into two or three phases in equilibrium [3]. More complex oxide bronzes than the phases of $M_xT_yO_z$ are known to exist. For example, two transition metals may occupy the covalent

subarray, or on the other hand, M atoms may be introduced by a more complex substitutional mechanism in which the T_yO_z network expands with the loss of T atoms [3].

The study of oxide bronzes is interesting not only because of the great variety in their structures, but also in the width of their compositional ranges, which are generally greater than those of other non-stoichiometric binary compounds. This width gives rise to the possibility of a considerable change in the electrical properties as we traverse the different phases, a possibility that is further enhanced in the recently studied phases by the increased complexity of their chemical formulae. In addition to either metallic or semiconducting properties, these oxide bronzes possess the versatility of liquid mixtures in terms of compositional variety. It has been proposed that such compounds offer a rich storehouse for future technology [2].

HYDROGEN BRONZES OF TRANSITION METAL OXIDES

Hydrogen bronzes are non-stoichiometric, hydrogen insertion analogues of oxide bronzes, represented by the formula, H_xMO_n or $H_xMM'O_n$. They are formed by the ambient temperature reaction of hydrogen with a wide range of binary and ternary transition-metal oxides. The phase diagrams of these compounds are composed of biphasic regions containing solids of fixed composition in equilibrium, separated by single-phase regions of variable hydrogen content. Table 1.1 lists all known phases of tungsten and molybdenum hydrogen bronzes, the materials of concern to this investigation. Powder X-ray diffraction has demonstrated that the lattice parameters of the parent oxide do not change very much on hydrogen insertion, implying that the metal-oxygen framework is retained in most cases. In some cases, a few amorphous products

are formed at high values of x and this can be attributed to a structure collapse of the parent oxide. Hydrogen insertion depends on both the structural factors and the redox characteristics of the metal oxidation states involved.

Table 1.1
Hydrogen Bronzes of Tungsten and Molybdenum Oxides

Oxide	Established Phase Range	Color/ crystal structure	x_{\max}	References
<i>I) Corner-sharing octahedra</i>				
WO ₃	0.09 < x < 0.16	Dark blue / tetragonal A	0.4	[4, 5]
	0.31 < x < 0.5	Dark blue / tetragonal B		
	0.5 < x < 0.6	Dark blue / cubic		
β -MoO ₃		Dark blue / cubic	1.23	[6, 7]
<i>hex</i> -WO ₃	0.1 < x < 0.47	Dark blue / cubic	0.5	[8-10]
<i>II) Edge-sharing octahedra</i>				
α -MoO ₃	0.2 < x < 0.43	Blue / orthorhombic	1.7	[11-14]
	0.85 < x < 1.03	Blue / monoclinic		
	1.55 < x < 1.72	Red / monoclinic		
	$x = 2$	Green / monoclinic		

Initial investigations of hydrogen bronzes focused on the apparent similarities between the electronic and structural properties of the hydrogen bronzes and the alkali metal hydrogen bronzes (alkali metal ions are located in cavities present in the parent oxide matrix). The analogies in electronic properties of alkali metal bronzes and hydrogen bronzes are successfully drawn because both these classes share a common

redox insertion process given by the reaction, shown in Equation 1.1, where A= H or alkali metal, and A_i represents an ionized donor located at an interstitial site and e_M is an electron donated to a metal based orbital.



The high formal oxidation state of M in MO_n assures the existence of a suitable acceptor orbital, leading to, either, the progressive filling of a broad conduction band as in metallic conductors like A_xWO_3 , or localization of the electron at a particular metal site leading to formation of semiconductors such as $A_xV_2O_5$. The formation of a semiconductor or a metallic conductor depends on the parent metal oxide and not on the nature and location of A_i . It is known that the mode of attachment of hydrogen in H_xMO_n does not control the electronic properties, but it is presumed to be important in influencing the actual crystal structure adopted by the bronze and will also affect the properties that depend on hydrogen mobility. For this reason, analogies drawn between structures of alkali metal bronzes and their hydrogen counterparts are misleading. In the alkali-metal bronzes, the alkali metal has a definite ionic radius, which is usually greater than 0.2 nm, whereas the hydrogen atoms in the hydrogen bronzes are attached to oxygen as $-OH$ or $-OH_2$ groups, with a bond length of about 0.1 nm. This same mode of hydrogen attachment is found in many of the naturally occurring oxy-hydroxides and oxide hydrates such as haggite, $V_4O_4(OH)_6$, and protodoloresite, $V_3O_3(OH)_5$. Complete crystal structure determinations have been carried out for most of the hydrogen bronzes and based on these results it would be wise to classify the hydrogen bronzes as oxy-hydroxides $MO_{n-x}(OH)_x$ rather than as $H_x^+MO_n(xe)$, which might seem to imply the

chemically unrealistic possibility of the existence of isolated protons in the hydrogen bronzes.

LOCATION OF HYDROGEN IN HYDROGEN BRONZES

Complete structural characterization of these types of bronzes is difficult due to three main reasons:

- 1) Conventional X-ray diffraction often cannot be used because the products obtained using the usual ambient temperature preparative routes are poorly crystalline and frequently inhomogeneous.
- 2) Sometimes, even when single crystals of these bronzes are available, X-ray diffraction techniques are not of much use because these techniques are not suitable for determination of the exact location of hydrogen atoms in presence of heavier metal atoms.
- 3) The products formed are invariably non-stoichiometric and a random or partially ordered arrangement of hydrogen atoms amongst a surplus of available and near equivalent sites is the most likely outcome.

Powder neutron diffraction provides the solution for the first two difficulties. This technique measures only the Bragg reflections, by which only the sites and occupancies of the average unit cell are determined; however, no information can be obtained on the local ordering or clustering of hydrogen. Therefore, for complete structural determination, other techniques that probe the local proton environment, such as NMR, and neutron scattering methods, such as incoherent inelastic neutron scattering (INS) or elastic neutron scattering, are necessary to supplement the data obtained. INS has an

advantage over IR and Raman spectroscopies in that it is applicable to metallic materials for which IR and Raman spectroscopies are not. It is also sensitive to vibrational modes involving hydrogen atom displacement. Despite all the available techniques, complete structural determinations have been completed for a relatively few phases of the bronzes listed in Table 1.1. They are:

Group I) $H_{0.5}WO_3$ and $\beta-H_{0.99}MoO_3$

Group II) $H_{0.34}MoO_3$ and $H_{1.7}MoO_3$

The compounds belonging to Group I have the ReO_3 type of structure [15], a cubic phase based on corner-sharing MO_6 octahedra that are linked at vertices via two-coordinated oxygen (Figure 1.1).

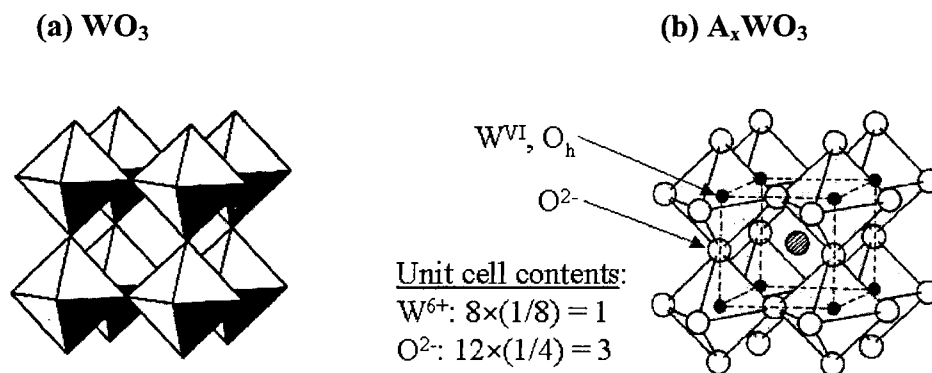


Figure 1.1: Structures based on ReO_3 Structure, a) WO_3 b) A_xWO_3 [Adapted from P. G. Dickens and A. M. Chippindale, Chem. Solid State Mater., 2, 101, (1992)]

Figure 1.1 (b) shows the structure of alkali metal tungsten bronze with the alkali metal placed in the center of the cavity. The structure of the tungsten hydrogen bronze is

similar to that shown above, except that the hydrogen atom is attached to one of the corner sharing oxygen atoms.

Among the Group II compounds, $H_{0.34}MoO_3$ [16, 17] has orthorhombic geometry, while $H_{1.7}MoO_3$ [18] has a monoclinic structure. Both these bronzes have structures similar to α - MoO_3 , which has a layered structure of double chains of edge-sharing MO_6 octahedra linked through vertices to form corrugated layers. α - MoO_3 has three types of oxygen atoms- two-coordinate (O_2), three-coordinate (O_1), and terminal (O_3) types of oxygen. All the phases of α - H_xMoO_3 have this same basic heavy-atom framework. $H_{0.34}MoO_3$ has hydrogen atoms located within the MoO_3 layers attached to bridging two-coordinate oxygens (O_2) as $-OH$ groups [20] (Figure 1.2a). In $H_{1.7}MoO_3$ most but not all of the hydrogen atoms are located at the terminal oxygen (O_3) as $-OH_2$ groups [22] (Figure 1.2b). The structures of the remaining phases of bronzes in Table 1 are undetermined in the sense that their average unit cells are still undefined by diffraction methods. Crystallographic data only provides the dimensions and types of Bravais lattice, which establishes the fact that the hydrogen bronzes are topotactically related to the parent oxides, but provides no information about the exact location of hydrogen. In such cases, vibrational spectroscopic methods, like IR and Raman spectroscopies, and proton NMR spectroscopy play a key role in obtaining information about the mode of attachment of hydrogen.

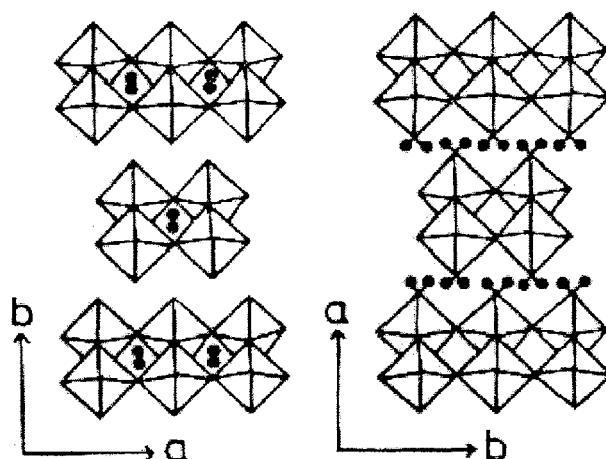


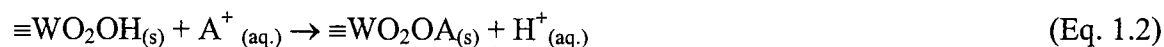
Figure 1.2: (a) Structure of $H_{0.34}MoO_3$, (b) Structure of $H_{1.7}MoO_3$ [Adapted from P. G. Dickens and A. M. Chippindale, *Chem. Solid State Mater.*, 2, 101, (1992)]

APPLICATIONS OF METAL BRONZES

The longest known and best studied oxide bronzes are those of tungsten, but in recent years analogous compounds of molybdenum, vanadium, niobium, tantalum and titanium have been prepared and found to have similar properties. Several reviews cover different aspects of the hydrogen insertion compounds formed by transition metal oxides. Unlike their parent oxides, the hydrogen bronzes are formally mixed-valence compounds and are often deeply colored. They possess high conductivity and can behave as good metallic conductors or semiconductors. This controllable variation in electronic properties has been exploited in electrochromic displays, which utilize the color changes induced by hydrogen insertion [19]. The hydrogen bronzes can also be used to construct sensors that respond to conductivity or optical changes in oxides on hydrogen incorporation [20]. It was speculated that these hydrogen bronzes could also be used as hydrogen storage materials based on the hydrogen recovered from the bronzes upon heating in the case of favorable systems with high values of x [21]. Investigations have

also been carried out on the function of H_xMO_n as a hydrogen source in hydrogenation reactions and the reactivity of the inserted hydrogen towards neutral Lewis bases such as NH_3 and organic amines [22, 23].

Ion-exchange properties of bronzes can be assumed due to their ionic structure and have been widely reported [24, 25]. It is reported that the lattice forming ions are not exchanged, but the protons of the water molecules are adsorbed on the surface [26] are exchanged according to the equation 1.2, where $\equiv WO_2OH$ is the active site on the bronze site where the ion exchange takes place.



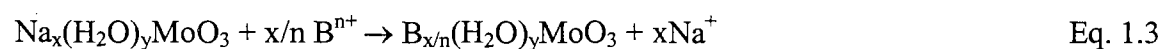
The ion exchange equilibrium is given by $\{(100-f)/vf\} = 1/Z(c_e + c_o)$ where the amount of water (%) adsorbed on the surface is given by f ; v gives the volume of the solution (cm^3) and z gives the amount of cations bound in the monomolecular adsorption layer (the ion exchange capacity of the bronze in $mol\ g^{-1}$). C_o ($mol\ cm^{-3}$) is a parameter characteristic for the particular system and c_e is the equilibrium concentration of the exchanging ion in solution. The equilibrium concentration, c_e , can be calculated by the measurement of f and the knowledge of the original concentration (c) of the solution and is given by the equation

$$c_e = \{(100-f)/100\} \times c$$

The constants $1/z$ and c_o/z of the above equation are characteristic of a particular system [27]. The potassium ion exchanging capacity was determined for some tungsten bronze

samples in this manner and they were found to have higher ion exchanging capacity than the corresponding tungsten trioxide sample [27].

Many insertion compounds can be prepared by following ion exchange methods. Most of the successful reactions reported involved layered oxides rather than those having framework structures. In the latter case, ion exchange is usually incomplete and the products formed are often amorphous. One example is the exchange of hydrated alkali-metal cations in $\text{Na}_x(\text{H}_2\text{O})_y\text{MoO}_3$ by ion exchange methods from an aqueous electrolyte [28] according to the equation 1.3



The replacement of sodium ions by other alkali and alkaline earth metal ions is rapid. The electrolyte solutions must be buffered and neutral in order to avoid a partial replacement of the cations by protons [29]. Ion exchange in dilute acids produces phases $\text{H}_x(\text{H}_2\text{O})_y\text{MoO}_3$ which on dehydration produce phases of H_xMoO_3 [30].

Besides ion-exchange properties, there have not been many reports that discuss the various types of chemical transformations that are possible using these bronzes. In this investigation it was determined that the bronzes could be effective for dechlorination of chlorocarbons and removal of heavy metal contaminants from wastewater samples. It is known that halocarbons and heavy metals are the most common contaminants of groundwater and one of the more complex technical challenges faced by scientists and environmental-engineers is the remediation of water contaminated with these materials. Earlier remediation efforts involved extraction and treatment of groundwater with the sole objective of restoring aquifers to pristine conditions. As these efforts progressed, it became apparent that the groundwater could not be restored to an uncontaminated

condition in a reasonable period of time or economically by “pump and treat” operations. Groundwater researchers attributed this difficulty in restoration to the complexity of the aquifer. Many leading environmentalists took up the challenge to advance the development of novel remediation techniques. One such innovative method has been the use of permeable reactive barriers (PRB), which has been considered by many groundwater chemists to be one of the major advances in groundwater treatment over the last ten years. The concept of a PRB is a relatively simple one, in which groundwater contaminants are destroyed or immobilized in a subsurface treatment zone [31]. The PRB is placed in the subsurface to intersect the flow of the contaminant plume and it can typically be oriented vertically or horizontally depending on the direction of the movement of the contaminated plume. Figure 1.3 (a) shows the lateral orientation of a PRB, in which a PRB is placed downstream to a chemical plume in order to prevent it from migrating further. Figure 1.3(b) shows the vertical orientation of a PRB, in which a PRB is placed immediately below a contaminant source and prevents the plume from entering the aquifer. Most of the known practical applications of PRB’s have been to prevent laterally spreading plumes. The PRB is designed in a way such that it is permeable and the groundwater flow is not impeded. However, PRB’s can alter existing ambient hydraulic conditions and care must be taken in designing a PRB so as to avoid any unintended consequences.

The use of reactive barriers to prevent the spread of pollutants in aquifers is a promising technology that can greatly curtail any environmental endangerment. Furthermore, the reagents used for construction of reactive barriers are generally also amenable to application in pump and treat operations or for treatment of wastewaters. In

1989, the use of granular iron was proposed for in situ remediation of groundwater containing chlorinated organic contaminants. Since that time, the technology has been adopted at numerous sites and has been applied to remediation of other types of organic compounds, inorganic species, and radionuclides [32-35].

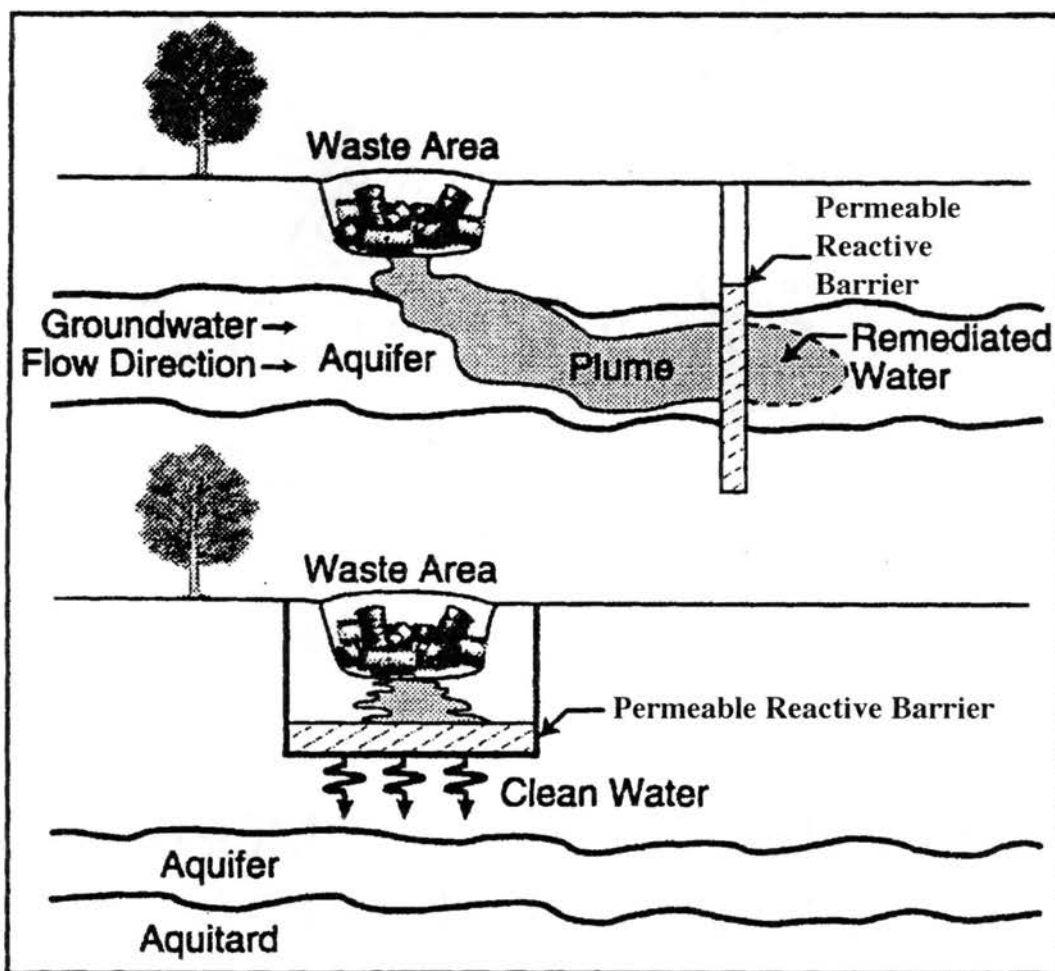


Figure 1.3: Typical Representation of Permeable Reactive Barriers (PRB): (a) Lateral Orientation. (b) Vertical Orientation [Adapted from S. D. Warner and D. Sorel in “Chlorinated Solvent and DNAPL Remediation”, Edited by S. M. Henry and S. D. Warner, ACS Symposium Series 837, (2003), 36-50]

In this investigation, we determined the reactivity of tungsten and molybdenum hydrogen bronzes to a variety of environmental contaminants such as chlorocarbons,

heavy metals and radionuclides. During the course of this research, other unusual and useful transformations of organic compounds were also discovered.

CONCLUSIONS

It is concluded that the hydrogen bronzes are structurally distinct compounds with hydrogen directly bonded to the oxygen atoms within the oxide framework. At low hydrogen contents, the bronzes are considered to be mixed-valence oxy-hydroxides and the structures adopted contain only $-OH$ groups. At higher hydrogen contents, $-OH_2$ groups are present and the compounds are considered as oxide hydrates.

This thesis makes an attempt to discuss the various types of chemical transformations that take place by the use of these bronzes. The next chapter discusses the synthesis and characterization of these bronzes. The remainder of the thesis will be devoted to the study of several different types of chemical transformations that might be possible utilizing these bronzes. The following three chapters discuss the reactions with chloromethanes, chloroaromatics and alkenes, respectively. The final chapter will be devoted to the study of remediation of wastewaters using these bronzes and also will discuss the feasibility of using these bronzes as PRB's for metal reduction.

REFERENCES

-
1. F. Wholer, *Ann. Chim. Phys.* (1923), 43, 23
 2. P. G. Dickens; and M. S. Whittingham, *Q. Rev., Chem. Soc.* (1968), 22(1), 30
 3. P. Hagenmuller in "*Comprehensive Inorganic Chemistry*", Vol. IV, pp 541-605
 4. P. J. Wiseman; P. G. Dickens, *J. Solid State Chem.*, (1973), 6(3), 374
 5. P. G. Dickens ; and R. H. Jarman, *J. Electrochem. Soc.*, (1981), 28(6),1390

-
6. E. M. McCarron, *J. Chem. Soc., Chem. Commun.*, (1986), 336
 7. J. B. Parise; E. M. McCarron III; and A. W. Sleight, *Mater. Res. Bull.* (1987), 22(6), 803
 8. B. Schlasche and R. Schollhorn, *Rev. Chim. Miner.*, 19, (1982) 534.
 9. M. Figlarz, *Prog. Solid State Chem.*, (1989), 19, 1.
 10. P. G. Dickens; S. J. Hibble; S. A. Kay; and M. A. Steers, *Solid State Ionics*, (1986), 20, 209
 11. O. Glemser and G. Lutz, *Z. Anorg. Allg. Chem.*, (1951), 264, 17
 12. J. J. Britill and P. G. Dickens, *Mat. Res. Bull.* (1978), 13, 311
 13. P. G. Dickens and J. J. Britill, *J. Electron. Mater.* (1978), 7, 311
 14. R. Schollhorn, R. Khulmann and O. J. Besenhard, *Mat. Res. Bull.* (1976), 11, 83
 15. J. B. Parise, E. M. McCarron and A. W. Sleight, *Mat. Res. Bull.* (1987), 22, 803
 16. P. G. Dickens, J. J. Britill and C. J. Wright, *J. Solid State Chem.* (1979), 28, 185
 17. F. A. Schroeder and H. Weitzel, *Z. Anorg. Allg. Chem.* (1977), 435, 247
 18. P. G. Dickens, A. T. Short and S. Couch-Baker, *Solid State Ionics*, (1988), 28-30, 1294
 19. B. W. Faughnan and R. S. Randall, in *Display Devices in Topics in App. Phys.* (Springer-Verlag, Berlin (1980))
 20. P. J. Shaver, *Appl. Phys. Lett.* (1967), 11, 255
 21. A. R. Berzins and P. A. Sermon, *Nature*, (1983), 303, 506
 22. R. Schollhorn, T. Schulte-Nolle and G. Steinhoff, *J. Less Common Metals*, (1980), 71, 71
 23. J. P. Marcq, G. Poncelet and J. J. Fripiat, *J. Catal.* (1984), 87, 339
 24. L. Bartha, A. B. Kiss and T. Szalay, *Int. J. of Refractory Metals and Hard Materials* (1995), 13, 77
 25. R. H. Jarman and P. G. Dickens. *J. Electrochem. Soc.*, (1982), 129, 2276
 26. T. Szalay, A. Ludanyi and B. A. Kiss, *J. Mater. Sci.*, (1987), 22, 3543

-
27. T. Szalay, *Kem. Kozl.*, (1980), 54(1), 125
 28. R. Schollhorn, R. Khulmann and O. J. Besenhard, *Mat. Res. Bull.* (1976), 11, 83
 29. S. J. Hibble, A. M. Chippindale and P. G. Dickens, *J. Electrochem. Soc.*, (1985), 2688
 30. A. Mendiboure, H. Eickenbusch, R. Schollhorn and G. Subba Rao, *J. Solid State Chem.* (1987), 71, 19
 31. McMurty, D. C.; Elton, R. O., *Environmental Progress.* 1985, 4(3), 168
40
 32. D. R. Burris, R. M. Allenking, V. S. Manoranjan, T. J. Campbell, G. A. Loraine, and B. L. Deng, *J. Environ. Eng.*, (1998),124, 1012
 33. L. Charlet, E. Liger, and P. Gerasimo, *J. Environ. Eng.*, (1998),125, 25
 34. T. L. Johnson, W. Fish, Y.A. Gorby, and P. G. Tratnyek, *J. Contaminant Hydrology*, (1998), 29, 379
 35. S. F. Ohannesin and R. W. Gillham, *Ground Water*, (1998), 36, 164

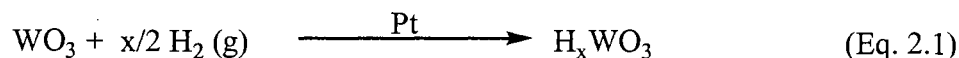
CHAPTER 2

SYNTHESIS OF TUNGSTEN AND MOLYBDENUM HYDROGEN BRONZES

BACKGROUND

The reduction of highly valent transition metal oxides with dissociated hydrogen at ambient temperatures often produces non-stoichiometric hydrogen insertion compounds called hydrogen bronzes, having the general formula H_xMO_n . The structure of the bronzes are usually derived with small changes from the structure of the parent metal oxide and the amount of hydrogen inserted depends on both the structure of the parent metal oxide and the oxidation state of the metal in the parent metal oxide. The reduction of metal oxides can take place by a variety of methods such as:

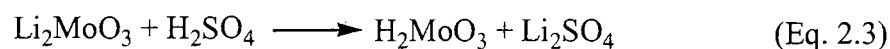
1) Hydrogen Spillover method: Hydrogen insertion takes place via heterogeneous reduction with H_2 in the presence of a noble-metal catalyst (Equation 2.1) [1- 3].



2) Dissolving Metal Reduction: Reduction occurs via nascent hydrogen generated by reaction of an active metal with an acid (Equation 2.2) [4].

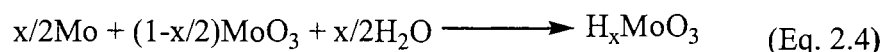


3) Ion-exchange method: Hydrogen insertion compounds are formed by ion-exchange reactions from the corresponding alkali- or hydrated alkali-metal insertion compounds (Equation 2.3) [5-7].

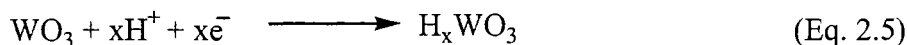


It is of importance to note that the product formed by this method retains the Li_2MoO_3 structure [7,8], and is structurally different from the bronze formed by the Zn/HCl method [9].

4) Hydrothermal synthesis [10]: Hydrogen bronzes are synthesized hydrothermally by a comproportionation reaction (Equation 2.4)



5) Electrochemical reduction in aqueous media [5,11]: In this method, hydrogen can be incorporated into oxides of tungsten [12] and molybdenum [13] by cathodic reduction in aqueous solutions (Equation 2.5). Thus hydrogen bronzes of tungsten and molybdenum are formed electrochemically from aqueous solutions of mineral acids.



Most of the preparations of bronzes are carried out under an inert atmosphere since the majority of the hydrogen bronzes are sensitive to oxygen. The hydrogen content of the bronze is determined by redox titration, thermogravimetric analysis, or from the curve of E versus x when the electrochemical method of synthesis is used. The bronzes are classified on basis of their color, crystal structure and hydrogen content. Bronzes that differ widely in their hydrogen content show different phases and are classified separately. Table 2.1 shows the classification of all known phases of tungsten and molybdenum hydrogen bronzes.

Table 2.1

Classification of hydrogen bronzes of tungsten and molybdenum

Oxide	Established Phase Range	Color	Crystal Structure
α -MoO ₃	0.2<x<0.43	Blue	Orthorhombic
	0.85<x<1.03	Blue	Monoclinic
	1.55<x<1.72	Red	Monoclinic
	x = 2	Green	Monoclinic
WO ₃	0.09<x<0.16	Dark blue	Tetragonal A
	0.31<x<0.5	Dark blue	Tetragonal B
	0.51<x<0.6	Dark blue	Cubic

The blue orthorhombic phase (0.2<x<0.43) of molybdenum bronze and the dark blue, tetragonal B phase (0.31<x<0.5) of tungsten bronze were used as reagents for the experiments reported within this thesis.

Most methods of synthesizing bronzes, discussed above, involved the use of high temperatures, corrosive reagents and vigorous conditions. Recent research has focused on exploring simple means of inserting hydrogen into transition metal oxides such as MoO₃ and WO₃. P. G. Dickens *et al* [14] suggested that any reducing couple with $E^0 < 0.34$ V should, in principle, reduce the above mentioned oxides and hence mild reducing agents could be employed for the reduction. Alcohols and glycols are excellent reducing agents for the preparation of metal particles from their salts[15]. Ayyappan *et al* [16] reported the successful synthesis of the transition metal bronzes by using alcohols and glycols as

reducing agents. In our research we extended this study further by carrying out synthesis by using a series of alcohols, the results of which are discussed in this chapter

EXPERIMENTAL

All reagents were commercial grade (ACS Reagent grade or higher) and were used without further purification. X-ray powder diffraction (XRD) patterns were recorded on a Bruker AXS D-8 Advance X-ray powder diffractometer using copper K_{α} radiation. Quantitative standards for determination of percent composition of molybdenum hydrogen bronze (MB) were prepared by mixing carefully weighed amounts of MoO_3 and MB. Crystalline phases were identified using a search/match program and the PDF-2 database of the International Centre for Diffraction Data (ICDD) [17].

Thermogravimetric studies (TGA) were performed using 10-20 mg samples on a Seiko ExStar 6200 TGA/DTA instrument under a 50 ml/min flow of dry air. The temperature was ramped from 25°C to 600°C at a rate of $5^{\circ}\text{C}/\text{min}$. The surface areas were measured on a Quantachrome Nova 1200 surface area analyzer via nitrogen adsorption isotherms, using the BET method and six points in the range of 0.05 to 0.30 P/P_0 .

Screening tests using various alcohols for synthesis of molybdenum hydrogen bronzes

A 2.88 g. sample of molybdenum trioxide (MoO_3) and alcohol were mixed in a 1:20 ratio in a 100 ml glass media bottle. The bottle was sealed and placed in a furnace at 120°C for 24 hours. The bottle was then removed from the furnace, cooled to room temperature and the mixture was filtered through a $45\mu\text{m}$ nylon membrane filter. The solid was collected, dried in a vacuum oven and the composition was determined by X-ray powder diffraction.

Preparation of Molybdenum Bronze

A round bottom flask was charged with 30.00 g of MoO_3 , 300 ml of n-butanol and 5 ml of concentrated HCl. The mixture was refluxed for 6 hours at which time it had turned a very dark blue color. At this point, the reaction mixture was cooled to room temperature and was filtered through a fine sintered-glass filter funnel. The dark blue solid was washed with n-butanol and was then dried in a vacuum oven at room temperature. The yield was 29.50 g (98% \pm 0.2). The XRD pattern of the product corresponded to that of $\text{Mo}_2\text{O}_5(\text{OH})$ in the ICDD data base.

Preparation of Tungsten Bronze

Tungsten trioxide (30.0 g) and 56.8 g of granular zinc metal, 5 ml of water, and a large stirring bar were placed in a 1000 ml filtration flask. A paraffin oil-filled bubbler was attached to the flask's hose connector with a short length of Tygon tubing. Next a dropping funnel containing 200 ml of concentrated hydrochloric acid was placed in the mouth of the flask using a one-hole rubber stopper to make an air-tight connection. The flask was then placed in a water bath and the hydrochloric acid was added drop-wise to the magnetically-stirred reaction mixture (caution must be exercised with this reaction since it vigorously evolves hydrogen gas, an explosion hazard). The yellow solid rapidly turned blue. After the HCl addition was complete and hydrogen evolution had stopped, the reaction mixture was filtered through a 45 μm nylon membrane filter and was thoroughly washed with water. After drying in a vacuum oven at room temperature the yield of dark royal blue solid was 30.5 g (99% \pm 0.2) (the excess mass is due to hydration of the product). The XRD pattern of the product corresponded to that of $\text{W}_3\text{O}_9(\text{OH})$ in the ICDD data base.

Reactions between molybdenum hydrogen bronze and alcohols

Reactions between molybdenum hydrogen bronze and alcohols were performed in teflon-lined stainless steel bombs using an excess of the blue reagent (2.5 g) and 0.25 g of the alcohol at 150⁰C, under autogenous pressure. The amount of reactants and products in the reaction mixtures were determined by cooling the bombs, sampling the headspace with a gas-tight syringe, and analyzing by gas chromatography/mass spectroscopy. Compounds were identified by comparison of their mass spectra to the NIST database. Product identity was confirmed by measuring the retention times of authentic samples of the compounds identified by mass spectroscopy.

RESULTS AND DISCUSSION

This study utilized a series of test reactions between MoO₃ and a variety of alcohols in order to determine the effectiveness of the alcohols for the production of the bronze. The alcohols used in this study were methanol, ethanol, propanol, *isopropanol*, butanol, *isobutanol*, *secbutanol*, *tertbutanol*, 3-methyl-1-butanol, allyl alcohol and benzyl alcohol. The reactions were carried out at 120⁰C for 24 h in order to limit the conversion of MoO₃ to the molybdenum bronze to less than 25%. In this fashion, the rate of the redox reactions were approximated by the initial slopes method. The extent of conversion of MoO₃ to molybdenum bronze was determined by X-ray powder diffraction using the areas of one X-ray reflection due to MoO₃ ($2\theta = 25.10^{\circ}$ A) and one due to molybdenum bronze ($2\theta = 26.10^{\circ}$ A). A calibration curve (Figure 2.1) was constructed using the raw data presented in Table 2.2, for six different standards.

Table 2.2

XRD data for various MoO₃ :Molybdenum bronze (MB) mixtures

MoO ₃ :MB	MoO ₃ area	MB area	Ratio MoO ₃ /MB
80:20	21.21	75.36	0.28
75:25	25.54	57.23	0.45
60:40	26.63	29.11	0.92
50:50	46.69	33.72	1.38
60:40	48.85	24.70	1.98
20:80	48.95	19.42	2.52

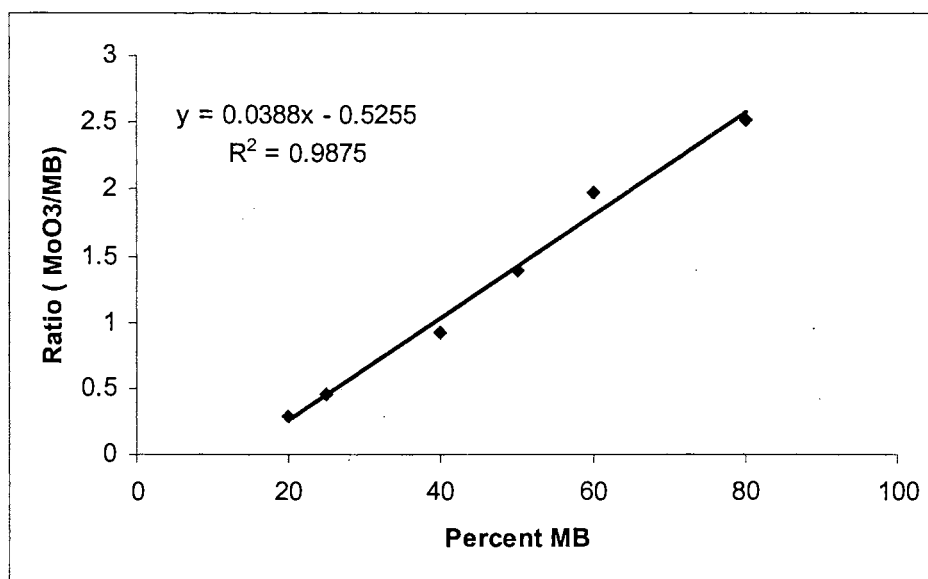


Figure 2.1: (Graph1) Graph of Percent MB Vs. Ratio ($Area_{MoO_3} / Area_{MB}$)

The ratio of the areas of the two peaks was used rather than the raw areas to eliminate errors due to sample size or placement in sample holder. Using the linear fit to the calibration curve, the amount of molybdenum bronze in the products obtained from the

reaction of MoO₃ with alcohols could be calculated using Equation 2.6. The results are given in Table 2.3

$$\% \text{ Molybdenum Bronze} = (\text{Ratio of Areas} + 0.5255) / 0.0388 \quad (\text{Eq. 2.6})$$

Table 2.3
Percentage of bronze produced from alcohols

Alcohol	Percentage Molybdenum Bronze Produced
Methanol	0
Ethanol	13.6
Propanol	15.7
<i>iso</i> Propanol	0
Butanol	21.7
<i>iso</i> Butanol	3.8
<i>sec</i> Butanol	0
<i>tert</i> Butanol	0
3-Me-1-butanol	13.6
Methoxyethanol	12.8
Allyl Alcohol	14.6
Benzyl alcohol	19.4

All of the primary alcohols with the exception of methanol were effective in the synthesis of the bronze with butanol giving the greatest yield of the bronze. The failure of *tert*-butanol to reduce MoO₃ is not surprising since it contains no α -hydrogen atoms. The lack of reaction of *isopropanol* and *sec*-butanol with MoO₃ indicates considerable steric

constraints on the redox reaction. Indeed, iso-butanol with a methyl branch on the β -carbon was also ineffective for the synthesis of molybdenum bronze. Only when the methyl group is introduced into the gamma position (as in 3-Me-1-butanol) does it not interfere with the bronze production. The ability of alcohols to reduce MoO₃ likely involves a carbocation mechanism in which a hydride ion is first extracted. In order to gain a better understanding of the hydrogen insertion process, the alcohols (filtrate) obtained on the reaction between MoO₃ and alcohols were analyzed. Aldehydes were found to be the major products. The results of the analysis are given in Table 2.4.

Table 2.4
Analysis of alcohol used in molybdenum bronze synthesis

Alcohol	Major Product	Minor Product
Propanol	Propanaldehyde (95%)	Di- <i>iso</i> -propylether, di- <i>n</i> -propyl ether, <i>isopropyl</i> -propylether (5%)
Butanol	Butyraldehyde (96%)	Sec-butylether, dibutylether, isobutyl-butylether (4%)
Benzylalcohol	Benzaldehyde (95%)	Dibenzyl ether (5%)

The aldehydes are observed as the oxidation products but small amounts of ethers are also observed. It was suspected that the hydrogen bronze catalyzed the conversion of the alcohols to the ethers. This was confirmed by separate experiments between the bronze and alcohols (Table 2.5).

Table 2.5**Results of reaction between molybdenum bronze and alcohols**

Alcohol	Major Product	Minor Product
Propanol	di- <i>isopropyl</i> ether (95%)	<i>Isopropyl-propyl</i> ether (4%), di-propyl ether (1%)
Butanol	di- <i>secbutyl</i> ether (97%)	di-butyl ether (3%)
Benzyl alcohol	di-benzyl ether (99%)	

Note, that the major ether products from butanol and propanol have undergone a rearrangement of the alkyl groups from primary to secondary moieties. This suggests a carbocation mechanism. Also, the fact that both the alkyl groups are rearranged in the major ether products suggests that the isomerization of alcohols occurs prior to condensation to the ether. Both results indicate a possible Brønsted acid catalyzed mechanism that is shown in Figure 2.2 for propanol. The preponderance of diisopropyl ether suggests that isomerization of the alcohol occurs more rapidly than ether formation so that the dipropyl ether and propyl isopropyl ether are formed only in small amounts in the early part of the reaction.

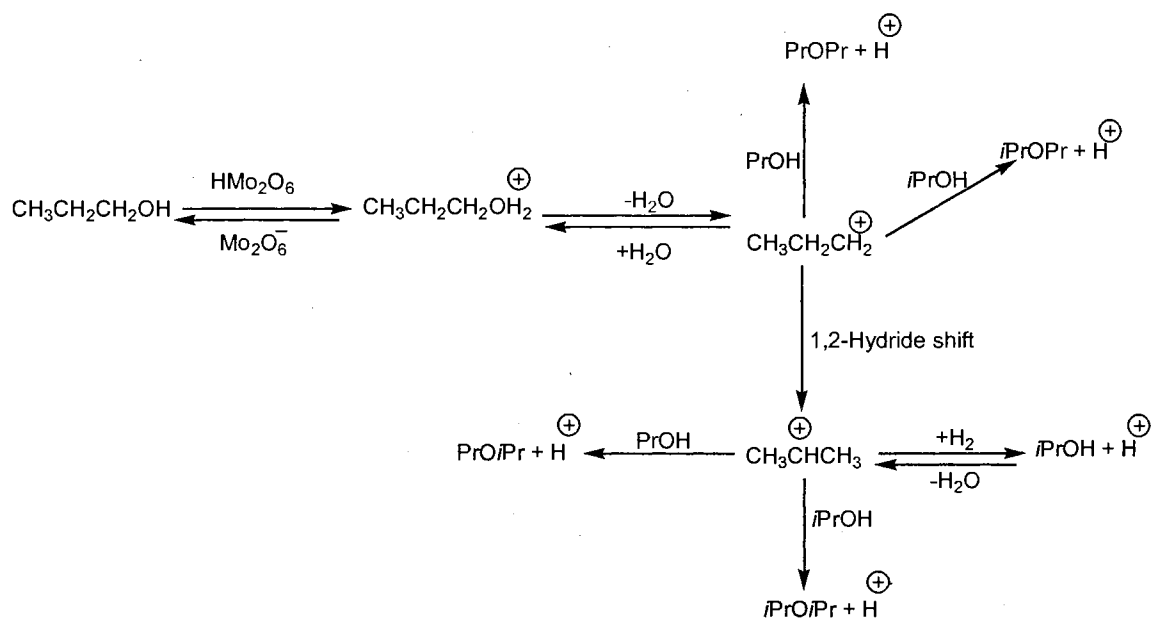


Figure 2.2: Proposed Mechanism for Reaction of Alcohols with Molybdenum Blue

The formation of ethers in the interaction of the molybdenum hydrogen bronze with the alcohols suggests that the bronze has considerable acidity. This possibility was tested by the reaction of acetonylacetone with molybdenum hydrogen bronze. The interaction of acetonylacetone with both acids and bases is shown on Figure 2.3. It produces 2,5-dimethyl furan on reaction with an acid and 3-methylcyclopent-2-ene-1-one on reaction with a base. Therefore, based on the products obtained, it can readily be determined whether the reaction is acid catalyzed or base catalyzed [18].

Acetonylacetone on interaction with molybdenum hydrogen bronze produces 2,5-dimethyl furan as the product establishing the fact that molybdenum hydrogen bronze possesses considerable acidic character. Reaction of the bronze with fluorescent pH indicating dyes established that the surface acidity of the molybdenum hydrogen bronze was less than 0 based on the change in fluorescence of Eosin Y from green to non-fluorescent when adsorbed on molybdenum bronze [19].

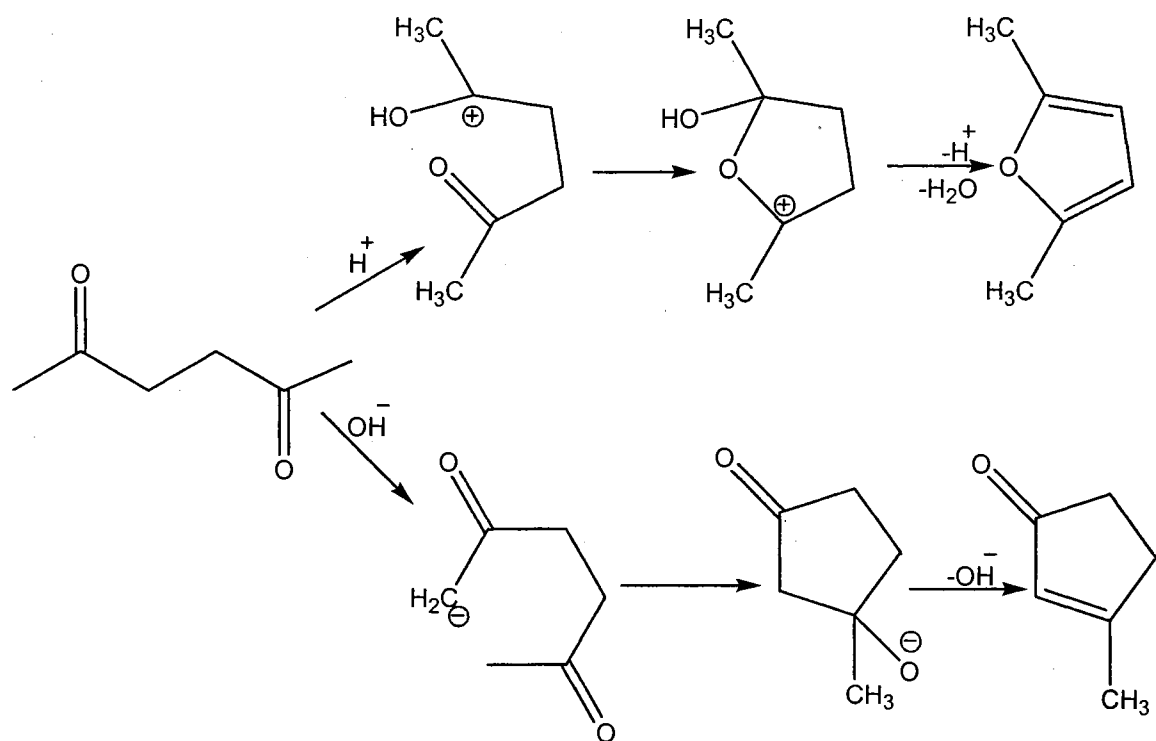


Figure 2.3: Interaction of acetylacetone with acids and bases

The reaction of alcohols with MoO_3 undergoes a lag period with very little or no blue coloration present and undergoes rapid acceleration once the blue becomes visible.. This suggests an autocatalytic effect in which the molybdenum bronze catalyzes the alcohol/ MoO_3 reaction. In keeping with its acidity, this likely occurs through protonation of the alcohol by the bronze. A test of this hypothesis using HCl as an acidic catalyst showed that all primary and secondary alcohols rapidly reduced MoO_3 under acidic conditions. Once butanol was established to be the best alcohol for the synthesis of the bronze, bulk synthesis of the bronze was carried out as described earlier. Using catalytic amount of acid enabled rapid conversion of MoO_3 to the bronze within 6 hours in 98% yield. Tungsten hydrogen bronze was not obtained on reaction of tungsten trioxide with alcohols under the reaction conditions used for these investigations, hence the tungsten

hydrogen bronze was prepared from zinc/HCl mixture was described earlier in experimental section.

CHARACTERIZATION OF THE BRONZES

The tungsten and molybdenum hydrogen bronzes synthesized were characterized by X-ray powder diffraction, infrared spectroscopy, thermogravimetric analysis and scanning electron microscopy. The BET surface areas of the bronzes were determined by nitrogen adsorption methods

BET Surface Area Analysis

The specific surface area of the molybdenum hydrogen bronze synthesized was 22.21 m²/g (\pm 0.01 m²/g) and that of tungsten hydrogen bronze was 20.45 m²/g (\pm 0.01 m²/g) using 9 measurements for 9 independently synthesized samples.

X-ray Powder Diffraction

The X-ray powder diffraction pattern of the molybdenum hydrogen bronze obtained from butanol matched that of Mo₂O₅(OH) in the ICDD database (ICDD # 14-0041). A similar pattern was obtained for the molybdenum hydrogen bronze synthesized from zinc/HCl.

The X-ray pattern of tungsten hydrogen bronze synthesized from zinc/HCl corresponded to the pattern of tetragonal W₃O₉(OH) in the ICDD database (ICDD # 23-1449).

Infrared Spectroscopic Data: The infrared spectral data was obtained using KBr pellets.

The data is as follows:

Mo₂O₅(OH) (KBr/ cm⁻¹): 3450cm⁻¹ (w), 998 cm⁻¹ (m), 857 cm⁻¹ (m), 572 cm⁻¹ (s)

W₃O₉(OH) (KBr/ cm⁻¹): 3325 cm⁻¹ (w), 1263 cm⁻¹ (s), 890 cm⁻¹ (m), 425 cm⁻¹ (w)

Thermogravimetric Analysis: Dickens and coworkers [20] studied the thermochemistry of the bronzes and found that they lose hydrogen and water fairly easily in vacuum and at relatively low temperature. Orterstag and Collins [21] reported that the bronzes decompose between 470K and 670K. Our experiments confirm the above results for the decomposition range for both tungsten and molybdenum bronze.

Scanning Electron Microscopy (SEM): The morphology of the tungsten and molybdenum hydrogen bronzes prepared were studied by SEM. SEM images of MoO_3 and molybdenum bronze are shown in Figure 2.4 (A) and 2.4 (B) respectively. The images show that original size and morphology of the parent oxide are maintained in the bronze. The hydrogen intercalation reaction therefore proceeds without reconstruction of the parent oxide. This might suggest that reduction with alcohol takes place at the outside edges and the electrons and the hydrogen atoms are shunted inwards as the reduction proceeds. This could account for the fact that partial reduction gives only mixtures of MoO_3 and HMo_2O_6 with no intermediate reduced phases. SEM images of WO_3 and tungsten hydrogen bronze are shown in Figure 2.4 (C) and 2.4 (D) respectively. The bronze maintains the original size of the tungsten oxide, but the surface morphology has changed. The parent WO_3 has a fuzzy surface with many small agglomerates on the surface. In the final products these have mostly disappeared. This suggests that a dissolution/ reprecipitation reaction might have led to the growth of larger particles at the expense of smaller particles. Also, these larger particles have numerous visible stress cracks.

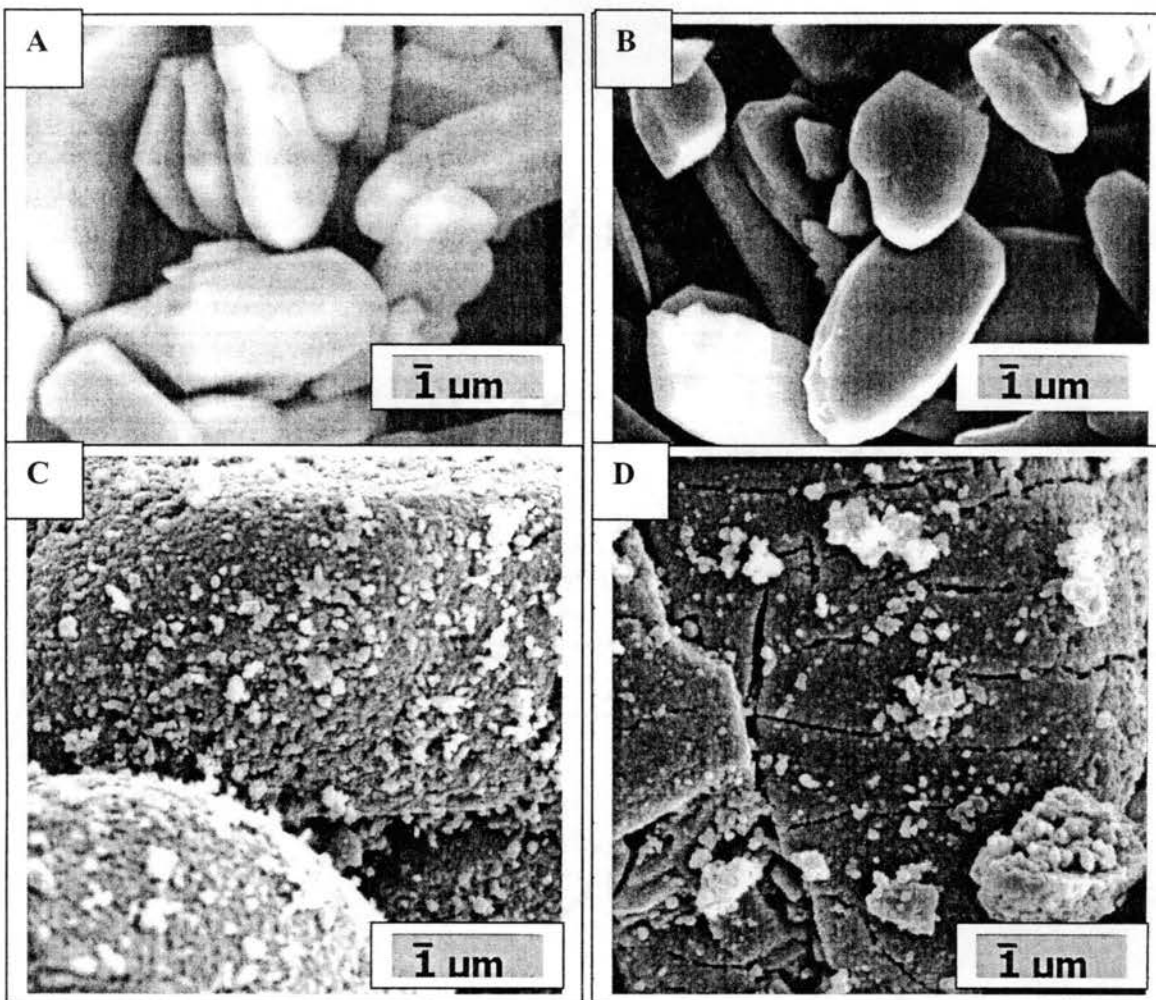


Figure 2.4: Scanning Electron Micrographs {from left to right and top to bottom} of (A) Molybdenum Trioxide (B) Molybdenum Hydrogen Bronze (C) Tungsten Trioxide and (D) Tungsten Hydrogen Bronze (SEM = 5000 × magnification)

REFERENCES

- 1 S. D. Lawrence, Part II Thesis, Department of Chemistry, Oxford University, 1984.
- 2 G. C. Bond and P. A. Sermon, *Catal. Rev.*, (1973), 8, 211.
- 3 G. C. Bond in "Spillover of Adsorbed Species", G. M. Pajonk, S. J. Teichner and J. E. Germain (eds), *Stud. Surf. Sci., Catal.*, (Elsevier)(1983), 17, 1
4. O. Glemser and C. Naumann, *Z. Anorg. Allg. Chem.*, (1951), 265, 289.
5. R. Schollhorn in *Intercalation Chemistry*, M. S. Whittingham and A. J. Jacobson (eds) (Academic Press, NY (1982)), 315.

-
6. R. Schollhorn , F. Klein-Reesink and R. Reimold. *J.Chem. Soc., Chem. Commun.* (1979), 399.
 7. J. Gopalakrishnan and V. Bhatt, *Mat. Res. Bull.*,(1987), 22 ,769.
 8. A. C. W. P. James and J. B. Goodenough, *J. Solid State Chem.*, (1988), 76, 87.
 9. J. B. Parise, E. M. McCarron and A. W. Sleight, *Mat. Res. Bull.*, (1987), 22, 803.
 10. J. J. Birtill, *D. Phil. Thesis*, Oxford University, (1977)
 - 11 M. T. Weller and P. G. Dickens, *Solid State Ionics*, (1983), 9-10, 1081
 12. B. W. Faughnan; R. S. Crandall; and P. M. Heyman, *RCA Rev.*, , (1975) , 36, 177
 13. R. Schollhorn, R. Kuhlmann and J. O. Besenhard, *Mat. Res. Bull.*, (1976), 11, 83.
 14. P. G. Dickens and A. M. Chippindale in *Proton Conductors* (Ed. Ph. Columban) Cambridge University Press, 1992.
 15. C. N. R. Rao, *Chemical Approaches to the Synthesis of Inorganic Materials*, John Wiley, Chichester, 1994.
 16. S. Ayyappan and C. N. R. Rao, *Mater. Res. Bull.*, (1995), 30(8), 947
 17. "Powder Diffraction File (PDF-2)" (International Centre for Diffraction Data, Newtown Square, PA).
 18. R. M. Dessau, *Zeolites*, (1990), 10, 205
 19. Lange's Handbook of Chemistry, 14th Edition, Section 8, Table 8.25; G. F. Kirkbright, " *Fluorescent Indicators*," Chap. 9 in *Indicators*, E. Bishop (Eds.), Pergamon Press, Oxford, (1972)
 20. P. G. Dickens, J. H. Moore and D. J. Neild, *J. Solid State Chem.* (1973), 7(2), 241
 21. W. Orterstag and C. V. Collins, *Mater. Res. Bull.*, (1967), 2, 217

CHAPTER 3

REACTION OF CHLOROMETHANES

INTRODUCTION

Cleavage of the carbon-halogen bond is of importance from a fundamental as well as a practical point of view. The cleavage of this bond has played a major role in elucidation of the mechanism of organometallic transformations, particularly oxidative addition to transition metal centers [1]. The formation of Grignard reagents, which has been a mainstay of organic synthesis for over half a century takes place by cleavage of a carbon-halogen bond [2]. From a practical point of view, breaking of the carbon-halogen bond, particularly the carbon-chlorine and the carbon-bromine bond is important since these compounds are generally toxic and carcinogenic in nature [3]. Most of the major classes of erstwhile pesticides that persist in the environment are chlorocarbons [4]. The most common chemical warfare agent, mustard gas (MD) is also a chlorocarbon [4]. Chlorofluorocarbons also play a major role in the destruction of the ozone layer. The cleavage of the carbon-halogen bond can be accomplished by the use of reducing reagents. Therefore, such agents can play an important role in the destruction of environmental contaminants such as freons, chlorinated solvents, and chlorinated pesticides.

The reductive transformation of chlorocarbons occurs via a number of processes. One interesting method of chlorocarbon reduction involves the passing of chloroorganics or CFCs through a packed bed of powdered sodium oxalate, $(\text{COONa})_2$, at 270 to 290°C

[5]. The generated reaction products are NaCl (as well as NaF in the case of CFCs), CO₂, and elemental carbon. Another approach for the reductive transformation of chlorocarbons involves the use of base metals. For example, Gillham and co-workers reported the degradation of halocarbons in groundwater in the presence of galvanized steel, stainless steel, aluminum, and iron [6]. Tratnyek and co-workers reported the reduction of chlorinated methanes by iron metal [7]. Further investigation indicated that increasing the clean surface area of iron increased the rate of degradation and that increasing the pH decreased the rate of degradation. Additionally, active metals such as sodium, zinc, or aluminum are highly reactive with chlorocarbons [8]. They operate by dechlorinating the chlorocarbon, producing a metal salt. This is highly advantageous in that the metal salt can be precipitated out of solution to allow for easy disposal of this solid waste. Unfortunately, these metals are highly reactive (in some cases, explosively) with water and air.

During an investigation of molybdate-based nucleophilic catalysts for hydrolytic dechlorination of chlorocarbons [9-12], a different type of reducing agent was discovered. In the course of this study, the use of solvents other than water was investigated as a means of enhancing the solubility of chlorocarbons and, thus, their interaction with heterogeneous and homogeneous catalysts. It was discovered that, the interaction of molybdenum trioxide and carbon tetrachloride in ethanol had a lengthy lag period in which chloride generation was gradual and the organic product was diethyl carbonate. However after 18 hours at 100°C, chloride generation accelerated by a factor of 50 and the organic product was found to be chloroform. Concomitant with this alteration in the dechlorination reaction was a change in color of the solid catalyst from white to blue. Subsequent analysis by X-ray powder diffraction and follow-up

experiments has shown the molybdenum trioxide had been converted to molybdenum blue, $\text{Mo}_2\text{O}_5(\text{OH})$ via an oxidation/reduction reaction with ethanol. This reaction is catalyzed by hydrochloric acid produced in the initial dechlorination process. These results prompted an investigation of the ability of molybdenum blue to react with chlorocarbons such as carbon tetrachloride, chloroform, and dichloromethane. These experiments and those of the related tungsten blue are reported herein.

EXPERIMENTAL

Hydrogen bronzes of tungsten and molybdenum were prepared according to the procedures given in Chapter 2. X-ray powder diffraction (XRD) patterns were recorded on a Bruker AXS D-8 Advance X-ray powder diffractometer using copper K_α radiation. Gas chromatographic/mass spectroscopic analysis (GC/MS) was performed on a Hewlett Packard G1800A instrument equipped with 30 m x 0.25 mm HP5 column (Crosslinked 5% PhME silicone). The temperature program used was an initial hold of 2 min at 35°C, a ramp of 5°C/min to 170 °C, and a final hold of 5 min. The helium flow rate was 1 ml/min and the injection port was set at 250°C.

Dechlorination Reactions

Reactions between molybdenum and tungsten blue were performed in Teflon-lined stainless steel bombs using an excess of the blue reagent (2.5 g) and 0.25 g of the chlorocarbon (CCl_4 , CHCl_3 , or CH_2Cl_2). The sealed reactors were placed in a digitally-controlled oven at various temperatures under autogenous pressure. The amount of reactants and products in the reaction mixtures were determined by cooling the bombs, sampling the headspace with a gas-tight syringe, and analyzing by gas chromatography/mass spectroscopy. Compounds were identified by comparison of their mass spectra to

the NIST database. Product identity was confirmed by measuring the retention times of authentic samples of the compounds identified by mass spectroscopy.

Dechlorination Reactions using excess chlorocarbon reagent

Reactions between tungsten blue and the chloromethanes were performed in sealed glass tubes using 0.25 g. of the blue reagent and 0.25 g of the chlorocarbon (CCl_4 , CHCl_3 , or CH_2Cl_2). The sealed glass tubes were placed in an oven at 150°C under autogenous pressure. The gas chromatography/mass spectroscopy analyses of the reaction mixture were done as described above

Absorption Equilibrium Constants

Tungsten blue (4.5 g) was placed in a 4.77 ml vial which was then sealed with a screw cap MiniInert valve. A 20 ml sample of air saturated with CCl_4 , CHCl_3 , or CH_2Cl_2 was withdrawn from a container containing the liquid chlorocarbon. The needle of the syringe was inserted into a vial so that it reached as close to the bottom as possible and then the plunger was compressed rapidly so that the vial was completely flushed with chlorocarbon-saturated air. In this manner, three samples of each tungsten blue/chlorocarbon combination were prepared along with three control samples for each chlorocarbon in which empty vials were used. After 12 hours equilibration at 25°C , the headspace of the vials were sampled with a gas tight syringe and 20 μL samples were injected into a GC/MS. The concentrations of the chlorocarbons were determined from the area of the chromatogram peaks using response factors that were obtained using chlorocarbon in pentane standard solutions. In the case of methylene chloride, which co-elutes with pentane, the response factor was determined using a saturated CH_2Cl_2 sample in air and the literature value for methylene chloride's vapor pressure at 25°C . The

amount of chlorocarbon adsorbed by the tungsten blue was calculated from the difference in chlorocarbon concentrations between the sample and control vials. The equilibrium distribution constants were then calculated as the ratio of the chlorocarbon concentration per gram of tungsten blue to the equilibrium gas-phase concentration of chlorocarbon.

RESULTS AND DISCUSSION

The reaction of molybdenum blue, $\text{Mo}_2\text{O}_5(\text{OH})$, with carbon tetrachloride at 150°C produced tetrachloroethene (PCE) as the major product. The formation of PCE is also observed in reductions of carbon tetrachloride with iron metal and is believed to result from coupling of dichlorocarbenes to give PCE or dimerization of trichloromethyl radicals to yield hexachloroethane [13], followed by reduction to PCE. Since the interaction of $\text{Mo}_2\text{O}_5(\text{OH})$ with CCl_4 in the presence of alcohols does not produce PCE but only CHCl_3 , it is likely that the dimerization of trichloromethyl radicals is the reaction mechanism leading to PCE formation (Figure 3.1). This hypothesis is reinforced by the fact that hexachloroethane reacts with tungsten blue to give PCE as the exclusive organic product. The formation of trichloromethyl radicals on the molybdenum blue surface suggests that the first step in dechlorination is electron transfer from a $\text{Mo}(\text{V})$ center to CCl_4 rather than hydride attack on the CCl_4 . However, a condensation reaction between the $\text{Mo}^{\text{V}}\text{-OH}$ linkage to yield what is essentially a trichloromethoxide ion attached to a $\text{Mo}(\text{V})$ center is also a possibility that cannot be ruled out. Whatever the first step, it is apparent that hydrogen transfer to the trichloromethyl fragment to yield chloroform is much slower than the coupling reaction to yield tetrachloroethene.

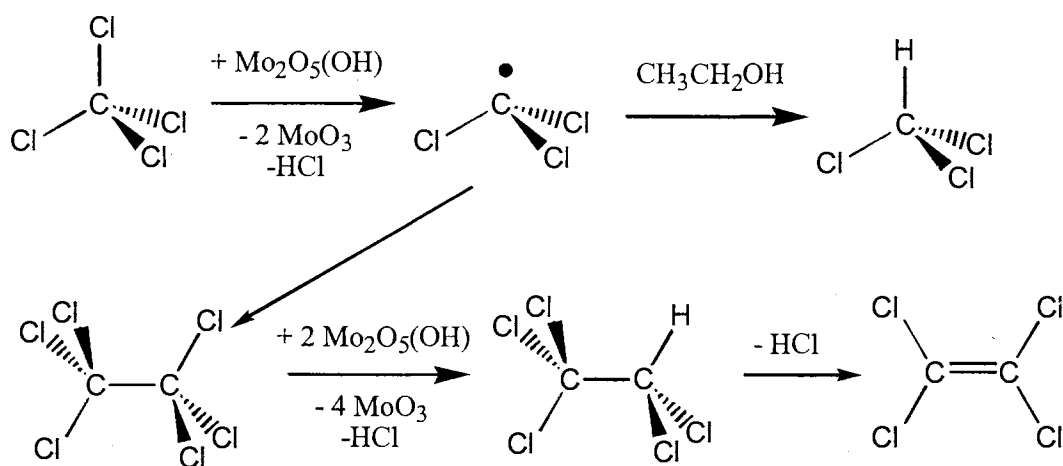


Figure 3.1: Proposed Mechanism for Reaction between CCl_4 and Molybdenum

Bronze

The formation of tetrachloroethene is unfortunate due to the fact that it is more toxic and refractory in the environment than CCl_4 . In order to avoid the radical coupling reaction, a tungsten hydrogen bronze, $\text{W}_3\text{O}_9(\text{OH})$, was used as the hydrodechlorinating reagent in place of molybdenum blue. With this substitution, carbon tetrachloride was reduced to chloroform without any detectable carbon-carbon bonded side products. The effectiveness of substitution of tungsten for molybdenum for the prevention of tetrachloroethene formation remains to be determined. It may be due to electronic factors but since the materials are structurally dissimilar (molybdenum blue has a layered structure while tungsten blue has a 3-dimensional structure with the hydrogen atoms in tunnels) steric interactions may also play a role. Kinetic factors may also influence the product distribution since the tungsten reagent is significantly more reactive towards oxidants than the molybdenum reagent.

At 150°C , the disappearance of CCl_4 was found to be exponential and was nearly complete after 24 hours (Figure 3.2(A)). A plot of the natural logarithm of the carbon

tetrachloride concentration versus time, shown in Figure 3.2(B), demonstrated that the reduction was pseudo-first-order in carbon tetrachloride and had a rate constant of $2.66 \times 10^{-3} \text{ min}^{-1}$ (from the slope of the graph). During the course of the reaction, the tungsten blue began to be converted to a yellow solid and started to display reflections in its X-ray diffraction pattern that were typical of tungsten trioxide. Infrared spectroscopy and elemental microanalysis of the spent reagent showed no build-up of organics or chloride on the tungsten blue.

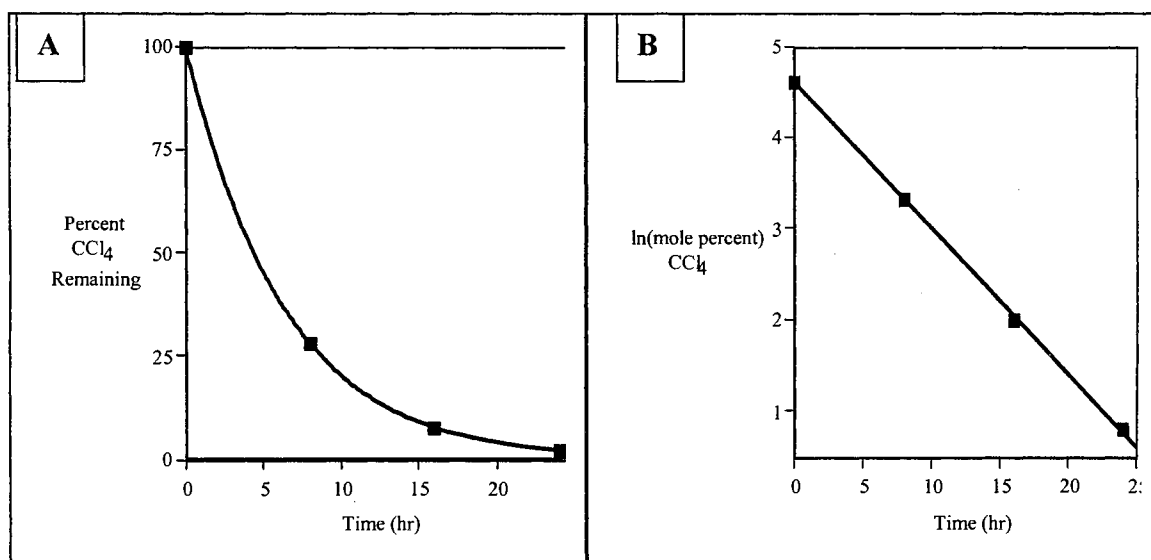


Figure 3.2: (A) Concentration of CCl₄ (mole percent) versus time for reaction with tungsten blue at 150°C. (B) First order reaction kinetics (ln of concentration versus time) for reaction of CCl₄ with tungsten blue at 150°C.

When chloroform and methylene chloride are reacted with excess tungsten bronze the organic products from these reactions are either too volatile to be observed by our GC/MS instrument or react away at a similar rate to their formation. Significantly, CH₂Cl₂ was not observed as a product from CHCl₃, under these conditions. The pseudo first order rate constants for disappearance of CCl₄, CHCl₃ and CH₂Cl₂ at 150°C with excess tungsten bronze are given in Table 3.1.

Table 3.1
Pseudo first order rate constants at 150°C

Chlorocarbon	Rate Constant (min⁻¹)
CCl ₄	2.66 × 10 ⁻³ (± 0.05)
CHCl ₃	1.93 × 10 ⁻³ (± 0.05)
CH ₂ Cl ₂	2.93 × 10 ⁻³ (± 0.05)

The pseudo first order rate constants for disappearance of CHCl₃ and CH₂Cl₂ at 150°C are 1.93x10⁻³ (± 0.05) min⁻¹ and 2.93x10⁻³ (± 0.05) min⁻¹, respectively. The two rate constants are close enough to each other to expect that if methylene chloride was formed, its steady state concentration would have been detectable providing that both chlorocarbons have similar adsorption equilibria with tungsten blue (see below). Also, it is notable that the rate constant for the methylene chloride reaction is higher than that of chloroform. This is opposite what is observed in iron-mediated reduction of chloromethanes in which carbon tetrachloride is sequentially dechlorinated via chloroform to methylene chloride (3). For these iron reductions, the initial rate of each reaction step became substantially slower with each step so that carbon tetrachloride

typically disappeared in several hours but no significant reduction of methylene chloride was observed after one month. These dissimilarities are suggestive of different solid-state reaction mechanisms (including adsorption equilibria) for the $W_3O_9(OH)$ reactions with $CHCl_3$ and CH_2Cl_2 . In order to try to shed some light on the mechanism of the chloroform reaction, deuteriochloroform was used as a substrate to see if there was an isotope effect. It was found that $CDCl_3$ reacted at the same rate as $CHCl_3$ and this absence of an isotope effect demonstrates that the cleavage of the C-H bond is not involved in the activated complex of the rate-determining step. Therefore, a possible mechanism where the hydrogen is abstracted leading to formation of dichlorocarbene in the rate-limiting step may be ruled out. The absence of an isotope effect however prompted carrying out the dechlorination reactions with an excess of halocarbon so that the initial halocarbon can effectively compete to adsorption and reactive sites on the bronze. In this manner, CH_2Cl_2 was found in the reaction products from $CHCl_3$ and CH_3Cl was detected in the CH_2Cl_2 reaction. CCl_4 was found to dechlorinate sequentially as $CCl_4 \Rightarrow CHCl_3 \Rightarrow CH_2Cl_2 \Rightarrow CH_3Cl$, eventually producing methane.

The apparent activation energies for the reactions of methylene chloride, chloroform and carbon tetrachloride with tungsten blue were determined by measuring the pseudo first order rate constants for three temperatures over a range of temperatures from 140-170°C. An Arrhenius plot of $\ln k$ versus $1/T$ yielded straight lines with slopes that corresponded to activation energies of 104 kJ/mol and 122 kJ/mol for $CHCl_3$ and CCl_4 , respectively. Table 2 shows the apparent activations energies for the chlorocarbons used in this study.

Table 3.2**Apparent Activation Energies of Chlorocarbons**

Chlorocarbon	Activation Energy (kJ/mol)
CCl ₄	122 (± 0.5)
CHCl ₃	104 (± 0.5)
CH ₂ Cl ₂	-12.6 (± 0.5)

Methylene chloride was actually found to react faster at lower temperatures and thus displayed a negative apparent activation energy. This occurs in heterogeneous reactions when the adsorption enthalpy, a negative number, is higher in magnitude than the true activation energy for the rate-controlling reaction step. In this situation, the apparent activation energy (equal to the sum of the adsorption enthalpy and the true activation energy) becomes negative. This means that adsorption equilibria play an important role in the tungsten blue/chlorocarbon reactions. For this reason, the equilibrium adsorption constants for CH₂Cl₂, CHCl₃ and CCl₄ on tungsten blue were determined by equilibrating chlorocarbon-saturated air with tungsten blue. The results of this characterization are presented in Table 3 and the constants are reported both in terms of per gram of catalyst and per unit surface area (the specific surface area of the tungsten blue was found to be 20.43 m²g⁻¹).

Table 3.3**Adsorption Data for Chlorocarbons onto Tungsten Blue at 25^oC**

Chlorocarbon	Surface Concentration (mmol/m ²)	Gas Phase Concentration (mmol/L)	K _D (L/m ²)	K _D (L/g)
CH ₂ Cl ₂	0.0297	4.21	7.05 × 10 ⁻³	0.144
CHCl ₃	7.30 × 10 ⁻⁵	2.81	2.60 × 10 ⁻⁵	5.31 × 10 ⁻⁴
CCl ₄	9.67 × 10 ⁻⁵	1.42	6.83 × 10 ⁻⁵	1.40 × 10 ⁻³

It was determined that the adsorption constants for CHCl₃ and CCl₄ were comparable to each other with the latter chlorocarbon having a slightly higher (2.6 times) adsorption constant. The higher adsorption constants for the more chlorinated compound is in keeping with Van der Waals forces being primarily involved in binding the chlorocarbons to the tungsten blue surface. By comparison, the K_D for adsorption of CCl₄ onto UO₂, calculated from Stakebake and Goad's data [14], is 5.10 × 10⁻³ L/m². However, this result is for CCl₄/UO₂ equilibria in the absence of air, so the lower value found in this study is not unexpected. In this experiment, the surface coverage by CCl₄ is much less than a monolayer (2.15%) based on the theoretical area of CCl₄ being 37 Å². It is quite likely that the CCl₄ occupies specific sites on the tungsten blue in accordance with Machin's observation that CCl₄ is adsorbed onto metal oxides in a localized manner and is dependent on the adsorbent structure [15]. Interestingly, methylene chloride has a much higher adsorption constant onto tungsten blue as compared to chloroform and carbon tetrachloride. The stronger binding of methylene chloride to tungsten blue is in

agreement with the observation of negative activation energy for the reaction between the two materials. More importantly, the fact that K_D for CH_2Cl_2 is 271 times that of CHCl_3 can explain why methylene chloride is not observed in the reduction of chloroform in presence of excess bronze. The higher binding of CH_2Cl_2 would allow it to be preferentially reduced providing that both chlorocarbons were competing for the same binding sites. Since the rate constant for the CH_2Cl_2 is greater than the rate constant for CHCl_3 , the steady state concentration of CH_2Cl_2 is low when the reaction of CHCl_3 is carried out using a large excess of tungsten blue. This also explains why CH_2Cl_2 is not observed in the reduction of CHCl_3 , when using excess reagent.

Mechanistic Studies

The reaction of carbon tetrachloride with tungsten bronze was chosen as a model reaction by which an attempt was made to propose a mechanism for the reaction. In order to predict a mechanism for the dechlorination reactions with tungsten bronze, it became necessary to take stock of the experimental evidence gathered so far:

- 1) Reactions carried out by varying the amount of tungsten bronze and varying CCl_4 concentrations establish the process to be first order in both reactants, thus the rate law can be given by $\text{rate} = k(\text{Tungsten bronze})(\text{CCl}_4)$
- 2) The only direct product observed for the reduction of CCl_4 is CHCl_3 , and is typical of the product derived from free organic radical intermediates. Similar reactivity has been observed in the reactions between alkyl halides and polyoxotungstates. Some of the reduced polyoxotungstates have been known to reduce organic radical intermediates to carbanions in solvents such as acetonitrile [16].

3) The best evidence for the presence of radical intermediates in dechlorination reactions can be obtained by trapping the intermediates with a variety of radical scavengers. However, no significant information could be obtained since in all cases tried, reaction of tungsten bronze with the scavengers was faster than the reaction with CCl_4 . This was also observed in the reactions of reduced polyoxotungstates with alkyl halides [17].

In an earlier research by Sattari and Hill [18], the fate of such radicals was determined by carrying out a reaction between polyoxotungstates and 2-methyl-2-phenyl-1-chloropropane (commonly called neophyl chloride, CPPM). The corresponding radical, neophyl radical, is known to rearrange by a 1,2-phenyl shift to the benzyldimethylcarbinyl radical. The oxidation of this radical takes place simultaneously and results in the benzyldimethylcarbinyl carbocation, which further produces well-documented products (the major product is the thermodynamically most stable alkene). Alkyl radicals and carbocation intermediates were ruled out for dechlorinations carried out using polyoxotungstates based on these experimental results [18]. In order to find out if dehalogenations with tungsten hydrogen bronze followed a similar pathway, the reaction between CPPM and tungsten hydrogen bronze was performed under the experimental conditions used in this study. The various products obtained from this reaction are shown in Figure 3.3.

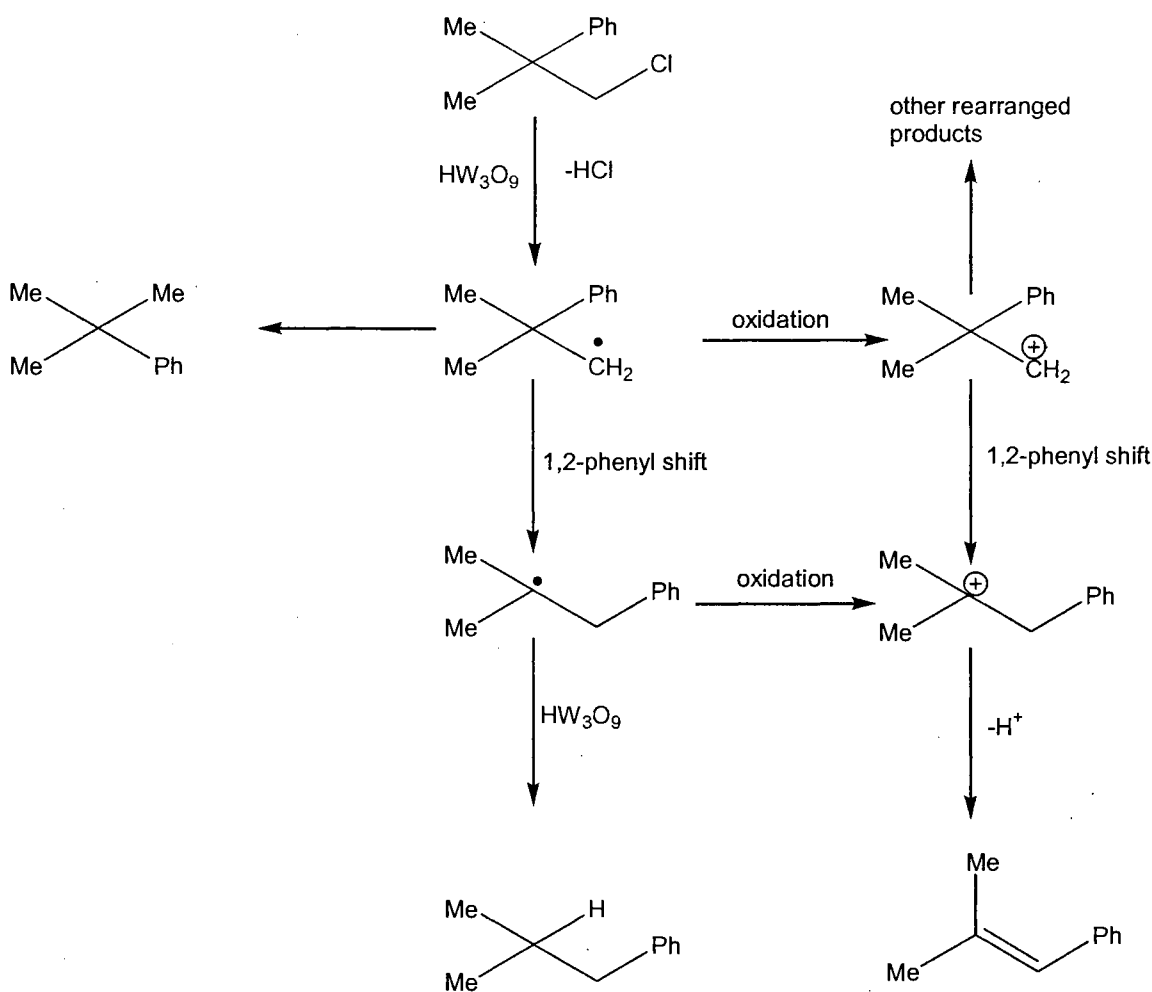


Figure 3.3: Reaction between 2-methyl-2-phenyl-1-chloropropane and tungsten hydrogen bronze

The formation of isobutylbenzene along with the most substituted alkene provides the evidence for the presence of both alkyl radicals and carbocation intermediates. Also observed are electrophilic aromatic substitution products from the reaction of carbocations with CPPM. Isomers of CPPM (species with 168 AMU parent ions and one chlorine present) are also observed by GC-MS analysis. These may be due to reactions of the alkene products with the evolved HCl. The results suggest that the initial reaction between CPPM and the bronze results in hydrodechlorination to yield the neophyl radical. This radical is subsequently oxidized by the bronze to the

carbocation. Experimental data obtained from pulse radiolysis studies [19], kinetic and product analysis studies [20] suggest that the oxidized forms of some polyoxotungstates oxidize organic radicals to carbocations at very high rates in solution.

All the data collected upto this point suggest that the reductive dehalogenation reactions proceed via the formation of radical intermediates. Generation of these species via dehalogenation reactions can proceed through two mechanisms, the electron transfer mechanism (ET) and the atom transfer process (AT). The general reaction pathway for reductive dehalogenation occurring through both ET and AT processes is shown in Figure 3.4

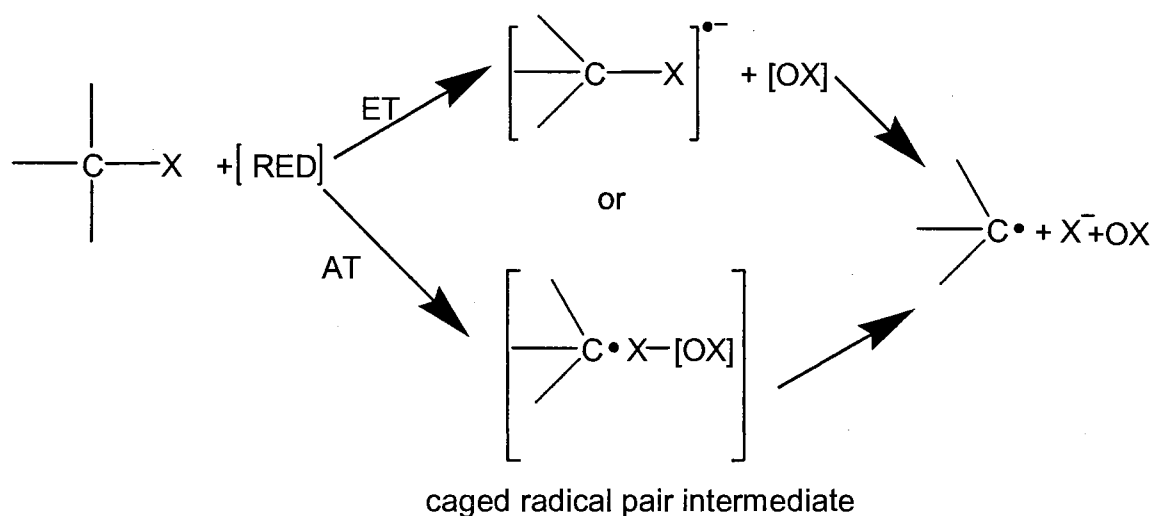


Figure 3.4: AT and ET mechanisms for reductive dehalogenations

The experimental evidence and background information available from literature do not allow us to rule out either electron transfer process or atom transfer process as operable for the dehalogenations of chloromethanes using tungsten hydrogen bronzes. The decreasing rate of dehalogenation with increasing degree of chlorination suggests an

AT mechanism. If it were ET one would expect the rate of reduction of the more easily reduced CCl_4 to be the fastest. However, more experimental information needs to be gathered to ascertain the mechanism. The best approach would be to use deuterated tungsten or molybdenum bronze to see if there is an isotope effect.

CONCLUSIONS

Molybdenum bronze was found to be unsuitable for reductive dechlorination of carbon tetrachloride in the absence of a solvent to act as a proton donor because coupling reactions dominated to produce tetrachloroethylene. Tungsten bronze, on the other hand, cleanly converted the chloromethanes according to the sequence $\text{CCl}_4 \Rightarrow \text{CHCl}_3 \Rightarrow \text{CH}_2\text{Cl}_2 \Rightarrow \text{CH}_3\text{Cl}$, eventually producing methane. Adsorption equilibria suggest that chloroform is reduced to methylene chloride but the latter compound is preferentially reduced further because of its stronger binding to tungsten bronze. The dehalogenations are fairly slow and follow a pseudounimolecular rate law, when excess of tungsten bronze is used. The carbon-halogen bond cleavage involves either halogen atom abstraction (atom transfer) or, electron transfer, which is dissociative in nature, in the rate determining step. More experiments are required to establish the exact process. These reagents show promise for reductive dechlorination reactions but the slow kinetics at ambient temperature might be restrictive for their environmental applications. Their ability to strongly adsorb chloromethanes may be a mitigating factor that would allow sufficient contact time between the reducing agent and the substrate in aquifers to allow chlorocarbon reduction to occur.

REFERENCES

1. J. P. Collaman.; L. S. Hegedus; J. R. Norton; and R. G. Finke in “*Principles and Applications of Organotransition Metal Chemistry*”, University Science Books, Mill Valley, CA; (1987), Chapter 5
2. M. S. Kharasch.; and O. Reinmuth, in “ *Grignard Reactions of Nonmetallic Substances*”, Prentic-Hill, NY, 1954
3. G. R. Lester, *Pollut. Prev.* (1991), 43
4. F. M. Menger; A. R. Erlington, *J. Am. Chem. Soc.*, (1990), 112, 8201
5. R. Crabtree; and J. Burdeniuc, *Science*, (1996), 271, 340
6. R. Gillham; and W. S. Orth, *Environ. Sci. Technol.*, (1996), 30, 66
7. P. Tratnyek; and L. J. Matheson, *Environ. Sci. Technol.*, (1994), 28, 2045
8. J. C. Dickerman.; T. E. Emmel; G. E. Harris; amd K. E. Hummel, in “*Technologies for CFC/Halon Destruction*”; EPA publication: Washington DC, 1989.
9. A. W. Apblett.; L. D. Byers; and L. E. Reinhardt, *American Chemical Society, Division of Environmental Chemistry, Preprints of Papers*, (1996), 36(2), 10
10. A. W. Apblett; L. D. Byers; and L. E. Reinhardt, *Extended Abstracts for Emerging Technologies in Hazardous Waste Management*, (1996), VIII, 724
11. A. W. Apblett; L. D. Byers; and L. E. Reinhardt, *American Chemical Society, Division of Environmental Chemistry, Preprints of Papers*, (1997), 37(1), 300
12. L. E. Reinhardt, *Ph. D. Thesis*, Tulane University, New Orleans, L A, 1997
13. H-M. Hung; and M. R. Hoffman, *Environ. Sci. Technol.* (1998), 32, 3011
14. J. L. Stakebake; and H. A. Goad, *J. Catal.* (1974), 32, 272
15. W.D. Machin, *J. Phys. Chem.* (1969), 73, 1170.
16. C. M. Prosser-McCartha; and C. L. Hill, *J. Am. Chem. Soc.*, (1990), 112, 3671
17. S. W. Benson, P. S. Nangia, *Acc. Chem. Res.*, (1979), 12, 223
18. D. Sattari and C. L. Hill, *J. Am. Chem. Soc.*, (1993), 115, 4649

19. E. Papaconstantinou, *J. Chem. Soc., Faraday Trans.*, (1982), 78, 2769

20. R. F. Renneke; M. Kadkhodayan; M. Pasquali; and C. L. Hill, *J. Am. Chem. Soc.*, (1990), 112, 3671

CHAPTER 4

REACTIONS OF BENZYLIC HALIDES

INTRODUCTION

Transition metal catalyzed dehalogenative coupling of organic halides, resulting in the formation of carbon-carbon bond is of great importance to organic chemistry [1]. These metals in low oxidation states have been extensively used as reagents for reductive coupling of benzylic halides. The earliest known coupling process to convert aromatic halides to coupled aromatic hydrocarbons utilized copper powder and was reported by Ullman in 1901 [2]. Since then, titanium [3], vanadium [4], chromium [5], tungsten [6] and nickel [7] have been used for the reductive coupling of benzylic halides. These catalysts could be prepared *in situ* by reducing the respective metal halide with strong reducing agents like lithium aluminium hydride or lithium metal in presence of naphthalene.

Metal complexes of nickel(I) [8, 9], cobalt(I) [10] and vanadium (II) [11] or metal carbonyls of nickel [12], cobalt [13], iron [14], molybdenum [15] and tungsten [6], as well as metallic iron [16] and nickel [17] have also been utilized as reagents for the reductive coupling of benzylic mono- and polyhalides. The biggest disadvantage of using most of the above coupling reagents was the moderate to low yields due to side reactions (e.g., the formation of toluene derivatives from hydrogenation of benzylic halides).

Another disadvantage was that the low-valent reagents prepared by the lithium aluminium hydride reduction of metal halides were incompatible with functional groups such as nitro or cyano. The cobalt (I), vanadium (II) complexes, and metallic iron were efficient in producing coupled products with benzylic halides, however, the examples reported were limited to only benzylic halides that did not contain nitro or cyano groups. Tungsten and molybdenum carbonyls were also reported as homocoupling reagents but their reactivity towards sensitive functional groups has not yet been reported. Tungsten carbonyls and tungsten hexachloride-lithium aluminium hydride (WCl_6 -LiAlH₄) systems have been found to cause coupling of benzylic dihalides and benzylic monohalides to give olefinic and bibenzyl derivatives, respectively [6]. Based on the experimental evidence, the reaction was believed to proceed via the formation of a carbene intermediate [6].

The dehalogenation of chlorocarbons such as carbon tetrachloride and chloroform using tungsten and molybdenum hydrogen bronzes was discussed earlier in Chapter 3. It was shown that the carbon tetrachloride reduction with tungsten hydrogen bronze produced chloroform as the major product while the reduction with molybdenum hydrogen bronze produced tetrachloroethene as the major product. Hence, tungsten bronze produced the hydrogenated product as the major product whereas molybdenum bronze produced the coupled product as the major product. The next logical step was to test the effectiveness of the tungsten and molybdenum hydrogen bronzes for the reduction of aryl halides such as benzylic mono and poly halides. This chapter addresses the results of such reactions.

EXPERIMENTAL

The molybdenum and tungsten bronzes, used here as reductive coupling agents, were prepared according to the procedures reported earlier in Chapter 2. X-ray powder diffraction (XRD) patterns were recorded on a Bruker AXS D-8 Advance X-ray powder diffractometer using copper K α radiation. Gas chromatographic/mass spectroscopic analysis (GC/MS) were carried out on a Hewlett Packard G1800A instrument equipped with 30 m \times 0.25 mm HP5 column (crosslinked 5% PhMe silicone). The temperature program followed was an initial hold of 2 min at 70°C, a ramp of 5°C/min to 270°C, and a final hold of 10 min. The helium flow was 1 ml/min. The injection port and detector were set at 250°C and 280°C respectively.

Reactions of the benzylic mono- and polyhalides with the metal bronzes

The reduction reactions were carried out in Teflon-lined stainless steel bombs using an excess of the blue reagent (2.5 g) and 0.25 g of the chloro-aromatic compound. These reactors were sealed and placed in a digitally-controlled oven at various temperatures under autogenous pressure. The amount of reactants and products in the reaction mixtures were determined by cooling the bombs, extracting with methylene chloride, sampling 1 μ l of this extract with a syringe, and analyzing by GC/MS. Compounds were identified by comparison of their mass spectra to the NIST database. Product identity was confirmed by measuring the retention times of authentic samples of the compounds identified by mass spectroscopy. For the reaction of benzyl chloride with tungsten bronze, the polymeric product obtained was purified by evaporation of the methylene chloride filtrate and redissolution in benzene, washing with water, drying over magnesium sulfate, and was finally precipitated by pouring into excess methanol. The

polymer thus precipitated was washed several times with methanol and dried in a vacuum oven. The purified polymer was used for the determination of its thermal stability, IR and elemental analysis. A polymer prepared by the reaction of benzyl chloride with FeCl₃ and was used to compare the IR data with that of the polymer prepared by using tungsten bronze.

RESULTS AND DISCUSSION

Table 4.1

Reactions Between Molybdenum Bronze and Benzylic Halides

Benzylic Halide	Product
α,α,α trichlorotoluene	Benzoic acid (100%)
$\alpha,\alpha,-$ dichlorotoluene	Benzaldehyde (100%)
benzyl chloride	Polybenzyl (100%)

Table 4.1 shows the results of the reactions between the benzylic halides and molybdenum hydrogen bronze. α,α,α trichlorotoluene produces benzoic acid exclusively whereas $\alpha,\alpha,-$ dichlorotoluene and benzyl chloride produced benzaldehyde and a polymeric product, respectively. These results suggest that molybdenum bronzes underwent substitution reactions with benzylic polychlorides to transfer a hydroxide and produce the hydrolysis products. The dehydroxylation of molybdenum bronze yielded a black solid that had a XRD pattern that did not match any known molybdenum containing phase. Dissolution in base followed by chloride analysis by ion selective electrode demonstrated a 15% chloride content. On this basis, it may be concluded that the product was a reduced molybdenum oxychloride, a previously unknown type of

molybdenum bronze. Since no coupled products were observed, the molybdenum bronzes could not be used as reagents for coupling of benzylic di- and tri- halides. However, they are effective for neutralizing these toxic compounds. Tungsten hydrogen bronze, on the other hand, reacted differently with the benzylic halides and produced coupled products, the results of which are given in Table 4.2 .

Table 4.2

Reactions Between Tungsten Bronze and Benzylic Halides

Benzylic Halide	Product
α,α,α trichlorotoluene	<i>cis</i> - and <i>trans</i> -1,2 -dichloro-1,2-diphenylethene (100%)
$\alpha,\alpha,$ - dichlorotoluene	<i>trans</i> -stilbene (77%), <i>cis</i> -stilbene (12%), 1,2-dichloro-1,2-diphenylethane (11%)
benzyl chloride	Polybenzyl (100%)

The reaction of α,α,α trichlorotoluene with tungsten hydrogen bronze resulted in the formation of a mixture of *cis*- and *trans*-1,2 -dichloro-1,2-diphenylethene (Figure 4.1). No diphenylacetylene was detected by GC/MS analysis. The *cis*- isomer was the major product and was obtained in 85% yield while the *trans* isomer was obtained in 15% yield.

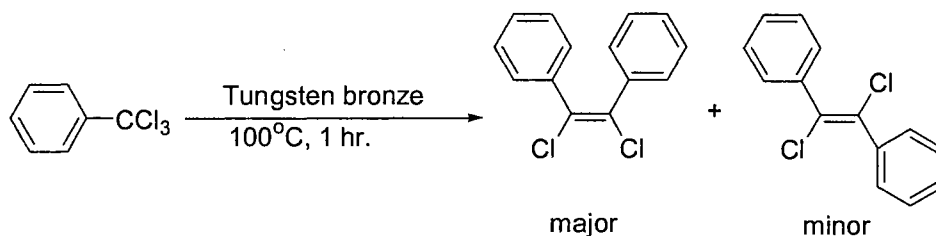


Figure 4.1: Reaction between tungsten bronze and α,α,α trichlorotoluene

The formation of the *cis* isomer suggests a surface-mediated coupling which would favor a mechanism in which the phenyl groups are facing away from the surface.

α,α -dichlorotoluene gave *cis*-stilbene as the major product in 77% yield. Small amounts of the *trans*-stilbene (12%) and 1,2-dichloro-1,2-diphenylethane (11%) were also produced in minor amounts (Figure 4.2). This result suggests that the dichloroethane derivative is formed first followed by hydrodechlorination to the stilbenes (Figure 4.3).

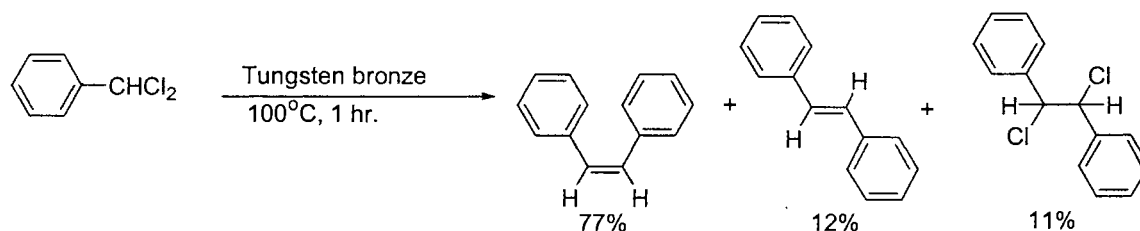


Figure 4.2: Reaction between tungsten bronze and α,α dichlorotoluene

Reductive coupling of benzylic polyhalides is known to occur either via a carbene or carbene-transition metal intermediate, or via a step-by-step dehalogenation mechanism. Coffey suggested a carbene mechanism for the reaction catalyzed by iron pentacarbonyl [14]. Later, carbenoid and carbene-transition metal complex intermediates were suggested on basis of trapping of the cyclopropane derivatives in the reaction of $\text{Ni}(\text{COD})_2$, $\text{Fe}(\text{CO})_5$, $\text{Co}_2(\text{CO})_9$ [18] or $\text{W}(\text{CO})_6$ [6] with benzylic dihalides. A step-by-step mechanistic pathway was also suggested for the reaction of benzylic polyhalides with $\text{Co}_2(\text{CO})_8$ [13] or metallic iron [19].

The reaction of α,α,α trichlorotoluene with tungsten hydrogen bronze was carried out in the presence of an excess of an electron-deficient olefin (cyclohexene) in order to attempt the trapping of a possible carbene intermediate. The formation of a cycloadduct could not be detected and hence the possibility of the reaction proceeding through a carbene intermediate was ruled out. The presence of cycloadducts could also not be detected in the reaction between tungsten bronze and α,α dichlorotoluene.

The coupling reaction between α,α,α trichlorotoluene and tungsten bronze, carried out under milder conditions (60°C , 1 hr), was found to produce 1,1-diphenyl-1,1,2,2-tetrachloroethane as the major product (70% yield). Hence, the reactions between tungsten bronze and benzylic tri-halides were believed to proceed in a stepwise manner as shown below (Figure 4.3).

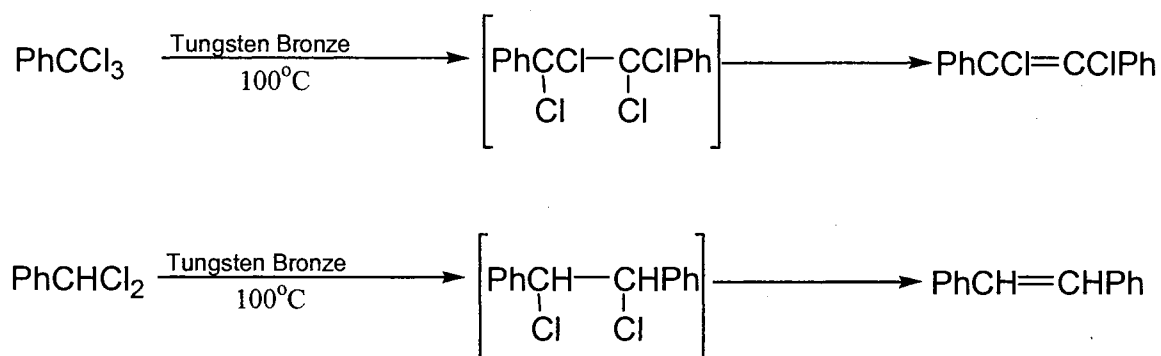


Figure 4.3: Stepwise mechanism for reaction between tungsten hydrogen bronze with α,α,α trichlorotoluene and α,α dichlorotoluene

1,2-dichloro-1,2-diphenylethane reacted with tungsten bronze at 100°C , to yield *cis*-stilbene (90% yield) and a small amount of *trans*-stilbene (10%). This result established that the second step in dehalogenation reactions of benzylic dihalides (α,α dichlorotoluene) with tungsten bronze proceeds by the sequence of reactions shown above (Figure 4.3).

The reaction of benzylic monohalides with tungsten or molybdenum bronze however did not produce bibenzyl (the homocoupled product expected) or toluene (the product expected if reduction reaction were to occur). The product actually obtained was a polymeric product, identified as para substituted benzyl polymer by infrared

spectroscopy. A similar reaction was observed on reaction of benzyl chloride with molybdenum hydrogen bronze.

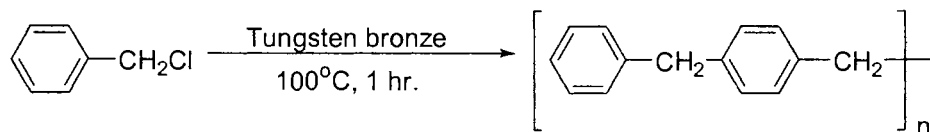
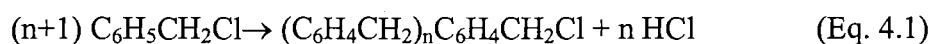


Figure 4.4: Reaction between benzyl chloride and tungsten bronze

Benzyl chloride, in presence of Lewis acid catalysts is known to undergo a self condensation reaction to produce polybenzyl with the evolution of HCl gas as shown in Equation 4.1.



The formation of polybenzyl is known to be a predominant side reaction in the various homogeneously [20, 21] and heterogeneously [22- 24] catalyzed benzylation reactions of aromatic compounds. Choudhary *et al* [24, 25] reported polycondensation reactions over Fe, Ga and In-containing solid catalysts and also studied the effect of temperature and solvent on the rate of these polycondensation reactions.

The polycondensation of benzyl chloride is believed to follow a typical Friedel-Crafts mechanism wherein the first step is the formation of a stable benzyl carbonium ion. In the second step, another molecule of benzyl chloride attacks the benzyl carbonium ion to form a dimer as shown in Figure 4.5. The dimer once formed competes with the benzyl chloride to be attacked by the benzyl carbonium ion. Earlier studies by Hass *et al* [26] showed that the presence of the chlorine atom in benzyl chloride considerably reduces its affinity to be attacked by the benzyl carbonium ion. At such a time, the dimer present is presumed to be preferentially attacked by the benzyl carbonium ion. Hence, the

Table 4.3**Reactions between Benzyl Chloride and Aromatic Substrates**

Substrate	Product
Benzene	Diphenylmethane (95%), bibenzyl (5%)
Toluene	4-benzyl toluene (65%), 2-benzyl toluene (31%), 4-phenyl toluene (3%), 1-phenyl toluene (1%)
Anisole	4-benzyl anisole (62%), 2-benzyl anisole (35%), 4-phenyl anisole (3%)
Napthalene	2-benzyl naphthalene (55%), 1-benzyl naphthalene (45%)

The experimental results obtained thus far suggest that the reaction of benzyl chloride with tungsten bronze follows the normal electrophilic substitution mechanism and the polymerized product obtained is formed due to the attack of the benzyl carbonium ion on the benzyl chloride. The effect of substituents at various positions on the substrate was studied in this investigation and the results are shown in Table 4.4.

Table 4.4**Reactions of various benzylic monohalides with tungsten bronze**

Substrate	Polymeric Product	Oligomers (dimers + trimers)	Alkylbenzenes
Benzyl chloride	100%	0%	0%
2-Me-benzyl chloride	78%	0%	22%
4-Me-benzyl chloride	82%	0%	18%
4-Cl-benzyl chloride	70%	0%	30%
2,6-dimethyl benzyl chloride	73%	0%	27%
2,4-dimethyl benzyl chloride	0%	66%	34%
2,4-difluorobenzyl chloride	0%	62%	38%

Substituents on the aromatic substrate do influence the product distribution from the substitution reaction. For example, benzyl chloride produces the polymer in nearly quantitative yield, while other substituted benzylic monohalides such as 4-methyl benzyl chloride, 2-methyl benzyl chloride undergo electrophilic aromatic substitution reaction to produce both polymer and minor amounts of alkyl benzenes. The latter result from hydrogenative dechlorination, so that, for example, o-xylene was produced from 2-methyl benzyl chloride and 4-methyl benzyl chloride produced p-xylene. The aromatic carbon-halogen bonds of the chloro- and fluoro- derivatives of benzyl chloride were unreactive towards tungsten hydrogen bronze. In general, substitution in the 2- position of the aromatic ring leads to oligomers, possibly due to steric and inductive effects. The polymerization termination step is hydrodechlorination, so, in the cases where oligomers

are observed (2,4-dimethyl benzyl chloride and 2,4-difluorobenzyl chloride), yields of the alkylbenzenes are also high.

The reaction between α -chloroisodurene and tungsten bronze gave unexpected products (Figure 4.6) and was therefore studied in greater detail, so as to see the effect of reaction time on the products obtained. Eight sets of batch reactors were set up to carry out 8 simultaneous reactions between 0.25 g of α -chloroisodurene and 2.5 g of tungsten hydrogen bronze according to the procedure described in the experimental section. One batch reactor was removed from the furnace at time intervals of 15 min, 30 min, 60 min, 90 min, 120 min, 150 min, 300 min and 600 min. The products were analyzed as described in the experimental section. The general reaction of α -chloroisodurene with molybdenum bronze is shown in Figure 4.6

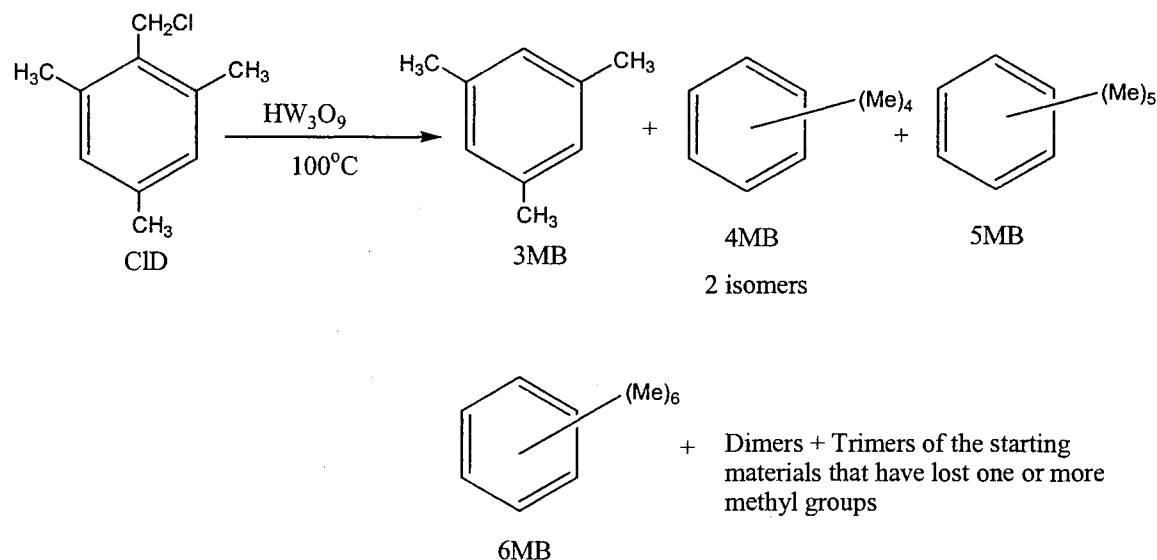


Figure 4.6: Reaction of α -chloroisodurene with Tungsten Bronze

α -chloroisodurene reacts with tungsten bronze to produce a variety of products that include trimethyl benzene (3MB), two isomers of tetramethyl benzene (4MB), pentamethylbenzene (5MB), hexamethylbenzene (6MB) and dimers and trimers of the

starting compound that have lost one or more methyl groups. For sake of simplicity the products were classified broadly into two categories. The methyl benzenes (3MB, 4MB, 5 MB and 6MB) were grouped together while the dimers and trimers of the starting compound were grouped separately (PAM). Table 4.5 shows the percentage of various products formed as a function of reaction time. A graph of the percentages of α -chloroisodurene and the reaction products obtained versus time is shown in Figure 4.7.

As seen from the plot shown in Figure 4.7 and Table 4.5, α -chloroisodurene reacts almost completely within a reaction time of 10 hours. The yield of the alkylbenzenes was 48% while the yield of the oligomerized product was 51%. The formation of coupled products takes place at short reaction times and seems to be the major product initially formed. At the start, the reaction probably proceeds by electrophilic aromatic substitution. This is supported by the detection of small amounts of the chloroaromatic derived from Friedel-Crafts alkylation of chloroisodurene with another chloroisodurene. However, this appears to react rapidly with another chloroisodurene to produce a trimer that is the first identifiable coupled product. This trimer is unusual in that it appears to have been demethylated, having a mass that corresponds to the loss of one methyl group. This result suggests that addition of the second tetramethylbenzyl group proceeds by displacement of a methyl group rather than a proton. The initially formed product appears to react away with time. The percentage of alkylbenzenes formed increases with time and finally at the end of 10 hours, the percentages of starting compound, alkylbenzenes and oligomers are 0.85, 47.67 and 51.48 respectively. Using FeCl_3 instead of the bronze, the major product obtained is a trimer of the starting compound minus a methyl group.

Table 4.5

Reaction between 0.25 g of α -chloroisodurene and 2.5 g of Tungsten Hydrogen

Bronze at 100°C

Time (min)	α -chloroisodurene (%)	Alkyl Benzenes (%)	PAM (%)
15	50.14	1.86	49
30	39.06	2.08	58.86
60	25.99	4.66	69.35
90	18.99	12.98	68.03
120	9.84	24.32	65.84
180	4.24	33.93	61.83
300	2.08	40.66	57.26
600	0.85	47.67	51.48

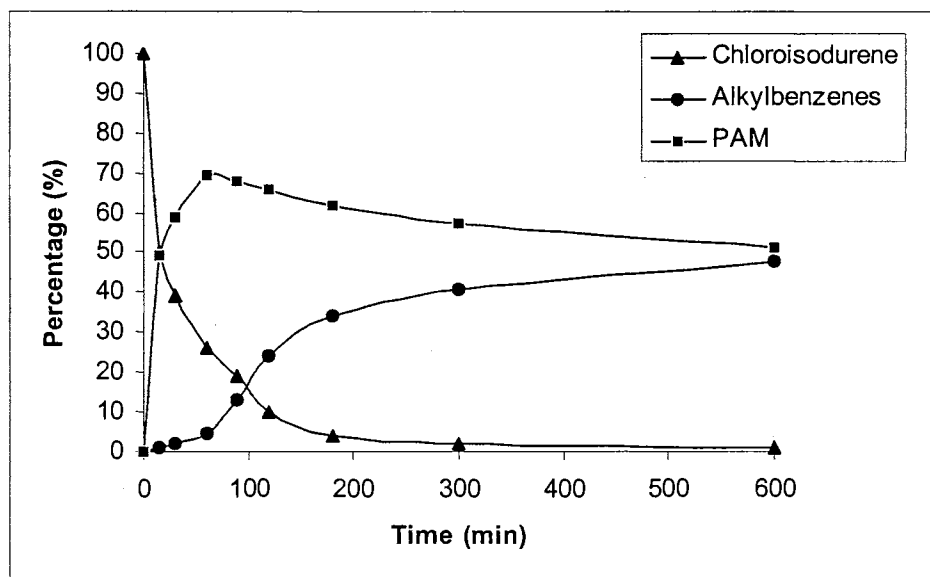


Figure 4.7: Graph of α -chloroisodurene reaction with tungsten hydrogen bronze

It has previously been shown that the reaction of polymethylbenzenes with concentrated sulfuric acid gives rearranged polymethylbenzenesulfonic acids. Under identical conditions halogenated polymethylbenzenes undergo isomerization as shown in Figure 4.8. Such a rearrangement is known as Jacobsen Rearrangement [27] and is believed to proceed by displacement of methyl cations by protons followed by realkylation.

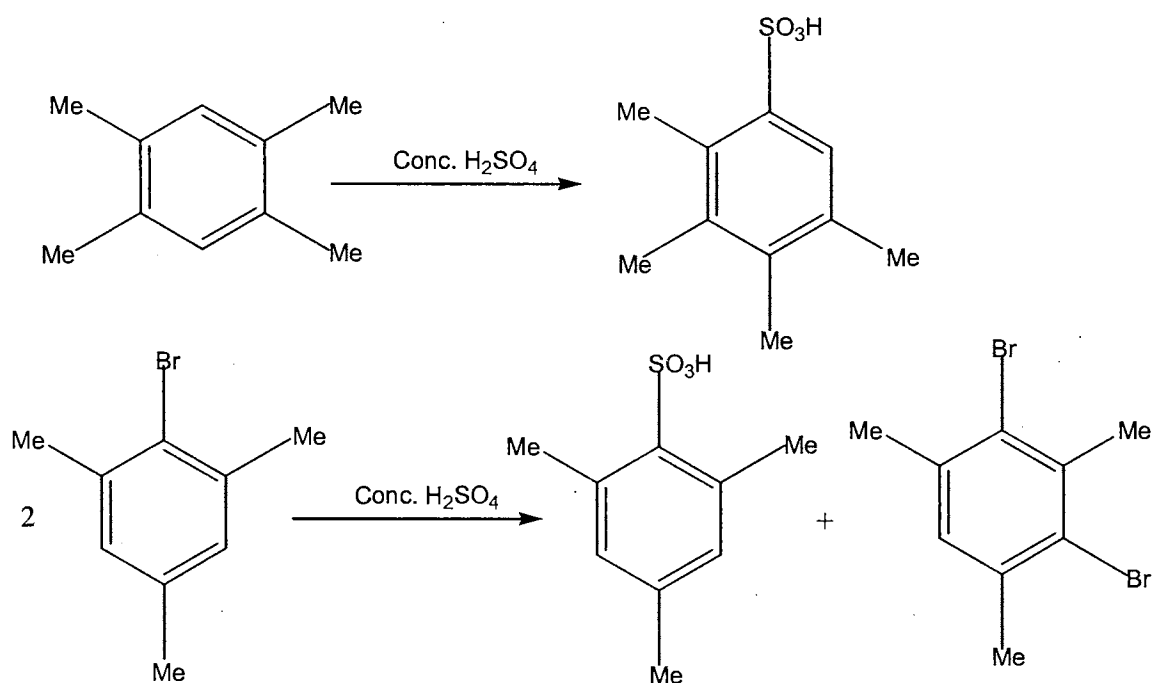


Figure 4.8 : General reactions of polyalkylbenzenes with acids

Many alkyl-aromatics are known to isomerize under acidic conditions and the alkyl group migrates from one aromatic ring to another. The reaction of α -chloroisodurene with tungsten bronze is believed to proceed by this alkylation-dealkylation mechanism and is a consequence of the high acidity of the bronze. Therefore, an experiment was carried out between durene and tungsten bronze to see if the scrambling of the methyl groups took place. It was found that this did indeed occur

and the products produced were 2,4,6-trimethylbenzene (25%); 1,2,4,5- and 1,3,4,5- isomers of tetramethylbenzene (30%); pentamethylbenzene (15%); hexamethylbenzene (30%) and a mixture of diarylmethanes (10%).

Reactions between α -chloroisodurene and tungsten bronze were also carried out in presence of the activated aromatic substrates, benzene, naphthalene, and anisole. Ar—CH₂—Ar products were obtained as the major product along with trimethylbenzene and the “normal” aromatic electrophilic substitution products (Ar-CH₂C₆H₂(CH₃)₃). The general reaction is shown in Figure 4.9. Deuterium incorporation into the bridge was not observed when deuterated aromatic substrates were used. The proposed mechanism for the formation of Ar—CH₂—Ar is shown in Figure 4.10.

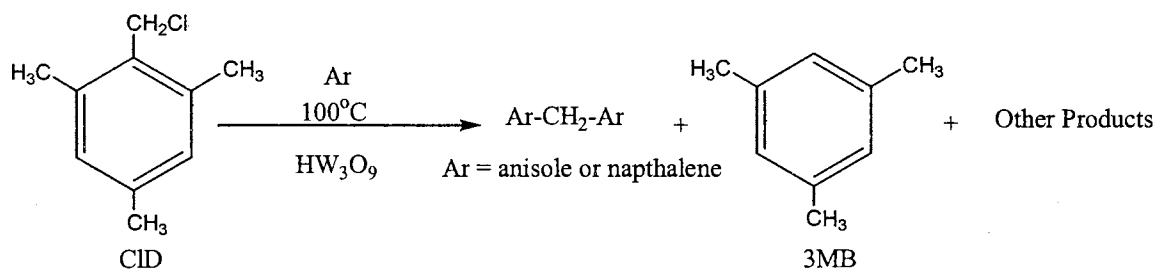


Figure 4.9 Reaction between CID and tungsten bronze in presence of aromatics

Table 4.6
Reaction between α -chloroisodurene and tungsten bronze in anisole

Product	Percentage (%)
1,3,5-trimethylbenzene	20
o-substituted Ar-CH ₂ -Ar	25
p-substituted Ar-CH ₂ -Ar	40
Ar-CH ₂ C ₆ H ₂ (CH ₃) ₃	9
Trimers	6

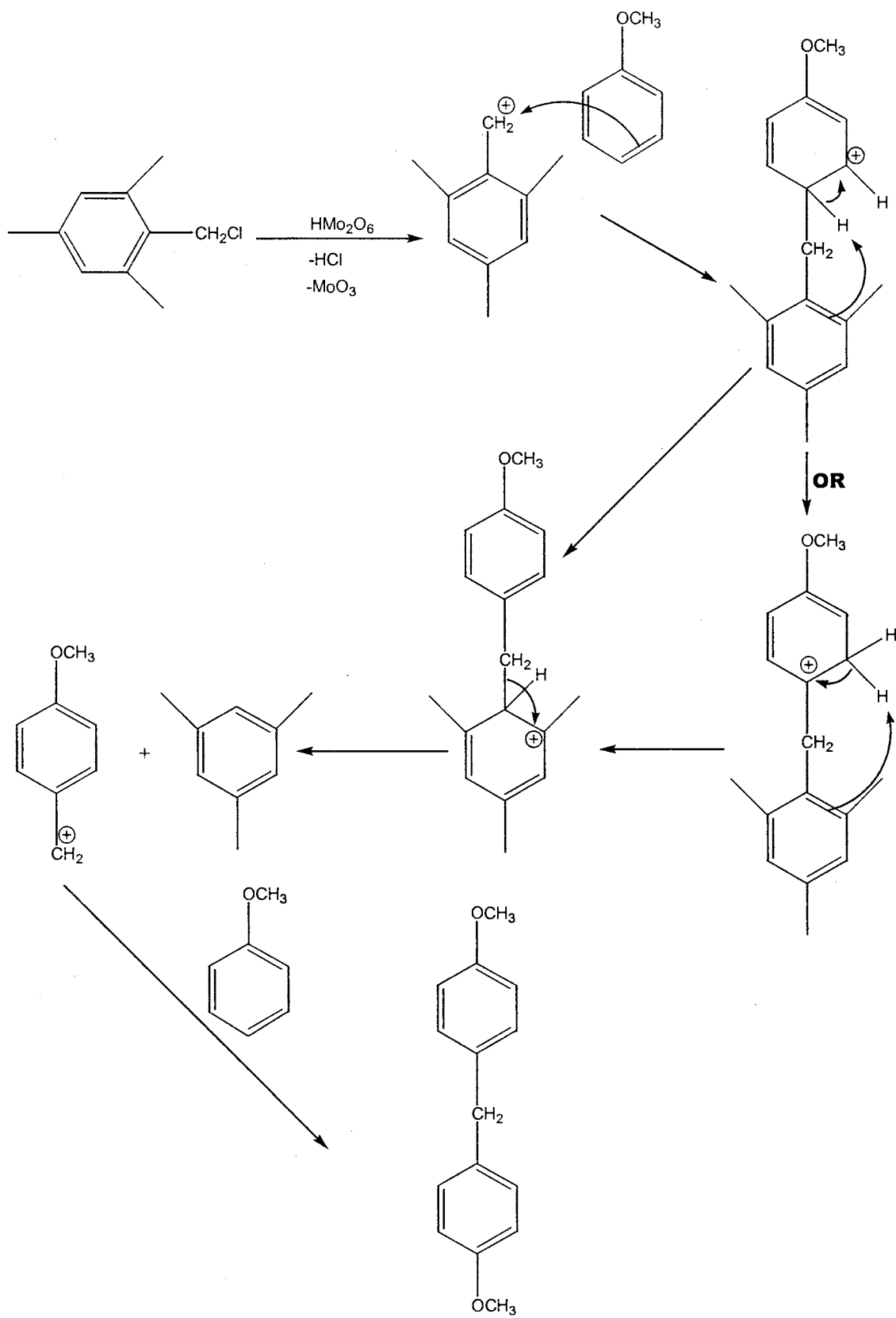


Figure 4.10: Proposed mechanism for the formation of $\text{Ar}-\text{CH}_2-\text{Ar}$

CONCLUSIONS

Molybdenum bronze was found to be useful for the conversion of benzylic halides to relatively non-toxic species by either polymerization or by the replacement of the halide by hydroxide and subsequent condensation. The latter products were obtained along with a novel molybdenum oxychloride. Tungsten bronze, on the other hand, produced a mixture of *cis* and *trans* dichlorostilbenes from α,α,α trichlorotoluene. It also reacted with α,α dichlorotoluene to produce *cis*-stilbene as a major product. A step-wise mechanism was suggested for these reactions on basis of absence of addition products when the reaction was carried out in presence of electron deficient species like cyclohexene. The reaction of the bronzes with benzyl chloride however produced a polymeric product and the reaction is believed to proceed via the formation of a benzyl carbonium ion followed by Friedel-Crafts aromatic substitution. These results show that tungsten bronze is an effective reagent for the reductive coupling reactions of benzylic polyhalides and that the reaction follows different mechanisms for the reaction with benzylic monohalides versus those of the benzylic polyhalides. Tungsten bronze was also found to be an effective reagent for catalyzing Jacobsen's rearrangement of poly substituted aromatics.

REFERENCES

1. M. F. Semmelhack, *Org. React.*, (1972), 19, 119
2. F. Ullman, J. Bielecki, *J. Chem. Ber.*, (1901), 34, 2174
3. G. A. Olah, G. K. S. Prakash, *Synthesis*, (1976), 607
4. T. -L. Ho and G. A. Olah, *Synthesis*, (1977), 170
5. Y. Okude, T. Hiyama and H. Nozaki, *Tetrahedron Lett.*, (1977), 3829

-
6. Y. Fujiwara, R. Ishikawa and S. Teranishi, *Bull. Chem. Soc. Jpn.*, (1978), 51, 589
 7. S. Inaba, H. Matsumoto and R. D. Reike, *Tetrahedron Lett.*, (1982), 23, 4215
 8. I. Hashimoto, N. Tsuruta, R. Ryang and S. Tsutsumi, *J. Org. Chem.*, (1970), 35, 3748
 9. N. Sadler, S. L. Scott, A. Bakac, J. H. Espenson, M. S. Ram, *Inorg. Chem.*, (1989), 28, 3951
 10. Y. Yamada and D. Momose, *Chem. Lett.*, (1981), 1277
 11. T. A. Cooper, *J. Am. Chem. Soc.*, (1973), 95, 4158
 12. E. Yoshisato and S. Tsutsumi., *J. Org. Chem.*, (1968), 33, 869
 13. D. Seyfert and M. D. Millar, *J. Organomet. Chem.*, (1972), 38, 373
 14. C. E. Coffey, *J. Am. Chem. Soc.*, (1961), 83, 1623
 15. H. Apler and D. D. Roches, *J. Org. Chem.*, (1976), 41, 806
 16. Y. Ogata and R. Oda, *Bull. Inst. Phys. Chem. Res. Tokyo*, (1942), 21, 616
 17. S. Inaba; H. Matsumoto and Reuben D. Rieke, *J. Org. Chem.*, (1984), 49(12), 2093
 18. J. Furukawa; A. Matsumura; Y. Matsuoka and J. Kiji, *J. Bull. Chem. Soc., Jpn.*, (1976), 49, 829
 19. Y. Ogata and H. Nakamura, *J. Org. Chem.*, (1956), 21, 1170
 20. L. Valentine and R. W. Winter, *J. Chem. Soc.*, (1956), 4768
 21. D. B. V. Parker; W. G. Davies and K. D. South., *J. Chem. Soc. B* (1967), 471
 22. K. Arata; A. Fukai and I. Toyoshima, *J. Chem. Soc., Chem. Commun.*, (1978), 121
 23. M. Hino and K. Arata, *Chem. Lett.*, (1979), 1141
 24. S. K. Jana; B. P. Kiran and V. R. Choudhary in “*Recent Trends in Catalysis*”, : V. Murugesan, B. Arabindoo, M. Palanichamy (Eds.), Narosa Publishing House, New Delhi, (1999), 106
 25. V. R. Choudhary, S. K. Jana and M. K. Choudhary, *J. Mol. Catal. A: Chem.*, (2001), 170, 251.

-
26. H. C. Haas; D. I. Livingston; and M. Saunders, *J. Polym. Sci.*, **(1955)**, 15, 503,
27. O. Jacobsen, *Ber.* **(1886)**, 19, 1209; **(1887)**, 20, 901

CHAPTER 5

REACTION OF ALKENES WITH METAL BRONZES

BACKGROUND

During the investigation of the dechlorination of CCl_4 by molybdenum bronze (Chapter 3), one possible mechanism that was investigated was the formation of dichlorocarbene as a reaction intermediate. Such an intermediate could dimerize or react with HCl to yield tetrachloroethylene or CHCl_3 , respectively. Therefore an attempt was made to trap the carbene by reaction with norbornene leading to a characteristic cyclopropane [1]. However when norbornene was added to a tungsten bronze/ CCl_4 reaction, analysis of the reaction mixture showed that norbornene completely and cleanly converted to norbornane without the formation of any addition products. Furthermore, complex reactions were observed with alkenes that were used as radical traps in the reaction of α -chlorinated benzenes with hydrogen bronzes. Therefore, the reactions of tungsten hydrogen bronze with various alkenes were studied, the results of which are presented in this chapter.

EXPERIMENTAL

Tungsten hydrogen bronze was prepared from zinc and hydrochloric acid according to the procedure described in Chapter 2. Reactions between the alkenes and the tungsten bronze were carried out in Teflon-lined stainless steel bombs using an excess of the blue reagent (2.5 g) and 0.25 g of the alkene. The sealed reactors were placed in a digitally-controlled oven at various temperatures under autogenous pressure. The amount of

reactants and products in the reaction mixtures were determined by cooling the bombs, sampling the headspace with a gas-tight syringe, and analyzing by gas chromatography/mass spectroscopy. Compounds were identified by comparison of their mass spectra to the NIST database. Product identity was confirmed by measuring the retention times of authentic samples of the compounds identified by mass spectroscopy. The products for the less volatile alkenes were isolated by extracting the reaction mixture with methylene chloride, and the extract was subjected to analysis by gas chromatography/mass spectroscopy. Compounds were identified as described above.

RESULTS AND DISCUSSION

Supported and unsupported tungsten and molybdenum oxide based catalysts are effective catalysts for olefin metathesis [2, 3], and isomerization reactions of alkenes [4, 5] and alkanes [6, 7]. It is known that metathesis, isomerization, cyclopropanation and polymerization are closely related alkene transformations. The surface chemistries of tungsten and molybdenum oxides have received considerable attention due to their high activity [8-10]. Experimental results obtained thus far suggest that the catalytic activity and selectivity of the products obtained vary widely with the extent of reduction of the catalyst and thus depend on the oxidation state of the tungsten or molybdenum present. In this chapter the reactions of various alkenes, ranging from linear alkenes, cycloalkenes, dienes, and aromatic alkenes, with tungsten and molybdenum hydrogen bronzes were carried out as described above and the results of the experiments are shown in Table 5.1.

Table 5.1

Alkenes used and the products obtained

Substrate	Reaction Time (days)	Composition of Reaction Mixture
Norbornene	1	Norbornane (100%)
Cyclopentene	14	<i>Cis</i> -decalin (67%), <i>trans</i> -decalin (33%)
Cyclohexene	14	1-Me-cyclopentene (82%), cis-1-4-dimethyl-decalin (5%), trans-1-4-dimethyl decalin (3%), bicyclohexyl (10%)
Dicyclopentadiene	14	No reaction
1-hexene	1	2-hexene (40%), 3-hexene (60%)
2-hexene	1	2-hexene (15%), 3-hexene (85%)
3-hexene	1	No reaction
1,3-hexadiene	1	3-hexene (100%)
Stilbene	1	mixture of dimerized products (100%)
Indene	14	Tetrahydro[1,2]benzanthracene (100%)
Styrene	12	Polystyrene (100%)
1,2-dihydronaphthalene	7	Naphthalene (75%), 1,2-dihydronaphthalene (25%)

Table 5.1 shows that the alkenes react differently producing a whole range of products including hydrogenated products, isomerized products, and coupled products. The first reaction carried out was that between norbornene and tungsten hydrogen bronze. Norbornane was the only product observed and was produced in 100% yield. It was suspected that the hydrogenation was influenced by the strained ring of norbornene so a reaction was carried out between cyclopentene and the tungsten bronze. The reaction proceeded cleanly with complete conversion of cyclopentene after 14 days to a mixture of *cis* and *trans* decalins with the *cis* decalin being the major product. Numerous investigations have been carried out on the acid catalyzed dimerization of 5 and 6 membered cyclic olefins [11-13]. The formation of decalins from cyclopentene systems was observed earlier during the research done by Onopchenko *et al* [14] and they

suggested that future researchers working with cyclopentene systems should look for decalin ring systems among the products of the reaction. Based on the results obtained, the proposed mechanism for the reaction between cyclopentene and tungsten hydrogen bronze is shown in Figure 5.1. An additional experiment performed using cyclopentyl chloride afforded *cis*- and *trans*- decalins in 92% yield with *cis*- isomer being the major product (75%). The remaining 8% was identified as bicyclopentyl. Under similar conditions molybdenum hydrogen bronze transformed cyclopentene into *cis*- and *trans*- decalins in 90% yield along with bicyclopentyl (10%), as a minor product.

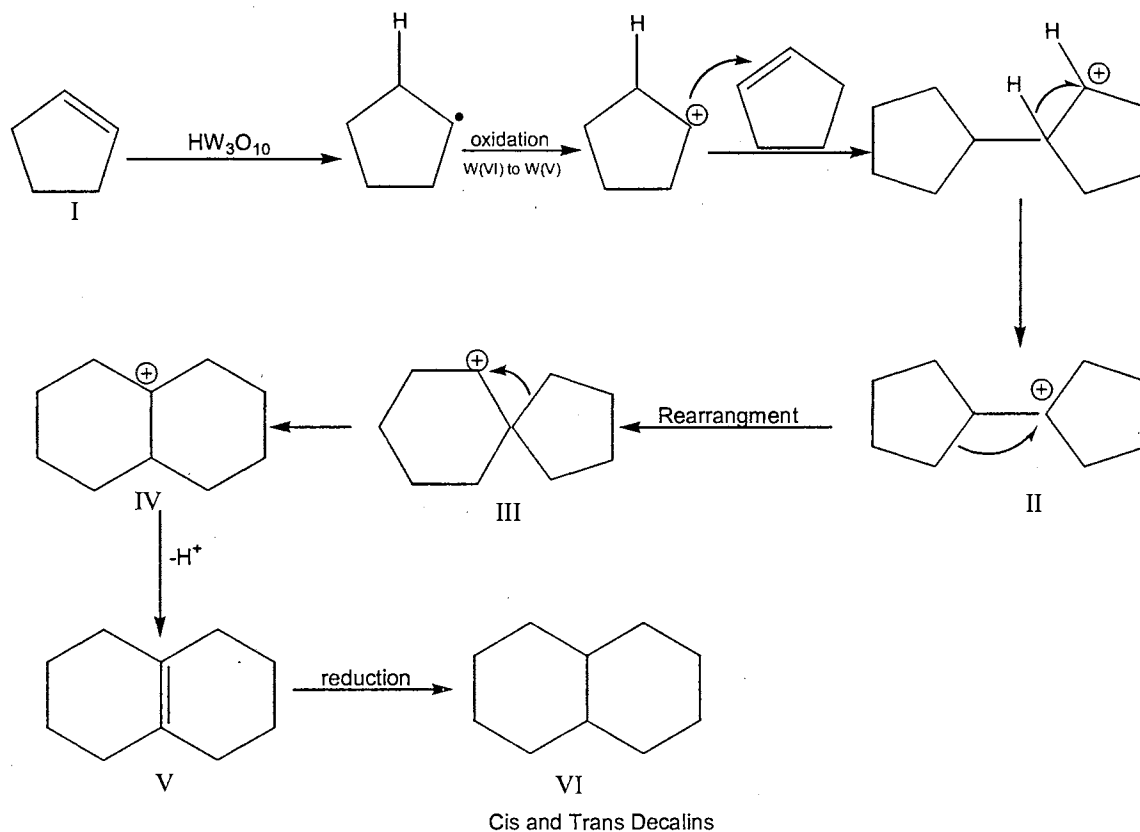


Figure 5.1: Reaction of Cyclopentene with tungsten bronze

In order to support the above mechanism, a control experiment was performed between 3-cyclopentylcyclopentene and tungsten bronze under the same experimental conditions, but for a shorter period of time (7 days). The reaction, however produced a

mixture of octalins (40%) (V) and a spirodecene (60%). The formation of spirodecene establishes structure III in Figure 5.1 to be an intermediate in the dimerization of pentene. Since it can be obtained by the deprotonation of structure III. It can be speculated that the above reaction would produce a mixture of decalins if the reaction were carried out for a longer period of time. For example, the reaction of cyclopentylcyclopentene with tungsten bronze in presence of cyclopentene for a period of 14 days produced a mixture of decalins in 70% yield with *cis* decalin being the major product. The remaining products were bicyclopentyl (5%) and a mixture of other cyclic alkenes (25%).

Similar dimerization products were expected from the reaction between cyclohexene and tungsten bronze, however the reaction products obtained were 1-Me-cyclopentene (72%), *cis*-1-4-dimethyl-decalin (5%), *trans*-1-4-dimethyl decalin (3%), and bicyclohexyl (20%). The results can be explained by rapid isomerization of the initially-formed cyclohexyl cation to the more stable methylcyclopentyl radical. Formation of 1-methylcyclopentene from cyclohexene over tungsten and molybdenum based catalysts has been reported earlier by Maire et al [7,15-18]. In presence of tungsten bronze, the later presumably goes on to form methyl substituted decalins according to the possible mechanism shown in Figure 5.1.

The formation of bicyclohexyl suggests that the cyclohexyl radical is an intermediate in the reaction. Previously, in Chapter 3, it was shown that 2-methyl-2-phenyl-1-chloropropane (CPPM) reacts to form a radical which is then oxidized to a cation by tungsten bronze. Thus, it can be speculated that the first step in the reaction is transfer of a hydrogen atom followed by oxidation to a cation. The formation of coupled radicals suggest that the latter reaction is slow. The possibility that the bicyclohexyl originated

from an electrophilic attack of cyclohexene on the cyclohexyl cation can be discounted based on the rapid isomerization of the latter cation. The formation of dicyclopentyl in the cyclopentene reaction could also be due to the dimerization of the radicals but, hydrogenation of proposed intermediate II (Figure 5.1) could also produce dicyclopentyl.

The suspicion that the methylated decalins were derived from methylcyclopentene was confirmed when a mixture of dimethyl decalins were obtained in 85% yield in a separate reaction of methylcyclopentene with tungsten bronze. Cyclic dienes such as cyclopentadiene did not react with either tungsten or molybdenum hydrogen bronze and was completely recovered at the end of the reaction.

The formation of decalins by the dimerization of cyclopentene prompted a reaction between indene (Figure 5.2 (A)) and tungsten hydrogen bronze. If dimerization were to occur, the major product would be either tetrahydronaphacene (Figure 5.2 (B)); or tetrahydro-[1,2]-benzanthracene (Figure 5.2 (C)); or tetrahydrochrysene (Figure 5.2 (D)) or a mixture of all of the above.

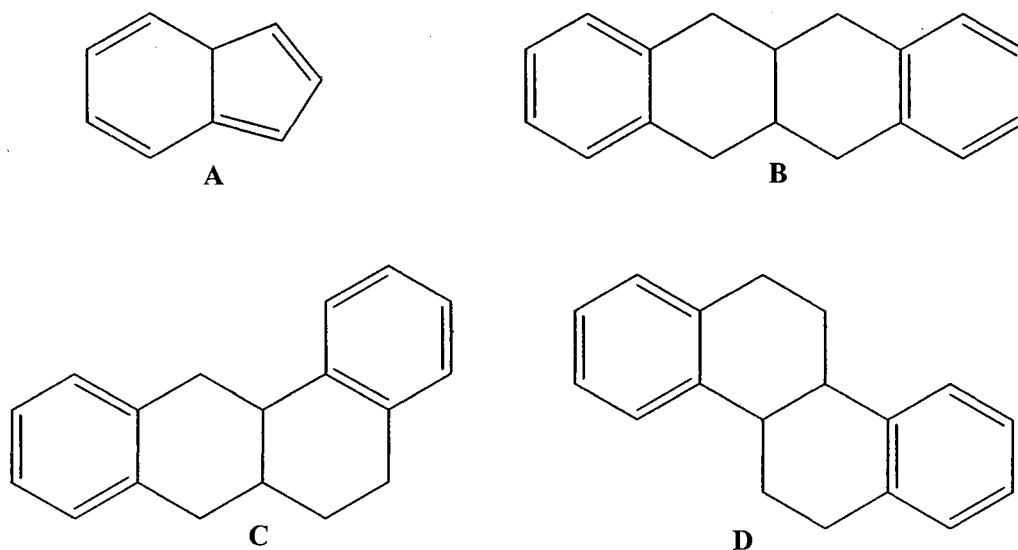
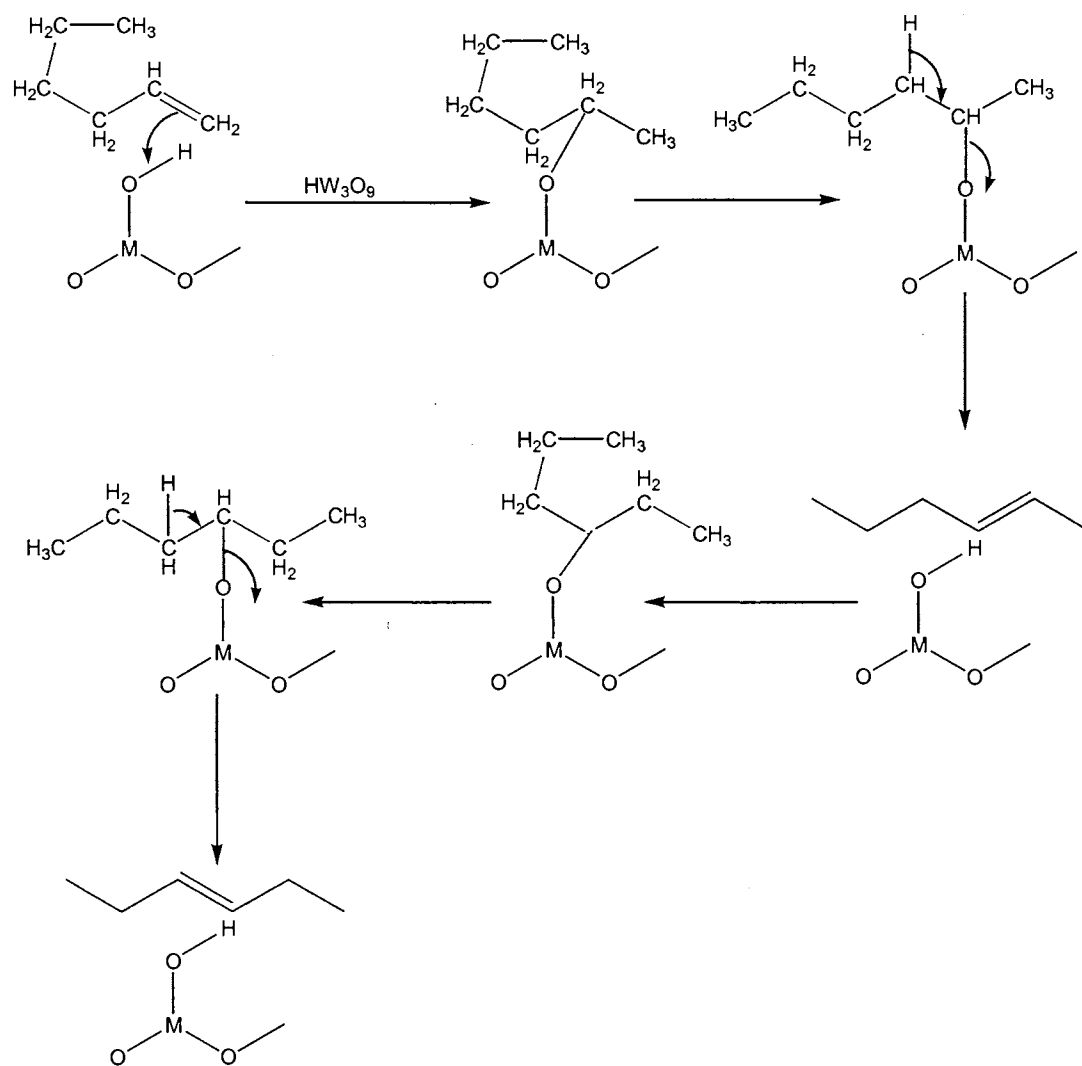


Figure 5.2: Possible products from the reaction between indene and tungsten blue

The GC-MS chromatogram of methylene chloride extract of the product of the reaction of indene with tungsten bronze showed a single peak having mass 234. This extract was evaporated and the residue was redissolved in CDCl_3 and the carbon (^{13}C) and proton (^1H) nuclear magnetic resonance spectra (NMR) were recorded. The ^{13}C -NMR spectrum shows 12 separate aromatic carbons ($\delta = 124.20, 124.27, 124.29, 124.48, 125.92, 126.01, 126.25, 126.35, 143.23, 143.49, 144.37$ and 146.40) and 6 separate aliphatic carbons ($29.74, 31.28, 36.91, 37.93, 43.71$ and 49.47). The tetrahydro[1,2]benzanthracene (Structure (C), Figure 5.2) product has two non-equivalent, non-symmetric aromatic rings and six different aliphatic carbons and has a structure most consistent with the data obtained. Structures (B) and (D) can be ruled out on basis of their symmetrical structure. Integration of the proton signals in the proton NMR spectrum shows multiplets in the aromatic region corresponding to 8 protons and 10 protons in the aliphatic region and that is consistent with the proposed structure (Figure 5.2 (C)). This identification of products is supported by the fact that at elevated temperature (200°C) dehydrogenation of the initially formed product occurs to yield [1,2]benzanthracene.

The reaction of tungsten bronze with simple linear alkenes such as 1-hexene produced isomerized products. 1-Hexene isomerized to yield a mixture of 2 and 3-hexenes with the 3-hexene being the major product. 2-hexene produced a mixture of unreacted 2-hexene and 3-hexene, while 3-hexene did not react and remains unconverted after a reaction time of 24 hours. Typically isomerization of alkenes favors structures with the double bond farther from the end of the carbon chain, in other words part of the driving force in most isomerization reactions would be to produce the highest possible

substitution of the double bond [19]. Similar isomerizations of 1-hexene were observed earlier by Agronomov and co-workers [20, 21], using reduced tungsten and molybdenum blacks that were obtained on reduction of the respective amalgams. The proposed mechanism for the isomerization of 1-hexene is shown in the Figure 5.3. 1,3-hexadiene produced 3-hexene as the only product (100% yield). This means that the terminal double bond is hydrogenated preferentially.



M= Mo or W

Figure 5.3: Proposed Mechanism for Reaction of 1-Hexene and Hydrogen Bronze

The aryl alkenes such as styrene and stilbene reacted differently and produced mainly oligomerized products. Styrene produced polystyrene in almost quantitative yield. The presence of polystyrene was confirmed by infrared spectroscopy of the extract. Stilbene produced dimerized products. The GC-MS chromatograms of the methylene chloride extracts of both the reactions showed the presence of dimerized products. The stilbene extract showed a single broad peak having a mass of 360 amu along with some minor peaks. Some of the minor products that could be identified were 1,2,3,4-tetraphenylbutadiene and 1,2,3-triphenyl azulene. These compounds suggest that the major product is 1,2,3,4-tetraphenylbutene. Dehydrogenation of this would yield the butadiene which presumably undergoes dehydrogenation and rearrangement to the azulene. The proposed mechanism for the formation of the dimerized alkene is shown in Figure 5.4.

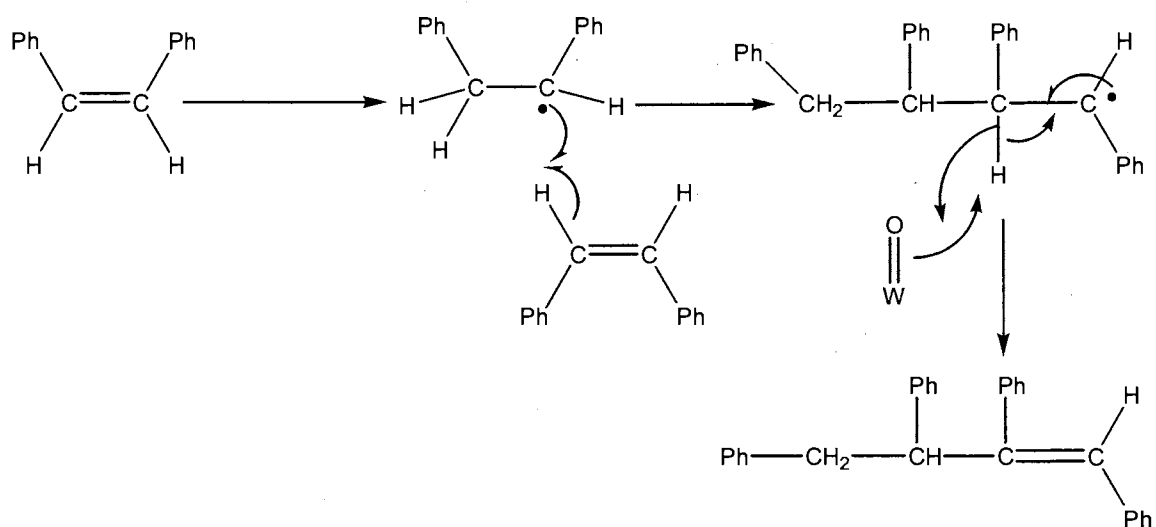


Figure 5.4: Proposed Mechanism for Dimerization of Stilbene

CONCLUSIONS

It may be concluded that the reaction of tungsten bronze gives a variety of products depending on the particular substrate. The initial reaction step appears to be

transfer of a hydrogen atom to give a radical. If the radical is stabilized by conjugation with a phenyl group, it survives sufficiently long to react with other alkenes to form dimers (as with stilbene) or polymers (as with styrene). When the radical is stabilized by conjugation with a second double bond, a second hydrogen atom transfer occurs to yield a product in which the diene has been hydrogenated at only one double bond.

Norbornylene is also hydrogenated possibly due to steric protection of the radical. In case of most alkenes, however, oxidation of the radical to a cation occurs and is followed by a normal sequence of reactions observed for reaction of these with strong Brønsted or Lewis acids. Thus n-alkenes are isomerized by double bond migration and cyclopentene derivatives yield decalins. Cyclohexene also yields dimethyldecalins by rearrangement of the initially formed cation to the methylcyclopentyl cation. Some of the above reactions were accompanied by dimerization of the initial radicals or hydrogenation or dehydrogenation of the initial products.

REFERENCES

-
1. A. W. Apblett; B. P. Kiran; and K. Oden, *ACS Symposium Series 837 (2003)*, (Chlorinated Solvent and DNAPL Remediation), 154
 2. P. A. Engelhard; J. Goldwasser; and W. K. Hall, *J. Catal.*, (1982), 76, 48
 3. R. Thomas; J. Moulijn, *J. Mol. Catal.*, (1980), 8, 161
 4. J. Houzvicka; and V. Ponec, *Catal. Rev.*, (1997), 39, 319
 5. V. Logie, *Ph. D. Thesis*, Strasbourg, (1998).
 6. Y. Holl; F. Garin; G. Marie; A. Muller; P. A. Engelhard; and J. Grosmangin, *J. Catal.*, (1987), 104, 225
 7. V. Keller; F. Barath; and G. Maire, *J. Catal.*, (2000), 189, 269
 8. P. E. Massoth, *Adv. Catal.*, (1978), 27, 265

-
9. I. E. Wachs, *Catal. Today*, (1996), 27, 437
 10. F. Morazzoni; C. Canevali; F. D' Aprile; C. L. Bianchi; E. Tempesti; L. Giuffre; and G. Airoidi, *J. Chem. Soc., Faraday Trans.*, (1995), 91(21), 3969
 11. H. S. Bloch and C. L. Thomas, *J. Am. Chem. Soc.*, (1944), 66, 1589
 12. A. E. Bearn and J. E. Leonard., *U. S. Patent 2,419,668* (1947)
 13. R. Criegee and A. Riebel, *Angew. Chem.*, (1953), 65, 136
 14. A. Onopchenko; B. L. Cupples; and A. N. Kresge, *Macromolecules*, (1982), 15, 1201
 15. F. Di-Gregorio; V. Keller, T. Di-Costanzo; J. L. Vignes; D. Michel; and G. Maire, *App. Catal. A: General*, (2001), 218, 13
 16. C. Bigey; L. Hilaire; and G. Maire, *J. Catal.*, (1999), 184, 406
 17. V. B. Kazanski; M. V. Frash; and R. A. Van Santen, *Appl. Catal., A: Gen.*, (1996), 146, 223
 18. V. B. Kazanski, *Acc. Chem. Res.*, (1991), 24, 379
 19. T. W. G. Solomons, *Organic Chemistry*, Wiley, New York, (1999)
 20. A. E. Agronomov; and G. V. Lisichkin, *Khimiya* (1972), 13(5), 582-5
 21. A. E. Agronomov; G. V. Lisichkin; V. V. Lunin; and M. S. Ketegenova, *Khimiya* (1969), 24(3), 113-6

CHAPTER 6

REACTIONS OF ACETYLENES WITH BRONZES

INTRODUCTION

In the previous chapter reactions of various alkenes with tungsten and molybdenum hydrogen bronzes was discussed. This chapter addresses at the reactions of various alkynes (acetylenes, $C\equiv C$) with molybdenum and tungsten hydrogen bronzes. Hydration of unsaturated carbon compounds is one of the simplest and environmentally benign methods for the formation of a carbon-oxygen bond and the formation of carbonyl compounds from the hydration of alkynes has been extensively studied [1-3].

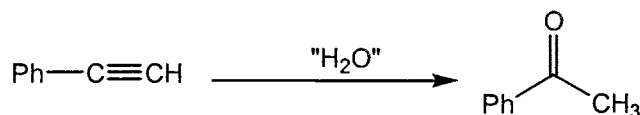


Figure 6.1: General Reaction for Hydration of an Alkyne

The hydration of alkynes catalyzed by mineral acids has been known for a very long time [4- 6]. These catalysts, however reacted with only electron-rich acetylene compounds, such as alkynyl ethers, alkynyl thioethers and ynamines, and gave the corresponding carbonyl compounds in satisfactory yields [1,7,8]. The reaction of simple alkynes is usually very slow in acids and requires the presence of other cocatalysts, typically toxic mercury (II) salts, to enhance the rate of reactivity of the carbon-carbon triple bond [9]. Recent research focuses on the use of transition metal complexes containing Ru^{II} [10], Ru^{III} [11], Rh [12], Pt [13] and other metal centers [14, 15], to catalyze the hydration alkynes, but the yields obtained were not satisfactory. More recently, Teles *et al*

reported the hydration of alkynes by Au^I species in presence of other acidic cocatalysts [16]. The reaction produced better yields than previously reported methods, however it did not proceed in absence of either the Au catalyst, the acidic cocatalyst or the solvent [17]. It is also worth noting that the hydration reaction did not take place in absence of solvents, the nature of ligands present on the catalyst determines its catalytic activity, and the presence of acidic cocatalysts like sulfuric acid further enhanced the yields of the reaction.

In Chapter 5, it was found that the reaction of molybdenum and tungsten hydrogen bronze were useful for the conversion of alkenes into a variety of products. Therefore the reaction of acetylenes with these reagents were investigated and the results are reported herein.

EXPERIMENTAL

The tungsten and molybdenum hydrogen bronzes were prepared by procedures reported in Chapter 2. Hydration reactions between the alkyne and the blue reagent were carried out in Teflon-lined stainless steel bombs using an excess of the blue reagent (2.5 g) and 0.25 g of the alkyne. The sealed reactors were placed in a digitally-controlled oven at a temperature of 100°C, under autogenous pressure for 8 hours. The amount of reactants and products in the reaction mixtures were determined by cooling the bombs, sampling the headspace with a gas-tight syringe, and analyzing by gas chromatography/mass spectroscopy. Compounds were identified by comparison of their mass spectra to the NIST database. Product identity was confirmed by measuring the retention times of authentic samples of the compounds identified by mass spectroscopy. The products for the less volatile alkynes were analyzed by extracting the reaction mixture with methylene

chloride, and subjecting the extract to analysis by gas chromatography/mass spectroscopy. Compounds were identified as described above.

RESULTS AND DISCUSSION

Molybdenum hydrogen bronze (MB) and tungsten hydrogen bronze (TB) reacted with various alkynes ($C\equiv C$) under the experimental conditions to produce the corresponding carbonyl compounds in excellent yields. The general reaction is shown in Figure 6.2 and the results obtained from the various reactions are tabulated in Table 6.1

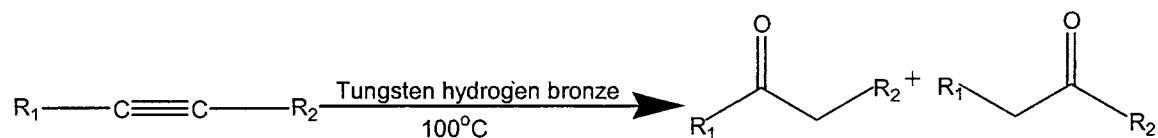


Figure 6.2: Reaction of $C\equiv C$ with tungsten and molybdenum bronzes

Table 6.1

Reactions of various C≡C with tungsten and molybdenum bronzes

Entry	Substrate	Catalyst	Major Product	Minor Products
1	PhC≡CH	MB TB	PhC(O)Me (99%) PhC(O)Me (94%)	1-Ph-Napthalene (1%) 2-Ph-Napthalene (2%) 1,3,5-tri-Ph-Benzene (2%) 1,2,4-tri-Ph-Benzene (1%)
2	<i>n</i> -BuC≡CH	MB TB	<i>n</i> -BuC(O)Me (80%) <i>n</i> -BuC(O)Me (65%)	1,2-hexane diol (20%)** 1,2-hexane diol (35%)**
3	<i>t</i> -BuC≡CH	MB TB	<i>t</i> -BuC(O)Me (34%) <i>t</i> -BuC(O)Me (28%)	
4	PhC≡CMe	MB TB	PhC(O)Et (75%) PhCH ₂ C(O)Me (25%) PhC(O)Et (71%) PhCH ₂ C(O)Me (29%)	
5	PhC≡CEt	MB TB	PhC(O)Pr (63%) PhCH ₂ C(O)Et (37%) PhC(O)Pr (66%) PhCH ₂ C(O)Et (34%)	
6	PhC≡CPh	MB TB	PhC(O)CH ₂ Ph (100%) PhC(O)CH ₂ Ph (100%)	
7	<i>n</i> -PrC≡CH	MB TB	<i>n</i> -PrC(O)Me (100%) <i>n</i> -PrC(O)Me (100%)	
8	<i>n</i> -PrC≡CMe	MB TB	<i>n</i> -PrC(O)Et (53%) <i>n</i> -BuC(O)Me (47%) <i>n</i> -PrC(O)Et (51%) <i>n</i> -BuC(O)Me (49%)	

MB: Molybdenum Hydrogen Bronze; TB: Tungsten Hydrogen Bronze

** 1,2- hexane diol believed to be formed by addition of two hydroxyl groups across C≡C

Table 6.1 shows that both terminal and internal acetylenes react almost equally well, with both the catalysts, provided that the substrates are not sterically hindered. The hydration of terminal alkynes followed the Markownikoff's rule and produced ketones as the only products (Entry # 1, 2, 3 and 7). An aldehyde would be produced if the hydration of alkynes took place by anti Markownikoff's rule. This is not observed and hence anti Markownikoff addition can be ruled out. Unhindered arylalkylacetylenes yield mixtures of ketones, the major product being the ketone containing the carbonyl group adjacent to the aliphatic moiety (Entry # 4 and 5). Symmetrical diphenylacetylene produced benzyl phenyl ketone in quantitative yield (Entry # 6). Unsymmetrical alkyl acetylenes produce a mixture of the two possible ketones in almost equimolar amounts (Entry # 8).

Most of the hydration reactions reported so far in literature are carried out in presence of solvents and use water as the direct source for the oxo group. In the reactions, reported herein the hydration of alkynes takes place in absence of a solvent or water and hence the ketone oxygen must be derived from the hydrogen bronze reagent. The proposed mechanism for the hydration of acetylenes, shown in the Figure 6.2, involves transfer of the hydroxyl from the metal bronze to the organic substrate. The intermediate is believed to be an enolate derived from the addition of a hydroxide across the acetylene. The reaction on completion gives the product ketone (mixture of ketones in some cases) and the catalyst gets reduced to a species in which one of the metal atoms is in a (+VI) state and the other one is in a (+IV) state, a more reduced state. The metal atom in the (+IV) state is believed to be a bare metal center. The same products were formed when tungsten hydrogen bronze was reacted with acetylenes and gave similar yields.

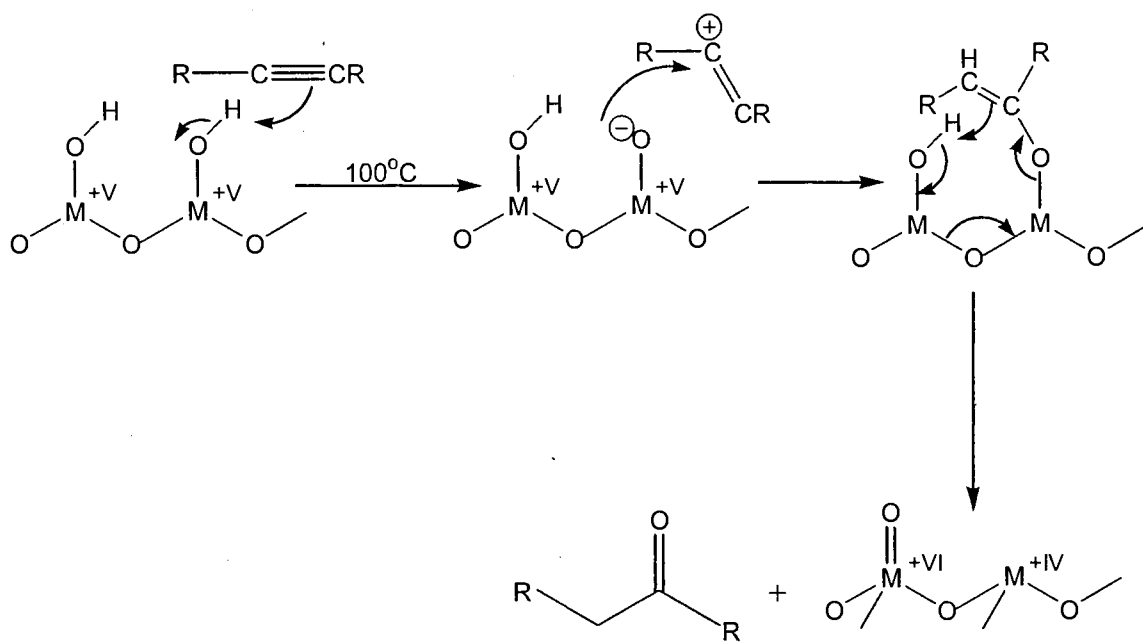


Figure 6.3: Proposed Mechanism for Hydration of Alkynes by Metal Bronzes

(M= Mo or W)

Table 6.1 shows that no oligomerized products were observed on reaction of the alkyne with molybdenum hydrogen bronze. Only the reactions between tungsten hydrogen bronze and the alkyne produced oligomerized products such as 1-phenylnaphthalene, 2-phenylnaphthalene, 1,3,5-triphenylbenzene and 1,2,4-triphenylbenzene in small quantities. The oligomerization is believed to involve the interaction of the bare W(+IV) center generated by the hydration reaction with the alkyne. As predicted by this hypothesis, subsequent reuse of the tungsten hydrogen bronze produced increased yields of the oligomerized products. Table 6.2 shows the effect of reuse of the catalyst on the yields of the oligomerized products for the reaction between phenyl acetylene and tungsten bronze. No oligomerized products were observed in the reaction between molybdenum hydrogen bronze and phenyl acetylene, even when molybdenum bronze was reused four times.

Table 6.2**Effect of Reuse of Tungsten Bronze in the Hydration Reactions**

Tungsten Bronze	Reaction Time (hrs)	Acetophenone (%)	Oligomers (%)
Fresh	8	94	6
Reuse # 1	8	93	7
Reuse # 2	8	90	10
Reuse # 3	8	84	16

Acetophenone was the only product obtained in 90% yields when hydration of diphenyl acetylene was carried out in alcohols such as ethanol or methanol. Alkyne oligomerization products were not observed. No reaction was observed when the hydration was carried out in various hydrocarbon solvents such as hexane and decane.

CONCLUSIONS

Molybdenum hydrogen bronze and tungsten hydrogen bronze are effective reagents for the hydration reaction of alkynes. The reaction produces high yields of the hydrated product (ketones), at relatively low temperatures and in absence of solvents. Minor amounts of oligomerized products are formed on reaction between tungsten hydrogen bronze and the alkyne under the experimental conditions. Molybdenum hydrogen bronze, therefore can be considered as a better reagent for the hydration reactions of alkynes (acetylenes), under the experimental conditions.

REFERENCES

1. J. March, *Advanced Organic Chemistry*, Wiley, New York, (1992), p. 762
2. P. F. Hudrlik; and A. M. Hudrlik in *The Chemistry of the Carbon-Carbon Triple Bond*, Part 1 (Eds.: S. Patai), Wiley, New York, (1978), p. 199
3. G. H. Schmid in *The Chemistry of the Carbon-Carbon Triple Bond*, Part 1 (Eds.: S. Patai), Wiley, New York, (1978), p. 275
4. A. Schrohe, *Chem. Ber.*, (1875), 8, 367
5. A. Bayer, *Ber.*, (1882), 15, 2705
6. Y. Izumi, *Catal. Today*, (1997), 33, 371
7. W. Drenth; and Hogeveen, *Recl. Trav. Chim, Pyas-Bas*, (1960), 79, 1002
8. A. D. Allen; Y. Chiang; A. J. Kresge and T. T. Tidwell, *J. Org. Chem.*, (1982), 47, 775
9. V. Jager; and H. G. Viehe in *Methoden Org. Chem.* (Houben-Weyl), 4th ed. (1952)., Vol. 5/2a, p. 726, (1977)
10. T. Suzuki; M. Tokunaga; Y. Wakatsuki, *Org. Lett.*, (2001), 3, 735,
11. T. Khan; S. B. Halligudi; and S. Shukla, *J. Mol. Catal.*, (1990), 58, 299
12. J. Blum; H. Huminer; and H. Alper, *J. Mol. Catal.*, (1992), 75, 153
13. W. Hiscox; and P. W. Jennings, *Organometallics*, (1990), 9, 1997
14. Y. Fukuda; and K. Utimoto, *J. Org. Chem.*, (1991), 56, 3729
15. K. Imai; K. Imai; and K. Utimoto, *Tetrahedron Lett.*, (1987) , 28, 3127
16. J. H. Teles; S. Brode and M. Chabanas, *Angew. Chem. Int. Ed, Engl.*, (1998), 37, 1415
17. J. H. Teles; and M. Schulz, *BASF AG, WO-A1 9721648*, (1997); *Chem. Abstr.* 127:121499, (1997)

CHAPTER 7

REACTIONS OF NITRILES WITH METAL BRONZES

INTRODUCTION

The formation of an amide from a nitrile has tremendous industrial and academic interest [1]. Amides have found use in a variety of industrial applications as additives in detergents, drug stabilizers, lubricants and in monomers [2]. Hydration of a nitrile to amide can be achieved by a variety of methods such as refluxing the nitrile in strong acidic [3, 4] and basic [5] conditions; using alkaline hydrogen peroxide [6]; metals [1] or metal oxides [7]; and by enzymatic routes [8]. Cheng-Ting and co-workers [9] reported the hydration of nitriles using MnO_2 supported on silical gel as a catalyst. However, the reaction required large reaction times, excess of MnO_2 , and hydrocarbon solvents to produce reasonable amounts of the amide. Most of the methods reported in literature suffer from drawbacks such as the use of strong acidic or basic medium, excessive use of organic solvents, elaborate procedures, less selectivity in the amide product caused by the hydrolysis of the product amide to an acid [10], or, long reaction times. The development of new hydration catalysts, or the modification of existing catalysts that will selectively hydrate the $\text{C}\equiv\text{N}$ bond without hydrolyzing the resulting amide product. In addition to being selective, the new catalyst must operate under reaction conditions that are mild enough to prevent the autocatalytic polymerization of amides to polyamides. The successful hydration of alkynes (acetylenes) to their corresponding

ketones using tungsten and molybdenum hydrogen bronzes was discussed in the previous chapter. The interaction of various nitriles with tungsten and molybdenum hydrogen bronzes is discussed in this chapter

EXPERIMENTAL

The tungsten and molybdenum hydrogen bronzes were prepared by procedures reported in Chapter 2. Hydration reactions between the alkyne and the blue reagent were carried out in Teflon-lined stainless steel bombs using an excess of the blue reagent (2.5 g) and 0.25 g of the nitrile. The sealed reactors were placed in a digitally-controlled oven at a temperature of 100°C, under autogenous pressure for 8 hours. The amount of reactants and products in the reaction mixtures were determined by cooling the bombs, sampling the headspace with a gas-tight syringe, and analyzing by gas chromatography/mass spectroscopy. Compounds were identified by comparison of their mass spectra to the NIST database. Product identity was confirmed by measuring the retention times of authentic samples of the compounds identified by mass spectroscopy. The products for the less volatile alkynes were analyzed by extracting the reaction mixture with methylene chloride and subjecting the extract to analysis by gas chromatography/mass spectroscopy. Compounds were identified as described above.

RESULTS AND DISCUSSION

Molybdenum hydrogen bronze (MB) reacted with various alkynes ($C\equiv N$) under the experimental conditions to produce the corresponding amides in excellent yields (>90%). Tungsten hydrogen bronze reacted similarly but also produced minor amounts (6%) of triazines when the alkyl group was sterically-undemanding ($R = \text{Me, Et, ClCH}_2$,

Pr). The latter products resulted from cyclotrimerization of three nitrile molecules. The general reaction is shown in Figure 7.1 and the results obtained are tabulated in Table 7.1

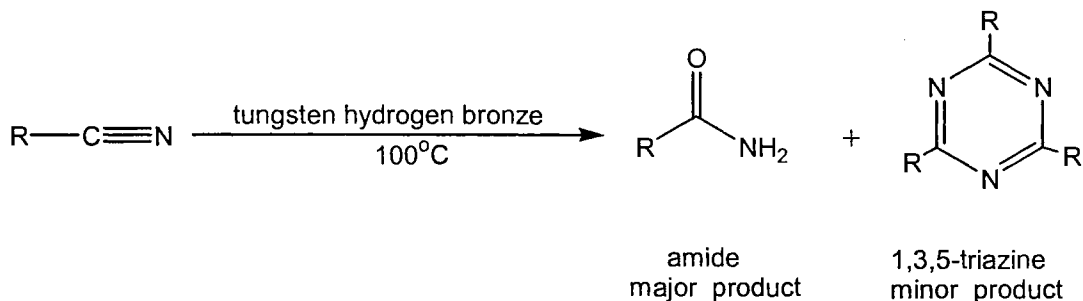


Figure 7.1: General Reaction for Conversion on a Nitrile to an Amide

Molybdenum hydrogen bronze reacts with nitriles and produces the corresponding hydrated products, amides high yields. No oligomerized products are observed. Table 7.1 shows the results of reaction between various nitriles and tungsten and molybdenum hydrogen bronze. High yields of amides (hydrated product) along with minor amounts corresponding cyclized triazines (oligomerized products) are obtained.

Table 7.1

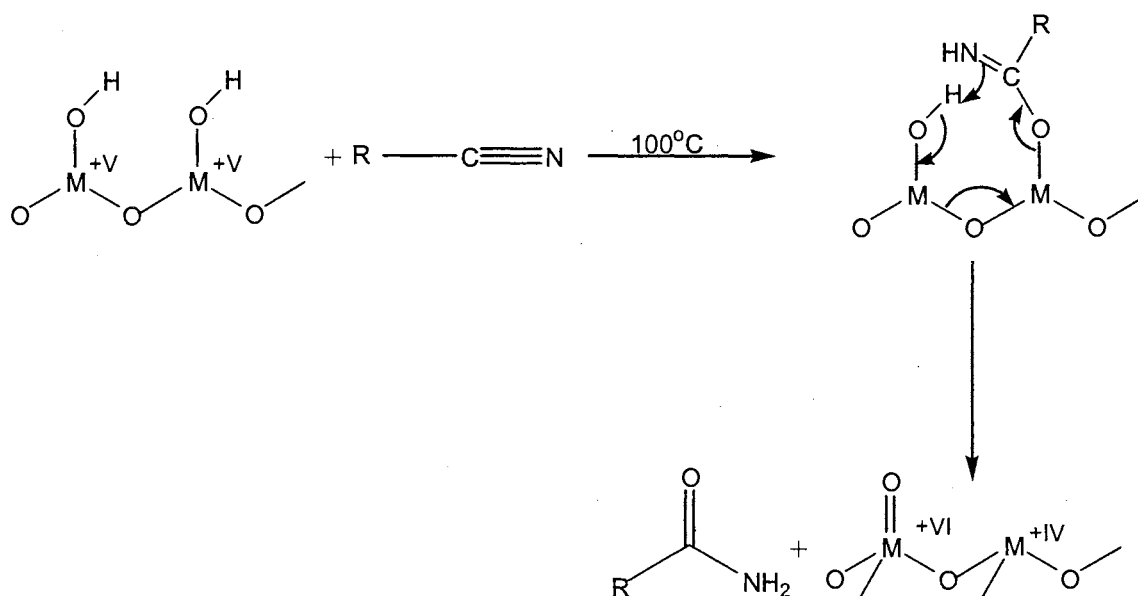
Reaction of Nitriles with Tungsten and Molybdenum Bronze

Nitrile	Catalyst	Unreacted Nitrile (%)	Major Product (Amide)	Minor Product (1,3,5-triazine)
CH ₃ CN	MB	0	CH ₃ C(O)NH ₂ (100%)	
	TB	0	CH ₃ C(O)NH ₂ (94%)	1,3,5-trimethyl-cyclotriazine (6%)
ClCH ₂ CN	MB	0	ClCH ₂ C(O)NH ₂ (100%)	
	TB	0	ClCH ₂ C(O)NH ₂ (97%)	1,3,5-trichloromethyl-cyclotriazine (3%)
Cl ₂ CHCN	MB	0	Cl ₂ CHC(O)NH ₂ (100%)	
	TB	0	Cl ₂ CHC(O)NH ₂ (100%)	
Cl ₃ CCN	MB	0	Cl ₃ CC(O)NH ₂ (100%)	
	TB	0	Cl ₃ CC(O)NH ₂ (100%)	
C ₂ H ₅ CN	MB	0	C ₂ H ₅ C(O)NH ₂ (100%)	
	TB	0	C ₂ H ₅ C(O)NH ₂ (96%)	1,3,5-triethyl-cyclotriazine (4%)
C ₃ H ₇ CN	MB	0	C ₃ H ₇ C(O)NH ₂ (100%)	
	TB	0	C ₃ H ₇ C(O)NH ₂ (98%)	1,3,5-tripropyl-cyclotriazine (2%)
Acrylonitrile H ₂ C=CHC≡N	MB	0	Polyacrylamide (100%)**	
	TB	0	Polyacrylamide (100%)**	
Adiponitrile NC(CH ₂) ₄ CN	MB	10	Adipamide (90%)	
	TB	8	Adipamide (92%) H ₂ NC(O)(CH ₂) ₄ C(O)NH ₂	
Benzonitrile	MB	12	Benzamide (88%)	
	TB	6	Benzamide (94%)	
Valeronitrile H ₃ C(CH ₂) ₃ CN	MB	15	Valeramide (85%)	
	TB	8	Valeramide (92%) H ₃ C(CH ₂) ₃ C(O)NH ₂	
Isovaleronitrile (CH ₃) ₂ CHCH ₂ CN	MB	13	Isovalermide (87%)	
	TB	7	Isovalermide (93%) (CH ₃) ₂ CHCH ₂ CN	

MB= Molybdenum Hydrogen Bronze, TB= Tungsten Hydrogen Bronze

** product identified by infrared spectroscopy

Since there is no external source of water, and the reaction is carried out in absence of a solvent, it is believed that the surface of the molybdenum or tungsten hydrogen bronze plays an important role in the hydration reaction. It is, therefore assumed that the surface hydroxyl groups present on the tungsten and molybdenum hydrogen bronze serve as the source of water in the above reaction. Hydration of nitriles to amines caused by surface hydroxyl groups of alumina are known and have been previously reported [11]. The proposed mechanism for the interaction of the nitriles with tungsten or molybdenum hydrogen bronzes is shown in Figure 7.2



M= W or Mo

Figure 7.2: Reaction of nitriles with tungsten and molybdenum bronzes

Upon completion, the reaction gives the product amide and the catalyst gets dehydrated. While Figure 7.2 shows one M(+V) center being reduced to + 4 state and another to +6, the high electrical conductivity of the bronze averages the distribution of electrons so that, overall the average oxidation state of the bronze remains unchanged.

Therefore this is not a redox reaction *per se* but the formal charge of the individual metal centers have changed. When tungsten hydrogen bronze was reacted with acetonitrile, acetamide was the major product observed along with small amounts of the oligomerized 1,2,3-trimethyl-2,4,6-triazine. Increase in reaction times, leads to increase in yields of the oligomerized products and subsequent reuse of the tungsten hydrogen bronze also produced increased yields of the triazine. Table 7.2 presents the data for the effect of reuse of the catalyst with respect to the yields of the oligomerized product. These observations suggest that the oligomerization took place due to the interaction of the bare W (+IV) center that was present on the bronze after the initial hydration reaction to produce the amide similar to what was observed for alkynes

Table 7.2

Effect of Reuse of Tungsten Bronze in Hydration of Nitriles

Tungsten Bronze	Reaction Time (hrs.)	Acetamide (%)	1,3,5-trimethyl-cyclotriazine (%)
Fresh	8	94	6
Reuse # 1	8	94	6
Reuse # 2	8	93	7
Reuse # 3	8	91	9
Reuse # 4	8	88	12

CONCLUSIONS

Tungsten and molybdenum hydrogen bronzes were effective as reagents in performing the hydration reactions of nitriles. Both the reagents produced high yields of the amide under mild conditions and in absence of a solvent. Molybdenum hydrogen bronze was seen to be more selective in the production of amides since no oligomerized products were observed, while tungsten hydrogen bronze produced minor amounts of triazines. The oligomerized products were believed to be formed due to the interaction between the nitrile and the bare M(IV) metal center produced on depletion of the surface OH group from the tungsten bronze.

REFERENCES

-
1. F. Matsuda, *Chemtech*, (1997), 7, 306
 2. R. Opsahl, "Amides", in *Encyclopedia of Chemical Technology*, J. J. Kroschwitz; M. Howe-Grand, Eds.: John Wiley and Sons, New York, (1991): Vol. 1, p 346
 3. J. March, *Advanced Organic Chemistry*, 4th Edition, (1992), p 887
 4. R. S. Varma; and D. Kumar, *Organic Lett*, (1999), 1(5), 697
 5. J. H. Hall; and M. Gisler, *J. Org. Chem.*, (1976), 41(23), 3769
 6. A. R. Katrizky; P. Pilarski; and L. Urogei, *Synthesis*, (1989), 949
 7. E. N. Zil'berman, *Russian Chem. Rev.* (Engl. Transl.), (1984), 53, 900
 8. M. A. Cohen; J. Sawden; N. J. Turner, *Tetrahedron Lett*, (1991), 31(49), 7223
 9. Cheng-Ting Liu; Mei-Hisu Shih; Hsiau-Wen Huang; and Chia-Juei Hu, *Synthesis*, (1988), 715
 10. N. C. Deno; R. W. Gaugler; and J. M. Wisotsky, *J. Org. Chem.*, (1966), 31, 1967
 11. H. Sharghi; and M. H. Sarvari, *Synthetic Commun.*, (2003), 33(2), 207

CHAPTER 8

HEAVY METAL REMEDIATION USING MOLYBDENUM BRONZE

INTRODUCTION

Heavy metals are a common contaminant of ground water and can arise from natural and anthropogenic sources. Remediation of such contaminated waters is problematic due to : (i) the presence of heavy metals in typically very low concentrations (100-500 $\mu\text{g/L}$); (ii) the ground water itself being found up to depths of several hundred meters below the surface; and (iii) the coexistence of alkali and alkaline-earth metals in much higher concentrations (30-300 mg/L), further complicating the remediation processes. In spite of all these difficulties, the remediation of ground water contaminated with metals is essential because of their high toxicity to humans and other living organisms [1, 2]. Since most of the heavy metals are cumulative poisons or exhibit biological effects in small doses, even low concentrations of heavy metals can be problematic.

Commonly used above-ground water treatment processes do not provide an adequate solution to heavy metal remediation. Processes converting soluble metal salts to corresponding insoluble hydroxides proved to be ineffective because the hydroxides still have a small but finite solubility. Calculated equilibrium concentrations for lead, cadmium and mercury [3], over the entire pH range, highly exceed the permitted values [4]. Another approach to above ground remediation, electrochemical reduction, takes advantage of the relative ease of reduction of heavy metal as compared to lighter, non-

toxic metals. However, the very high costs of this method makes it an unattractive alternative for ground-water remediation [5].

Reactive permeable barriers (PRB's) are among the most promising methods for the remediation of heavy-metal contaminated groundwater. The working of a PRB and the factors to be taken into account before using a particular material for construction of a PRB have already been discussed earlier in Chapter 1. PRB's have been designed and proved effective for a variety of heavy metals. PRB's consisting of zerovalent iron particles are one of the more successful technologies for this purpose. For example, iron reduces the mobile, soluble ions such as CrO_4^- to the non-toxic, insoluble and therefore immobile form Cr^{3+} . PRB's constructed using iron suffer from the drawback that they are nonspecific and react with a wide variety of dissolved species, leading to a period of life that is shorter than that would be expected from stoichiometric considerations [6-8]. In addition to iron, zeolites [9,10]; materials from biological sources such as seaweed, algae, and bacterial biomass [11,12]; humic acids and peat [13,14]; and activated carbon [15] have been tested as potential materials for construction of PRB's. The low cost of zeolites, high uptake selectivities [16] and their stabilities make them an attractive material for use in PRB's, but their low uptake capacities, slow reaction kinetics and low hydraulic conductivity work against them [17]. Materials from biological sources have low uptake capacities and selectivities [11,12]. Humic acid and peat have high selectivities towards heavy metals but have poor uptake capacities and also cannot be used in presence of calcium and magnesium [13,14]. Activated carbon also has poor uptake capacities and selectivities for the uptake of heavy metals. The objective of research described in this chapter was to explore the effectiveness of molybdenum

hydrogen bronze for the uptake of heavy metals. This chapter describes the results of the batch tests performed to test the efficiency of using molybdenum hydrogen bronzes as a potential remediation reagent.

Molybdenum hydrogen bronze, HMo_2O_6 is a promising reagent for environmental remediation. It has a number of unique properties which suggest it could perform better than other reductants for treatment of contaminated waters and the construction of permeable reactive containment barriers to prevent spread of pollutants within an aquifer. For example, when reductions of inorganic or organic pollutants are performed in a column-type reactor, the color change from royal blue to white would greatly facilitate monitoring of the column's remaining reductive capacity. Unlike other reductants that can be employed in the presence of water and oxygen (such as iron), molybdenum blue has an open layered structure that allows the entire reductive capacity to be used and enhances the rate of reaction by providing a tremendously increased area for the reaction to take place. Since both reduced and oxidized forms of the oxide materials have layered structures through which reactants and products can intercalate, passivation due to build up of oxidized product on the surface does not occur. This is in significant contrast to iron that can form a crust of rust that arrests further reaction of the iron particles with contaminant species. Finally, molybdenum blue is easily recycled after use in redox reactions since regeneration only requires treatment with hot butanol in the presence of a trace of HCl or with zinc/HCl. In fact, the regeneration process with butanol only produces butaraldehyde as a by-product and, in actual industrial production, this could be captured and sold as a commodity chemical.

EXPERIMENTAL

All reagents were commercial products (ACS Reagent grade or higher) and were used without further purification. Thermogravimetric studies were performed using 10-20 mg samples on a Seiko ExStar 6200 TGA/DTA instrument under a 50 ml/min flow of dry air. The temperature was ramped from 25 to 600°C at a rate of 5°C/min. Bulk pyrolyses at various temperatures were performed in ambient air in a digitally-controlled muffle furnace using ca. 2 g samples, a ramp of 10°C/min and a hold time of 4 hr. X-ray powder diffraction (XRD) patterns were recorded on a Bruker AXS D-8 Advance X-ray powder diffractometer using copper K_{α} radiation. Crystalline phases were identified using a search/match program and the PDF-2 database of the International Centre for Diffraction Data [18]. Scanning Electron Microscopy (SEM) photographs were recorded using a JEOL Scanning Electron Microscope. Colorimetry was performed on a Spectronic 200 digital spectrophotometer using 1 cm cylindrical cuvettes.

Measurement of the Uptake of Metals by Molybdenum Bronze

Molybdenum blue was tested for the ability to remove Pb^{2+} , Th^{4+} , UO_2^{2+} and Nd^{3+} from aqueous solution. HMo_2O_6 (1.0 g) was reacted with 100 ml of individual (approximately 0.1M) solutions of Pb^{2+} , Th^{4+} , UO_2^{2+} and Nd^{3+} . In all cases, nitrate salts were used with the exception of uranyl where both a nitrate and an acetate salt were tested. After stirring magnetically for a sufficiently long time for complete reaction, as indicated by complete disappearance of the blue color, the mixtures were separated by filtration through a 20 μ m nylon membrane filter. The solid products were washed copiously with distilled water and then were dried in a vacuum desiccator. They were subsequently characterized by infrared spectroscopy, thermal gravimetric analysis, and

X-ray powder diffraction. The filtrates were analyzed as shown in Table 8.1. The uranium and neodymium concentrations in the treated solutions were analyzed using UV/Visible spectroscopy ($\lambda = 415$ nm and 521 nm, respectively). Solutions were treated with nitric acid before analysis to ensure no speciation of metal ions would interfere with the measurement. Lead was determined gravimetrically as lead chromate [19]. Quantitation of thorium was performed colorimetrically using the blue complex ($\lambda = 575$ nm) formed between thorium and carminic acid [20].

Table 8.1

Methods used to analyze filtrates of metal uptake reactions

Element	Method of Analysis
Uranium	Ultraviolet / Visible Spectroscopy ($\lambda = 415$ nm)
Neodymium	Ultraviolet / Visible Spectroscopy ($\lambda = 521$ nm)
Lead	Gravimetrically as lead chromate
Thorium	Colorimetrically using the blue complex formed between thorium and carminic acid ($\lambda = 575$ nm)

Selectivity Determination

The selectivity of molybdenum blue for actinides was tested by competition experiments with calcium. Thus, the reactions between uranyl nitrate and molybdenum blue were repeated in the presence of 1.0, 2.0, and 5.0 molar equivalents of calcium nitrate per mole of uranyl ion and the uptake of uranium was determined by UV/Visible spectroscopy. The selectivity for heavy metals was tested by carrying out reactions between lead nitrate and molybdenum blue in presence of 1 molar equivalent of calcium

nitrate per mole of lead ions and the uptake of lead was determined gravimetrically as described earlier.

Recovery of Uranium from the Product Molybdate

Uranium was recovered from the iriginite phase by treatment with a strong base. Thus, 1.1 gram of the uranyl molybdate complex was stirred overnight with 100 ml 15% solution of ammonium hydroxide. The reaction mixture was separated by filtration through a 20 μm nylon membrane filter. The solid product was washed copiously with distilled water and then dried in a vacuum desiccator. The product was subsequently characterized by infrared spectroscopy, thermal gravimetric analysis, and X-ray powder diffraction. The filtrate was evaporated and the solid obtained was analyzed by infrared spectroscopy, thermal gravimetric analysis and X-ray powder diffraction.

Determination of Rate of Uranium Uptake

The rate of uranium uptake was determined was carried out by carrying out the following experiment. A 200 ml (0.1M) solution of uranium was stirred with 2 gm. of molybdenum bronze. Aliquots of 5 ml of the reaction mixture were withdrawn at regular intervals and the pH were measured. Uranium was quantified by the procedure described above. After completion of the reaction, the reaction mixture was filtered as described above. The residue and the filtrate were analyzed separately.

RESULTS AND DISCUSSION

Molybdenum bronze was tested for its ability to remove Th^{4+} (as a model for plutonium(IV)), UO_2^{2+} (of interest in its own right and as a model for PuO_2^{2+}), and Nd^{3+} (as a surrogate for the later transuranics , radioactive lanthanides, and Pu^{3+}) from aqueous solution. Also, the uptake of lead as a model heavy metal was investigated. The

experiments that were performed were designed to determine the capacity of the blue reagents for the various metals and attempt to identify the mechanism of metal uptake. Molybdenum bronze was reacted with an aqueous solution of each of the metals listed above. The stoichiometry was adjusted so that there was at least a one-fold excess of contaminant metal ions {on the basis of one molar equivalent of metal ion per M(V) site in HMo_2O_6 }.

The experimental conditions and results for the molybdenum bronze/metal ion reactions are listed in Table 8.2 while the results of the analyses and binding capacity calculations are given in Table 8.3. The results shown in Table 8.3 can be represented by the plot shown in Figure 8.2. These show that molybdenum blue has a remarkable capacity for absorption of actinides and heavy metals. Molybdenum blue absorbed 122% by weight of uranium, 37% by weight of thorium, 61.6% by weight of neodymium, and 110% by weight of lead. The substitution of acetate ions for nitrate ions had a small, negative effect on the uptake of uranium. These extremely high capacities bode well for the eventual application of these materials in environmental remediation.

Table 8.2

Experimental Conditions for Metal Uptake Reactions			
Metal Solution (0.1M)	Weight of Molybdenum Blue (g)	Weight of Solid Product (g)	Color of Solid Product
Uranium acetate	1.04	2.15	Yellow
Uranium nitrate	1.05	2.32	Yellow
Thorium	1.00	1.40	White
Neodymium	1.10	1.48	Grey
Lead	1.04	2.74	White

At the outset of research it was thought that adsorption of metals by molybdenum blue would occur either by ion-exchange or redox reactions. The latter possibility is negated because the colors of the final products are those of the contaminant metal ions in their oxidized states. The disappearance of the blue color of Mo(V) indicates that oxidation of the bronze has occurred. If the metal ions are not the oxidizing agents, the only other possibilities are nitrate ions or oxygen. Since uranyl acetate also forms a yellow product like uranyl nitrate, oxygen appears to be the oxidizing agent.

Another possible mechanism for the uptake of metals is a simple ion-exchange reaction (Equation 8.1) involving the hydrogen ions of the molybdenum blue.



The uptake of the metals in terms of milliequivalents per gram of molybdenum blue were 4.27 for neodymium, 5.14 for uranium, 5.29 for lead, and 1.59 for thorium. Thus, the moles of metal that can be absorbed by molybdenum blue varies with the charge of the metal ion as would be expected for an ion-exchange mechanism. Within the group of doubly-charged metal ions, the moles of metal absorbed are almost equivalent. In this case, the uptake of metals may be expressed as approximately 1.5 moles per mole of HMo_2O_6 and is therefore larger in magnitude than the number of Mo(V) centers. This result indicates that the molybdenum(VI) centers in molybdenum bronze also play a role in metal binding and a simple ion-exchange mechanism does not occur. The uptake of neodymium was 1.24 moles per mole of molybdenum bronze and that of thorium was 1.1 moles per mole of molybdenum bronze, and exceeds the capacity suggested by Equation 8.1.

Table 8.3

Results of Metal Uptake Experiments

Metal Solution	Initial Conc.	Final Conc.	Uptake (mmol)	Metal Capacity (mmol/g)	Metal Capacity (weight %)
Uranium Acetate	0.1 M	0.053 M	4.7	4.5	108%
Uranium Nitrate	0.1 M	0.046 M	5.4	5.1	122%
Thorium Nitrate	0.1 M	0.084 M	1.6	1.6	37.0%
Neodymium Nitrate	0.1 M	0.047 M	5.3	4.8	69.5%
Lead Nitrate	0.1 M	0.045 M	5.5	5.3	110%

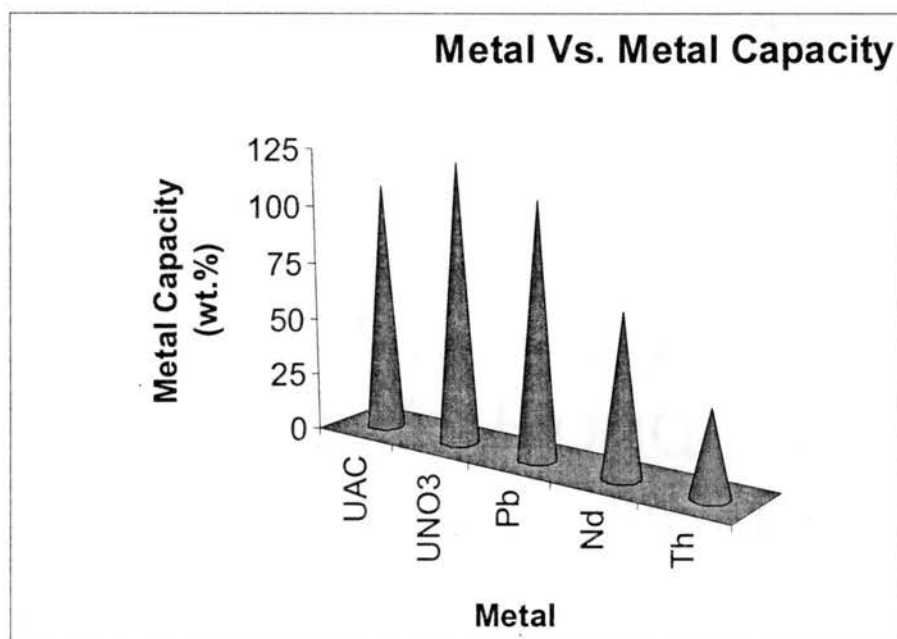


Figure 8.2: Graph of Metal Capacity versus Metal Solution

A major concern for the application of molybdenum bronze in the field is its selectivity for actinides and heavy metals as opposed to benign cations normally found in natural waters. Therefore, the selectivity of molybdenum bronze for uranyl ion over calcium ions was determined. The results are displayed in Table 8.4 and demonstrate that molybdenum bronze is highly selective for uranium. Figure 8.3 represents a plot of Uranium: Calcium ratio versus weight % of uranium absorbed. Even a five-fold higher concentration of calcium ions over uranyl ions had little effect on the absorption of uranium. The results show that molybdenum bronze is highly selective for uptake of uranium as compared to calcium.

Table 8.4.

Results of Competition Experiments Between Calcium and Uranium

Uranium: Calcium Ratio	Initial Uranium Concentration	Final Uranium Concentration	Weight Percent of Uranium Absorbed
1:0	0.1M	0.056M	122%
1:1	0.1M	0.055M	121%
1:2	0.1M	0.049M	100%
1:5	0.1M	0.052M	111%

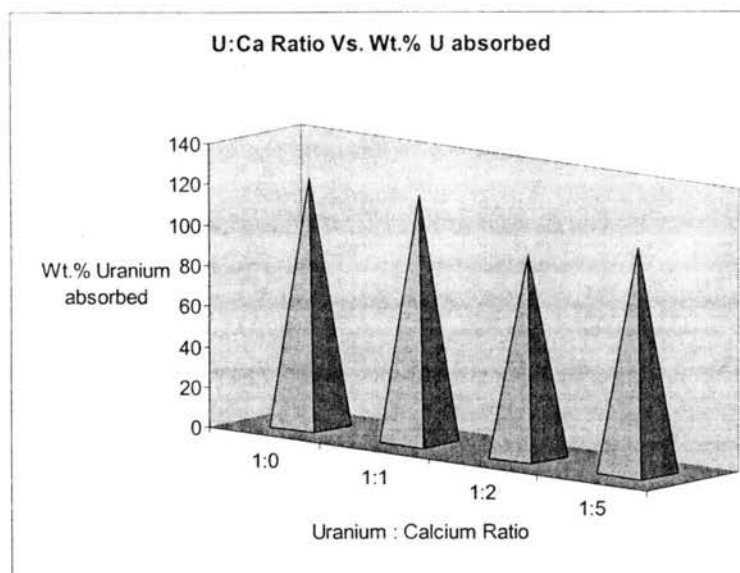


Figure 8.3: Graph of Uranium: Calcium Ratio Versus Weight Percent of Uranium Absorbed

Selectivity of molybdenum bronze for lead ion over calcium ions was also determined. The results are displayed in Table 8.5 and demonstrate that molybdenum bronze is highly selective for uranium. Even a five-fold higher concentration of calcium ions over lead ions had little effect on the absorption of uranium. The results show that molybdenum bronze is highly selective for uptake of lead as compared to calcium.

Table 8.5

Results of Competition Experiments Between Calcium and Lead

Lead: Calcium Ratio	Initial Lead Concentration	Final Lead Concentration	Weight Percent of Lead Absorbed
1:0	0.1M	0.045M	110%
1:1	0.1M	0.045M	110%
1:5	0.1M	0.050M	111%

Infrared spectral analysis of the various solid products and molybdenum blue was performed in order to gain a better understanding of the nature of the products and to

perhaps shed some light on the mechanism of metal uptake. The positions of the molybdenum-oxygen stretches are given in Table 8.6. Molybdenum blue was found to have a characteristic absorption at 857 cm^{-1} which is different from the bands observed in molybdenum trioxide. In all cases, except for neodymium, this band, attributable to Mo(V)-O stretching vibrations has disappeared. The neodymium compound is unusual because the molybdenum centers appear to be freely rotating in the solid so that there is rotational structure to the infrared absorptions making it difficult to assign the positions of the vibrations. Nevertheless, the data in Table 8.6 demonstrate that the solid products from reaction of molybdenum blue with uranium, uranium/calcium mixtures, and neodymium all contain network polymers based on MoO_6 octahedra, as demonstrated by multiple Mo-O stretches. By contrast, the lead product had a single strong Mo-O absorption at 786 cm^{-1} attributable to a tetrahedral MoO_4 center.

Table 8.6

Metal-Oxygen Stretching Frequencies Observed in the Infrared Spectra (cm^{-1})					
MoO₃	Mo Blue	U + Mo Blue	U + Ca + Mo Blue	Nd + Mo Blue	Pb + Mo Blue
	998				999 (w)
		970*	980*	972*	
884		892	901	913	
	857			866	
		840*	849*		
					786
569	572	551	533	572	
502				498	

* U-O stretches of the uranyl ion

In addition to the M-O stretching bands, the infrared spectra of the solids also contain bands attributable to a small amount of anions that are also absorbed from aqueous solution. The solids from reaction of molybdenum with uranyl, lead, and neodymium nitrate all display an infrared absorption at 1384 cm^{-1} . Notably, this band is due to ionic nitrate and not nitrate covalently-bound to the contaminant metals [21]. The product from uranyl acetate has weak bands at 1506 and 1436 cm^{-1} that are due to acetate ions – again the positions of these bands do not correspond to acetate bound to uranium (1514 and 1480 cm^{-1}) that was determined from the infrared spectrum of the starting material. The uptake of the anions indicates that when the metals are bound, the charge is not entirely compensated by the negative charge of the molybdate framework. Nevertheless, the absorptions for the extraneous anions are weak indicating a low degree of incorporation into the solid products. This conclusion was supported by the fact that the ceramic yields derived from heating the solids to 600°C in a thermal gravimetric analyzer were quite high (Table 8.7). Indeed, the majority of the weight losses occur between room temperature and 200°C and can be attributed to dehydration and dehydroxylation reactions.

Table 8.7

Results of TGA Experiments

Metal Salt	Temperature Range of Weight Loss	Ceramic Yield
Uranium Acetate	25-436°C	88.2%
Uranium Nitrate	25-469°C	90.2%
Thorium Nitrate	25-502°C	94.9%
Neodymium Nitrate	25-209°C	96.5%
Lead Nitrate	215-495°C	99.2%

X-ray powder diffraction analysis of the product from lead uptake by HMo_2O_6 revealed that it consisted mainly of PbMoO_4 (wulfenite, ICDD # 44-1486). (Figure 8.4). In this case, the interaction between HMo_2O_6 and Pb^{2+} is so strong that the molybdenum oxide layers are destroyed to yield a normal ortho-molybdate salt. The other metals, uranium and thorium also show similar behavior. The product of uranium uptake with molybdenum bronze was uranium molybdate ($\text{UMo}_2\text{O}_{12}\text{H}_6$, iriginite) while that of thorium uptake was $\text{Th}(\text{MoO}_4)_2$. Neodymium, however, behaved differently than uranium and thorium molybdate and formed an amorphous phase. However when heated to 800°C crystallization to neodymium molybdate, $\text{Nd}_2(\text{MoO}_4)_3$ occurred. This results suggest that the neodymium metal ions intercalate between the layers of HMo_2O_6 (staging) and react to give what might be phases that consist of negatively-charged slabs of MoO_6 octahedra with the contaminant ions residing between the layers, which then converts to the normal molybdate phase on heating. These results in combination with the infrared spectral data suggest that the mechanism of metal uptake by the molybdenum bronze is complete destruction of its layered structure and formation of a normal molybdate salt of the metal in which Mo is present as MoO_4 tetrahedra or MoO_6 octahedra

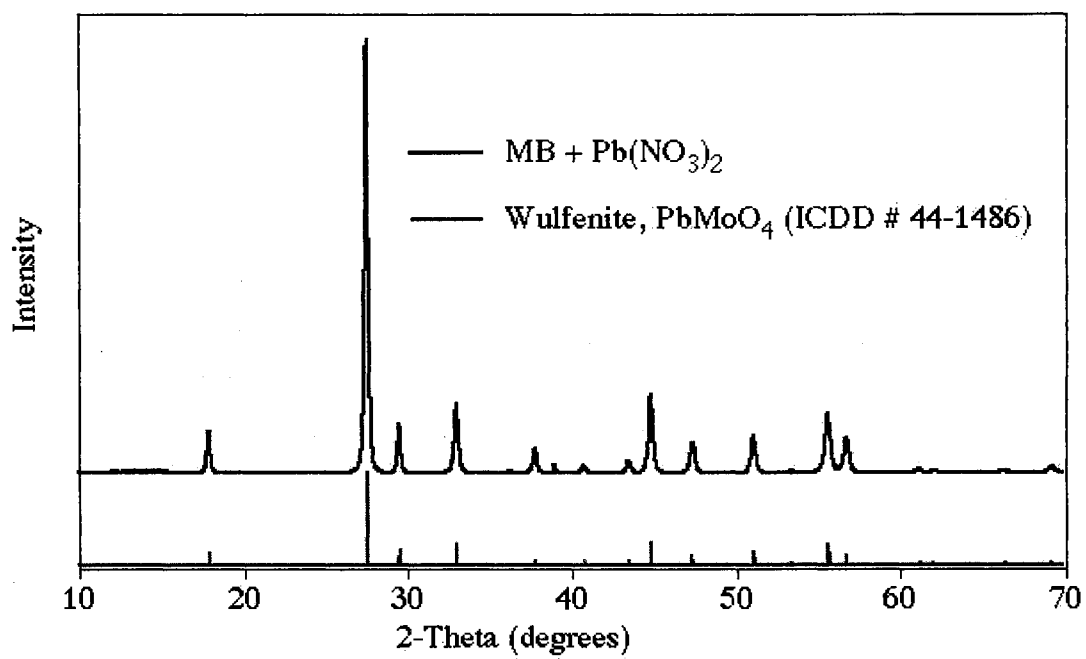


Figure 8.4: X-Ray Powder Diffraction Pattern For the Reaction Between Lead Nitrate and Molybdenum Bronze

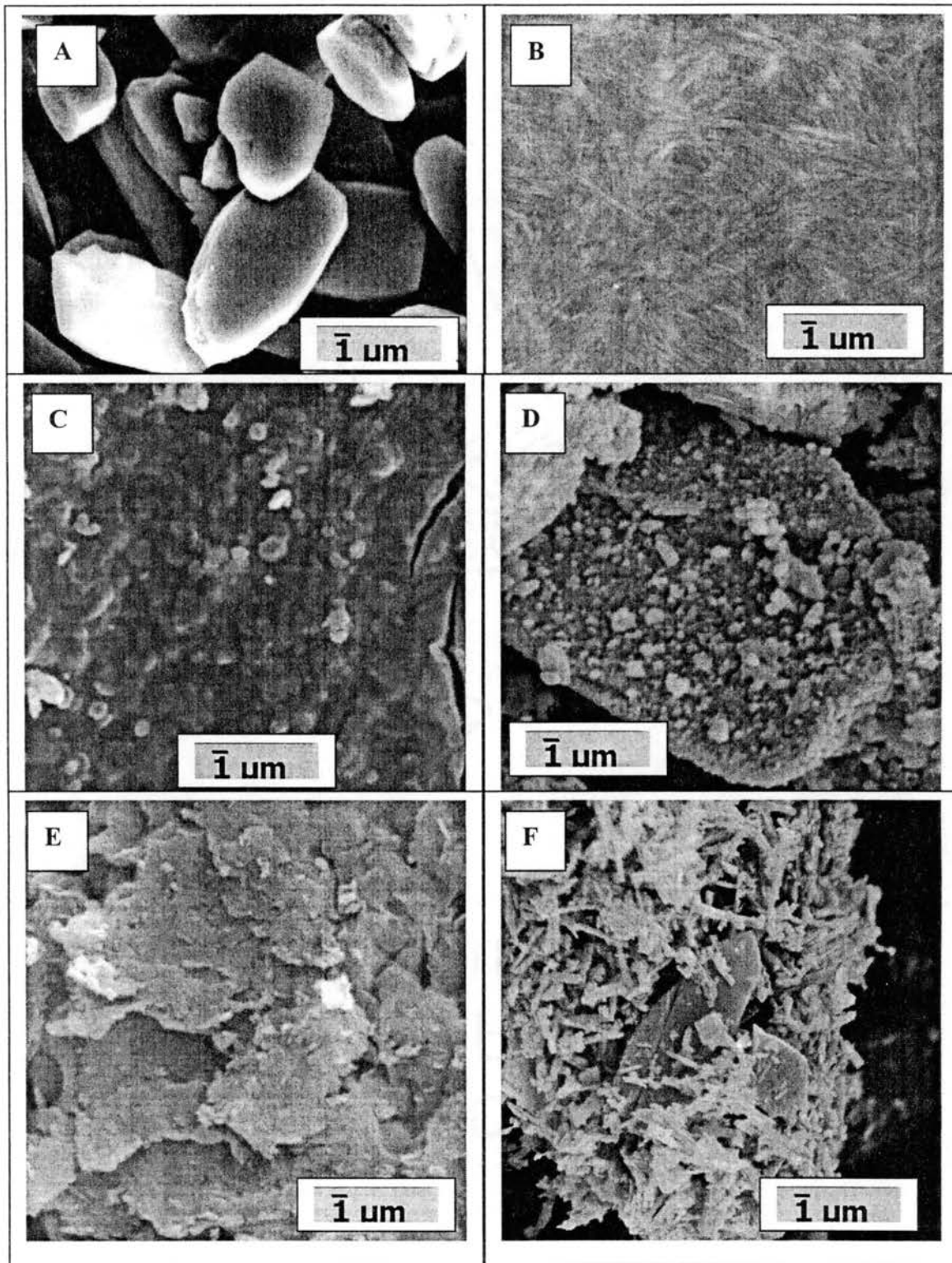


Figure 8.5: SEM pictures of (A) Molybdenum Bronze (B) Uranium Nitrate Product (C) Thorium Nitrate Product (D) Lead Nitrate Product and (E) Uranium Acetate Product (F) Neodymium Product (SEM= 5000 × magnification)

Figure 8.5 shows the SEM photographs of the solid products obtained from the reaction between molybdenum bronze and various metals. Figure 8.5(A) shows the SEM image of molybdenum bronze and 8.5(B), 5(C), 5(D), 5(E) and 5(F) show the images of the reaction products with uranyl nitrate, thorium nitrate, lead nitrate and uranyl acetate and neodymium nitrate respectively. All the reacted solids show a change from the original molybdenum bronze's morphology and particle size. The SEM image of the product of reaction between molybdenum bronze and uranyl nitrate, shown in figure 8.5(B), shows the product to consist of long fibers, a complete change of morphology from that of the original molybdenum bronze. The formation of fibers could occur by formation of reactive sites on the original molybdenum bronze surface followed by outward anisotropic growth. Since the structure of the product consists of uranium and molybdenum oxide/hydroxide chains, such a growth pattern would not be surprising. In the case of uranium acetate, however, the structure is one of thin flakes and not fibers. It is well documented that in hydrothermal synthesis, the nature of the anion exerts a strong influence on the morphology of the generated ceramic products. In particular, strongly-coordinating and chelating ligands such as acetate usually generate different morphologies as compared to non-coordinating anions such as nitrate. The difference in the morphologies of the uranyl nitrate and acetate products observed in this investigation might then suggest a second mechanistic possibility in which the molybdenum bronze particles are completely dissolved in a dissolution/precipitation process that generates new particles with different morphologies. Complete morphological rearrangement is also seen in the case of thorium nitrate (Figure 8.5 (C)), in which the product consists of very long relatively-flat glassy particles with embedded smaller particles. The overall

appearance is one of a partially melted solid. The product of lead nitrate reaction with the molybdenum bronze shows an almost identical SEM image as that of the original molybdenum bronze, except that the surface is not as smooth as the original bronze. The neodymium product consists of larger chunks similar to the starting molybdenum bronze along with small needle-like particles. This results suggests that intercalation of neodymium into molybdenum blue does occur leaving apparently intact particles behind. The presence of small needle-like phases may be due to delamination/ reaggregation of molybdate layers or be due to dissolution/reprecipitation reactions. Whatever the mechanism, both morphologies of the product are isomorphous to X-rays.

Recycling of Molybdenum Bronze in the Uranium Uptake Process

The uranyl molybdate product obtained on the reaction of molybdenum bronze with uranyl nitrate was treated with a 15% solution of ammonium hydroxide. The reaction was stirred overnight and the reaction mixture was separated by filtration. The X-ray powder diffraction pattern of the residue corresponded to ammonium uranate $\{(NH_4)_2U_3(OH)_2O_9 \cdot 2H_2O\}$, which has applications in the nuclear power industry. The ammonium uranate can be further converted to UO_3 upon heating to $600^\circ C$. Evaporation of the filtrate produced ammonium molybdate, $\{(NH_4)_2(Mo_2O_7)\}$, that was identified by XRD (ICDD Database #). Molybdenum trioxide (MoO_3) could be recovered on heating the ammonium molybdate product to $242^\circ C$ as determined by TGA.

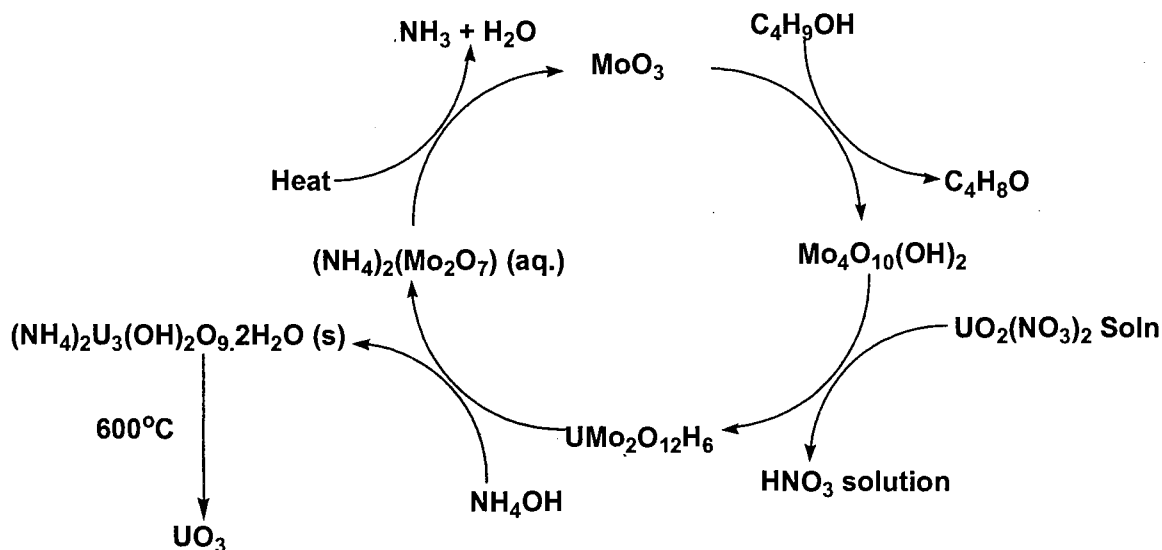


Figure 8.6: Complete Cycle of the Uranium Remediation Process

The results of the uranium recovery experiment suggest of a complete reaction cycle (Figure 8.6) in which uranium is selective absorbed by the molybdenum bronze forming a uranyl molybdate (iriginite) phase. Uranium, in form of ammonium uranate can be recovered from this molybdate phase by treatment with ammonium hydroxide. This ammonium uranate can be collected and sold to the nuclear power industry or can be heated to 600°C to produce UO₃. MoO₃ can be recovered by evaporation followed by heating of the filtrate. Hence a complete cycle can be developed in which the only reagents used are ammonium hydroxide and butanol along with heat; by-products produced are butanal, ammonia and water and the main reaction product is ammonium uranate. Potentially the ammonia could be recovered and reused and the butanol could be used industrially. In the experiment, the recovery of uranium from iriginite was 45% and the recovery of MoO₃ was 55%.

CONCLUSIONS

In conclusion, it has been demonstrated that molybdenum blue has an extremely high capacity for absorption of contaminant metals. Considerable information has been collected concerning the mechanism of metal absorption and the results obtained so far suggest that the formation of normal molybdate salts of the metal. However, in case of neodymium, it is believed that intercalation of the metal ions between the layers of HMo_2O_6 followed by reaction to yield solids in which the metal ions are trapped as counterions to the freshly-generated molybdate sites, precedes the formation of normal molybdate salts. These reactions are highly selective for heavy metals or metals that are chemically-soft or that have a large radii from water, and suggest considerable promise for application in environmental remediation and as reactive barriers for the prevention of the spread of contaminant plumes.

REFERENCES

-
1. B. A. Choudhary and R. K. Chandra, *Prog. Food Nutr. Sci.*, (1987),11(1), 55
 2. G. S. Shukla and R. L. Singhal, *Can. J. Physiol. Pharmacol.*, (1984), 62(8),1015
 3. C. Papelis; K. F. Hayes and J. O. Leckie, *HYDRAQL: a program for the computation of chemical equilibrium composition of aqueous batch systems including surface-complexation modeling of ion adsorption at the oxide/solution interface*, Stanford University, Stanford, CA, 1988
 4. United States Environmental Protection Agency, Office of Water.
<http://www.epa.gov/safewater>
 5. C. W. Fetter, *Contaminant Hydrogeology*, Macmillan Publishing Company: New York, (1993), Chapter 9
 6. D. W. Blowes; C. J. Ptacek; S. G. Benner; C. W. T. McRae; T. A. Bennett and R. W. Puls, *J. Contam. Hydrol.*, (2000), 45(1/2), 123

-
7. S. G. Benner; D. W. Blowes; W. D. Gould, R. B. Herbert and C. J. Ptacek, *Environ. Sci. Technol.*, (1999), 33(16), 2793
 8. D. W. Blowes, C. J. Ptacek and J. L. Jambor, *Environ. Sci. Technol.*, (1997), 31(12), 3348
 9. A. I. Bortun, S. A. Khainakov; V. V. Strelko; and I. A. Farbun, *Ion Exchange Developments and Applications: Special Publication- Royal Society of Chemistry*, (1996), 182, 305
 10. F. Sebesta; J. John; A. Motl; and E. W. Hooper, *Ion Exchange Developments and Applications: Special Publication- Royal Society of Chemistry*, (1996), 182, 346
 11. M. M. Figueria; B. Volesky; V. S. T. Ciminelli; and F. A. Roddick, *Water Res.*, (2000), 34(1), 196
 12. D. Kratochvil; and B. Volesky, *Water Res.*, (1998), 32(9), 2760
 13. L. M. Yates; and R. V. Wandruszka, *Environ. Sci. Technol.*, (1999), 33(12), 2076
 14. P. A. Brown; S. A. Gill; and S. J. Allen, *Water Res.*, (2000), 34(16), 3907
 15. A. Gierak, *Adsorpt. Sci. Technol.*, (1996), 4(1), 47
 16. A. I. Bortun; L. N. Burton; and A. Clearfield, *Solvent Extr. Ion Exch.*, (1997), 15(5), 909
 17. Z. Li; H. K. Jones; R. Bowman; and R. Helfferich, *Environ. Sci. Technol.*, (1999), 33, 4326
 18. "Powder Diffraction File (PDF-2)" (International Centre for Diffraction Data, Newtown Square, PA).
 19. A. I. Vogel, G. H. Jeffery, J. Bassett, J. Mendham, and R. C. Denney, *Vogel's Textbook of Quantitative Analysis*, (Longman Scientific and Technical: Burnt Mill, Harlow Essex, UK, (1989)), pp. 458-459.
 20. F. D. Snell, C. T. Snell, and C.A. Snell, "Thorium by Carminic Acid" in *Colorimetric Methods of Analysis*, Vol. IIA, (D. Van Nostrand Co.: Princeton, N.J., (1959)), pp. 518-519.
 21. K. Nakamoto, *Infrared and Raman Spectra of Inorganic and Coordination Compounds*, 4th ed. (John Wiley & Sons:, New York, (1986)).



VITA

Phani Kiran S. Bollapragada

Candidate for the Degree of

Doctor of Philosophy

Thesis: CHEMICAL TRANSFORMATIONS USING TUNGSTEN AND
MOLYBDENUM HYDROGEN BRONZES

Major Field: Chemistry

Biographical:

Personal Data: Born in Andhra Pradesh, India, on May 20, 1975

Education: Graduated from Loyola High School, Pune, India in June 1990; received Bachelor of Science degree in Chemistry from Pune University, India in June 1995; received Master of Science degree in Organic Chemistry from Pune University in June 1997. Completed requirements for the Doctor of Philosophy degree in Chemistry at Oklahoma State University in May 2003.

Experience: Employed by National Chemical Laboratory, Pune, India as a research assistant from November 1997 to July 1998. Employed by Oklahoma State University, Department of Chemistry, as a graduate research assistant, 1998 to present.

Professional Membership: American Chemical Society